Measurement and Control of the Longitudinal Phase Space at High-Gain Free-Electron Lasers.

Christopher Behrens

Deutsches Elektronen-Synchrotron (DESY)

33rd International Free-Electron Laser Conference
August 25, 2011, Shanghai

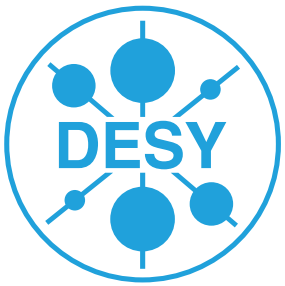

Motivation for Longitudinal Phase Space Diagnostics

Requirements of high-gain free-electron lasers including various seeded schemes

- Good electron beam quality in terms of energy spread, emittance, and peak current
- Time-resolved (i.e. longitudinal) information and control of these parameters
- Control of beam instabilities and corresponding diagnostics problems, e.g. COTR
- Measurement and tunability of electron and photon pulse lengths

Motivation for Longitudinal Phase Space Diagnostics

Requirements of high-gain free-electron lasers including various seeded schemes

- Good electron beam quality in terms of energy spread, emittance, and peak current
- Time-resolved (i.e. longitudinal) information and control of these parameters
- Control of beam instabilities and corresponding diagnostics problems, e.g. COTR
- Measurement and tunability of electron and photon pulse lengths

Measurement and control of the longitudinal phase space (t, δ)

- Longitudinal position $t = -z/c$ and relative energy or momentum deviation $\delta = \frac{\Delta p}{p_0}$
- 6-d beam transport matrix provide a powerful formalism to discuss the underlying physics

$$\begin{pmatrix} x_f \\ x'_f \\ y_f \\ y'_f \\ t_f \\ \delta_f \end{pmatrix} = \begin{pmatrix} R_{11} & R_{12} & R_{13} & R_{14} & R_{15} & R_{16} \\ R_{21} & R_{22} & R_{23} & R_{24} & R_{25} & R_{26} \\ R_{31} & R_{32} & R_{33} & R_{34} & R_{35} & R_{36} \\ R_{41} & R_{42} & R_{43} & R_{44} & R_{45} & R_{46} \\ R_{51} & R_{52} & R_{53} & R_{54} & R_{55} & R_{56} \\ R_{61} & R_{62} & R_{63} & R_{64} & R_{65} & R_{66} \end{pmatrix} \cdot \begin{pmatrix} x_i \\ x'_i \\ y_i \\ y'_i \\ t_i \\ \delta_i \end{pmatrix}$$

Motivation for Longitudinal Phase Space Diagnostics

Requirements of high-gain free-electron lasers including various seeded schemes

- Good electron beam quality in terms of energy spread, emittance, and peak current
- Time-resolved (i.e. longitudinal) information and control of these parameters
- Control of beam instabilities and corresponding diagnostics problems, e.g. COTR
- Measurement and tunability of electron and photon pulse lengths

Measurement and control of the longitudinal phase space (t, δ)

- Longitudinal position $t = -z/c$ and relative energy or momentum deviation $\delta = \frac{\Delta p}{p_0}$
- 6-d beam transport matrix provide a powerful formalism to discuss the underlying physics

$$\begin{pmatrix} x_f \\ x'_f \\ y_f \\ y'_f \\ t_f \\ \delta_f \end{pmatrix} = \begin{pmatrix} R_{11} & R_{12} & R_{13} & R_{14} & R_{15} & R_{16} \\ R_{21} & R_{22} & R_{23} & R_{24} & R_{25} & R_{26} \\ R_{31} & R_{32} & R_{33} & R_{34} & R_{35} & R_{36} \\ R_{41} & R_{42} & R_{43} & R_{44} & R_{45} & R_{46} \\ R_{51} & R_{52} & R_{53} & R_{54} & R_{55} & R_{56} \\ R_{61} & R_{62} & R_{63} & R_{64} & R_{65} & R_{66} \end{pmatrix} \cdot \begin{pmatrix} x_i \\ x'_i \\ y_i \\ y'_i \\ t_i \\ \delta_i \end{pmatrix}$$

★ Transverse Deflecting RF Structure in combination with an energy (dipole) spectrometer

- Single-shot capability and high resolution in both energy and time

The Principle: TDS in Combination with an Energy Spectrometer

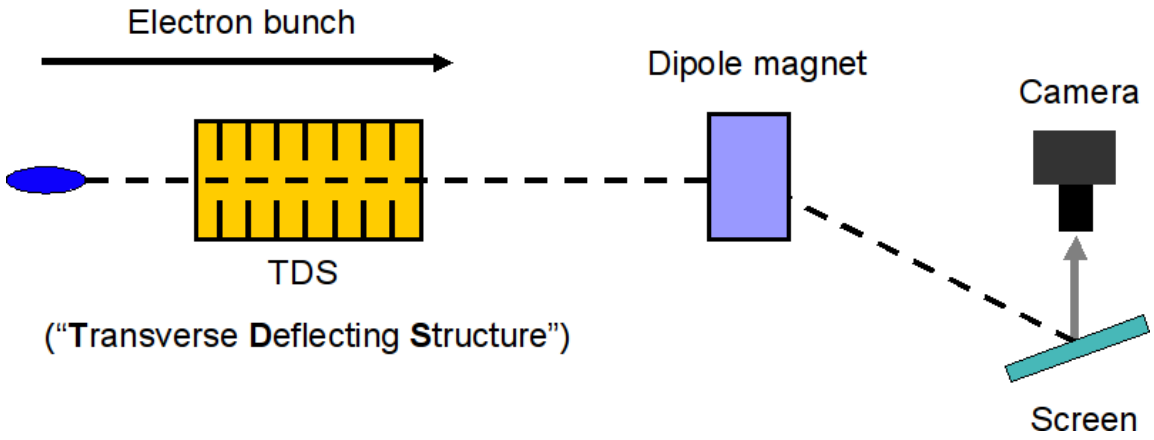

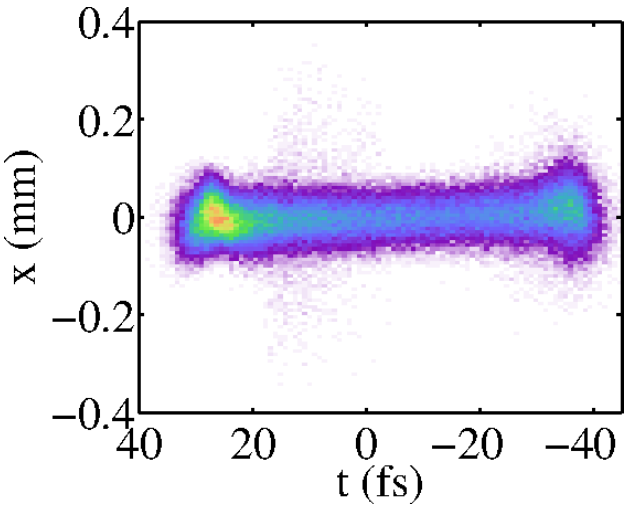

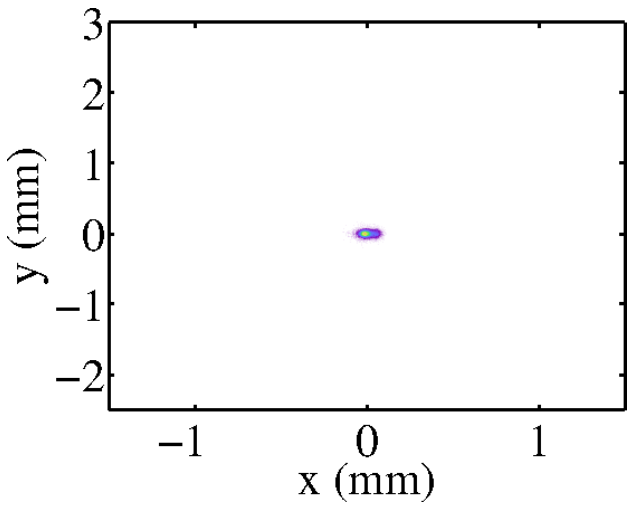

- Start with initial distributions in (t, x) and (x, y)

The Principle: TDS in Combination with an Energy Spectrometer

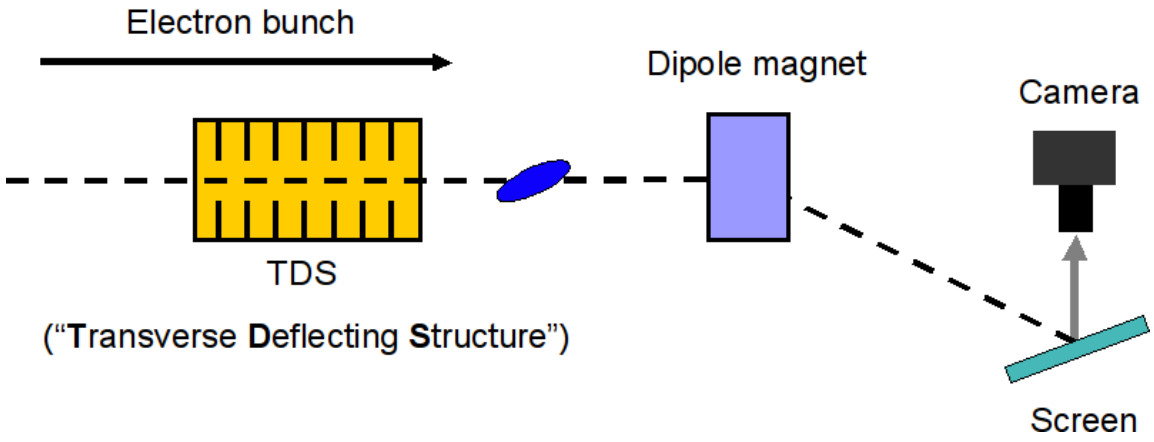

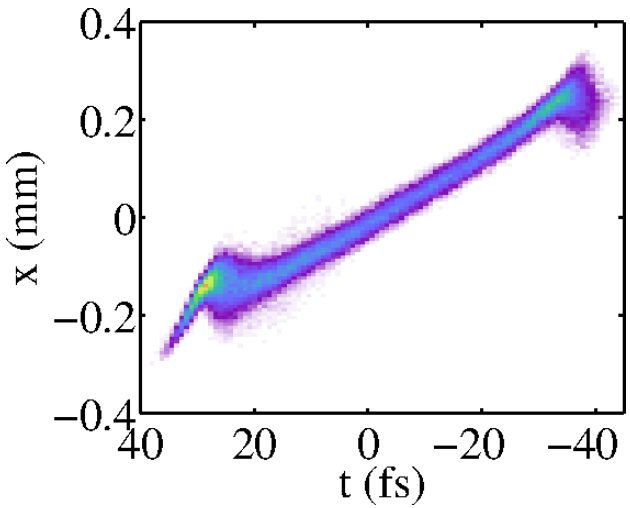

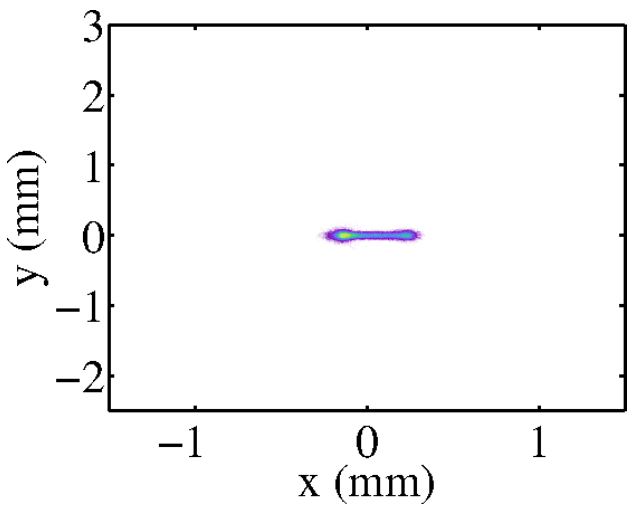

- TDS imposes a time-dependent transversal kick $\Delta x'(t) \sim \sin(t) \approx t$ (at zero-crossing)
- Appropriate beam transport optics (R_{12}) maps $\Delta x'(t) \rightarrow \Delta x(t)$, i.e. $\Delta x(t) \sim t$
- ★ Time information is translated to the horizontal position

The Principle: TDS in Combination with an Energy Spectrometer

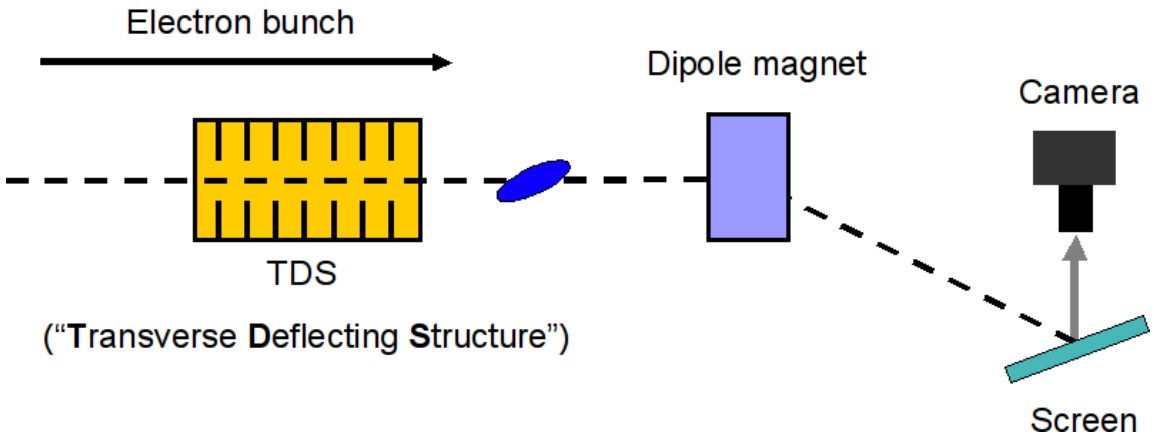

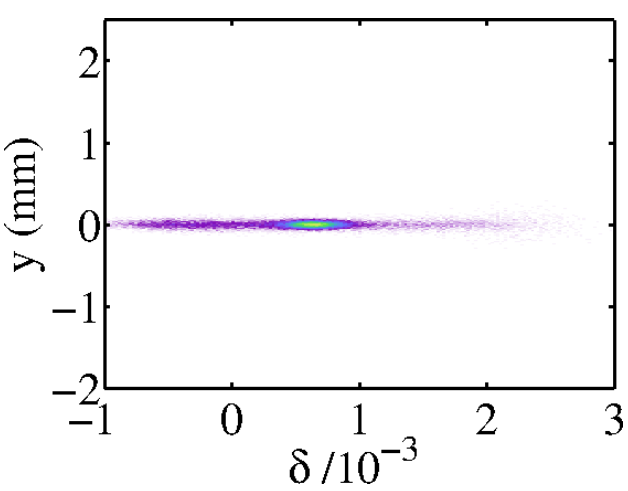

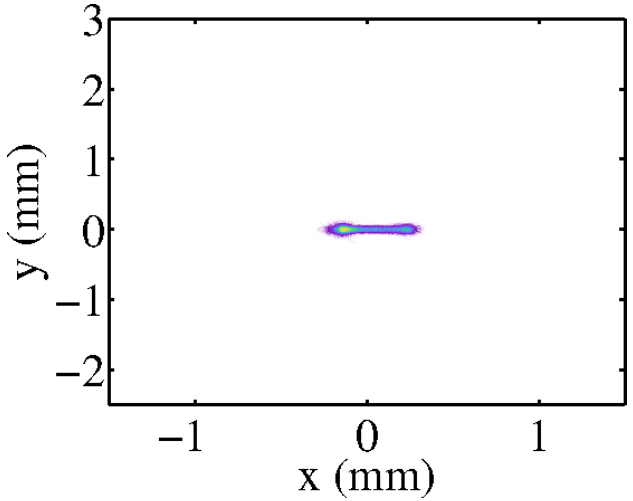

- Start again with present distributions in (δ, y) and (x, y)

The Principle: TDS in Combination with an Energy Spectrometer

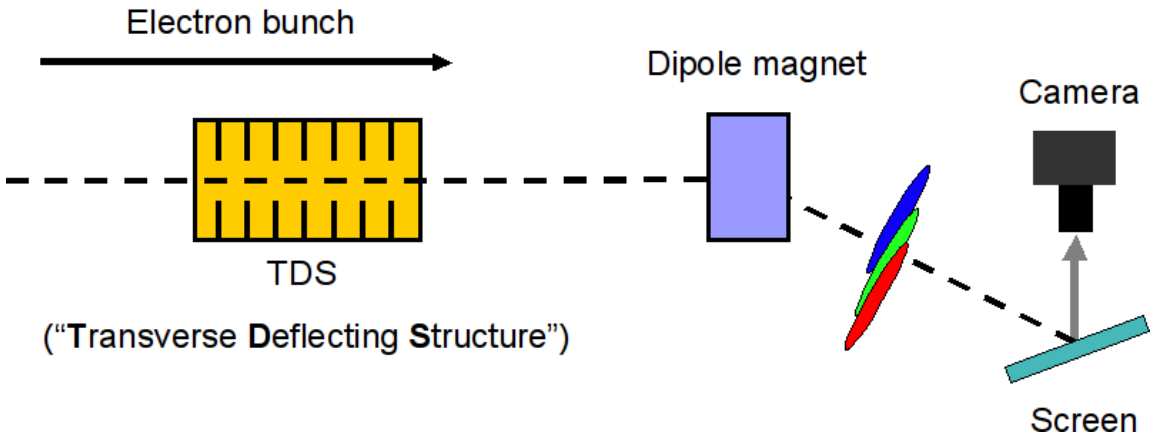

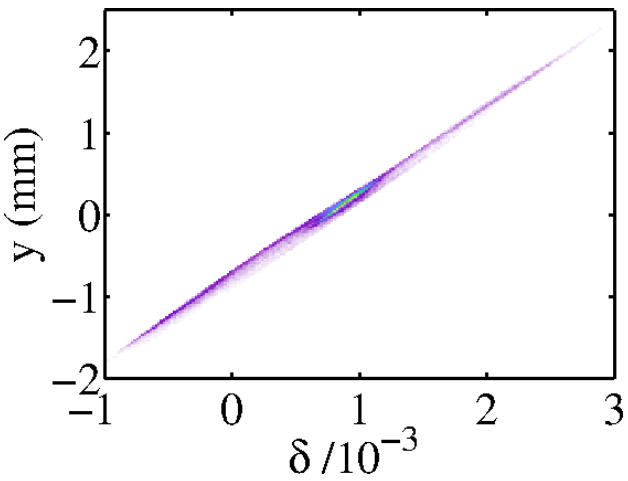

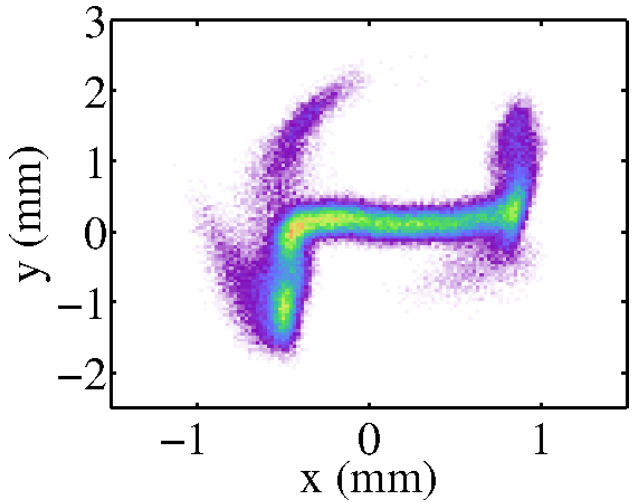

- Dipole magnet imposes a energy-dependent transversal kick $\Delta y'(\delta) \sim \delta$
- Appropriate beam transport optics (R_{34}) maps $\Delta y'(\delta) \rightarrow \Delta y(\delta)$, i.e. $\Delta y(\delta) \sim \delta$
- ★ Energy information is translated to the vertical position

The Principle: TDS in Combination with an Energy Spectrometer

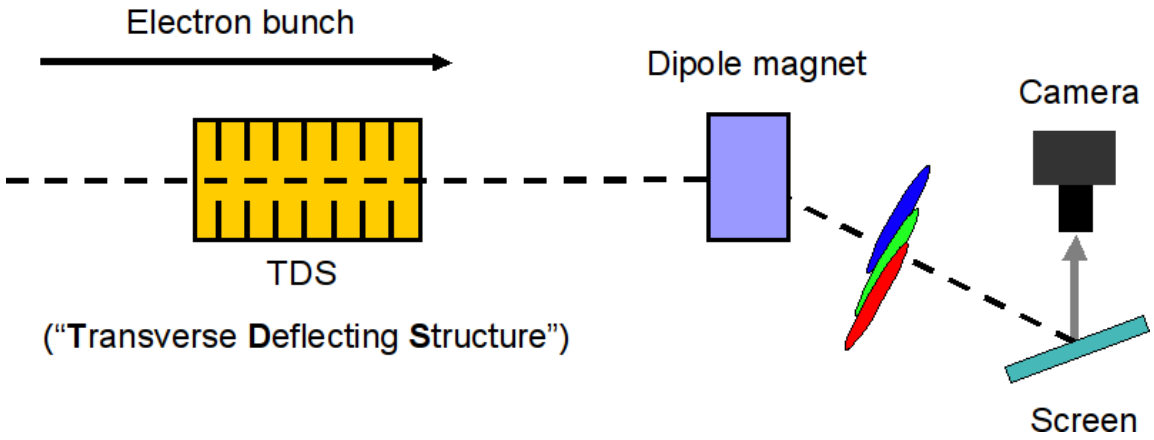

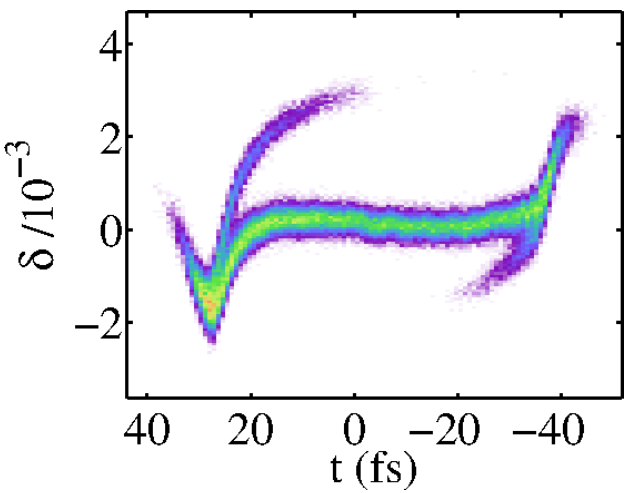

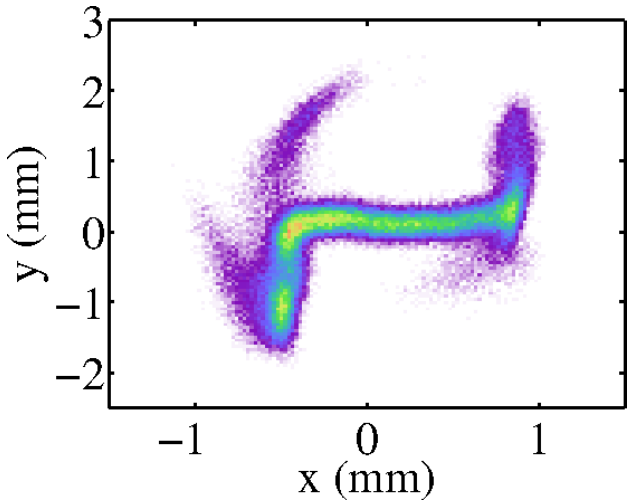

- ★ Transformation of the longitudinal phases space (t, δ) to (x, y)
- ★ Good agreement compared to the real longitudinal phase space
- ★ Simulation shows some discrepancy when looking into the details

Definition of Time and Energy Resolution (r.m.s)

Measureable beam size and time resolution using a TDS

- $x(s,t) = x_0(s) + S(s) \cdot t$ with shear function $S(s) = \frac{eV_0\omega}{E}\sqrt{\beta_1\beta_2(s)}\sin(\Delta\Psi_x(s))$ $\quad (S \hat{=} R_{15})$
- $\sigma_x = \sqrt{\sigma_{x_0}^2 + (S \cdot \sigma_t)^2} \Rightarrow$ r.m.s. definition of time resolution $\sigma_{R,t} = \sigma_{x_0}/S$

Definition of Time and Energy Resolution (r.m.s)

Measureable beam size and time resolution using a TDS

- $x(s,t) = x_0(s) + S(s) \cdot t$ with shear function $S(s) = \frac{eV_0\omega}{E}\sqrt{\beta_1\beta_2(s)}\sin(\Delta\Psi_x(s))$ $(S \hat{=} R_{15})$
- $\sigma_x = \sqrt{\sigma_{x_0}^2 + (S \cdot \sigma_t)^2} \Rightarrow$ r.m.s. definition of time resolution $\sigma_{R,t} = \sigma_{x_0}/S$

Measureable beam size and energy resolution using an energy spectrometer

- $y(s,\delta) = y_0(s) + D(s) \cdot \delta$ with dispersion function $D(s)$ $(D \hat{=} R_{36})$
- $\sigma_y = \sqrt{\sigma_{y_0}^2 + (D \cdot \sigma_\delta)^2} \Rightarrow$ r.m.s. definition of rel. energy resolution $\sigma_{R,\delta} = \sigma_{y_0}/D$

★ Small intrinsic beam sizes at screen position and large S and D improve resolution

Definition of Time and Energy Resolution (r.m.s)

Measureable beam size and time resolution using a TDS

- $x(s,t) = x_0(s) + S(s) \cdot t$ with shear function $S(s) = \frac{eV_0\omega}{E}\sqrt{\beta_1\beta_2(s)}\sin(\Delta\Psi_x(s))$ $(S \hat{=} R_{15})$
- $\sigma_x = \sqrt{\sigma_{x_0}^2 + (S \cdot \sigma_t)^2} \Rightarrow$ r.m.s. definition of time resolution $\sigma_{R,t} = \sigma_{x_0}/S$

Measureable beam size and energy resolution using an energy spectrometer

- $y(s,\delta) = y_0(s) + D(s) \cdot \delta$ with dispersion function $D(s)$ $(D \hat{=} R_{36})$
- $\sigma_y = \sqrt{\sigma_{y_0}^2 + (D \cdot \sigma_\delta)^2} \Rightarrow$ r.m.s. definition of rel. energy resolution $\sigma_{R,\delta} = \sigma_{y_0}/D$

★ Small intrinsic beam sizes at screen position and large S and D improve resolution

★ Intrinsic beam size could vary along the bunch

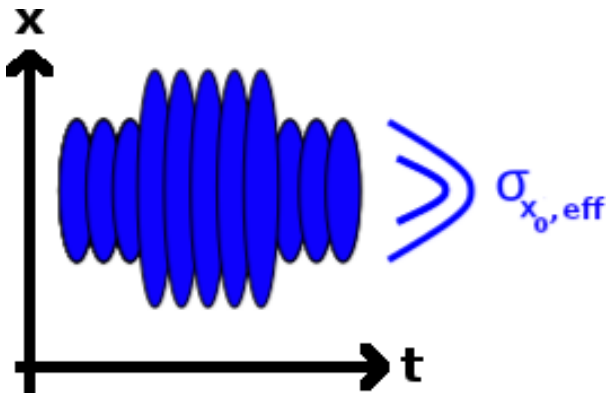

Definition of Time and Energy Resolution (r.m.s)

Measureable beam size and time resolution using a TDS

- $x(s,t) = x_0(s) + S(s) \cdot t$ with shear function $S(s) = \frac{eV_0\omega}{E}\sqrt{\beta_1\beta_2(s)}\sin(\Delta\Psi_x(s))$ $(S \hat{=} R_{15})$
- $\sigma_x = \sqrt{\sigma_{x_0}^2 + (S \cdot \sigma_t)^2} \Rightarrow$ r.m.s. definition of time resolution $\sigma_{R,t} = \sigma_{x_0}/S$

Measureable beam size and energy resolution using an energy spectrometer

- $y(s,\delta) = y_0(s) + D(s) \cdot \delta$ with dispersion function $D(s)$ $(D \hat{=} R_{36})$
- $\sigma_y = \sqrt{\sigma_{y_0}^2 + (D \cdot \sigma_\delta)^2} \Rightarrow$ r.m.s. definition of rel. energy resolution $\sigma_{R,\delta} = \sigma_{y_0}/D$

★ Small intrinsic beam sizes at screen position and large S and D improve resolution

★ Intrinsic beam size could vary along the bunch

★ Bunch could have a tilt

$\Rightarrow$ Definition describes the overall resolution

- The same is valid for the energy resolution

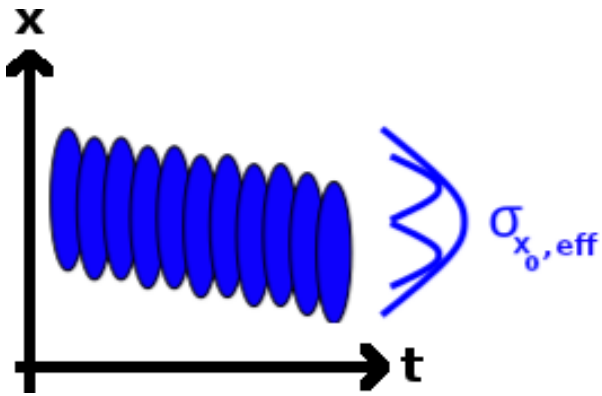

Calibration, Resolution, and Impact of Jitter: Time

Time calibration: Scanning of RF phase

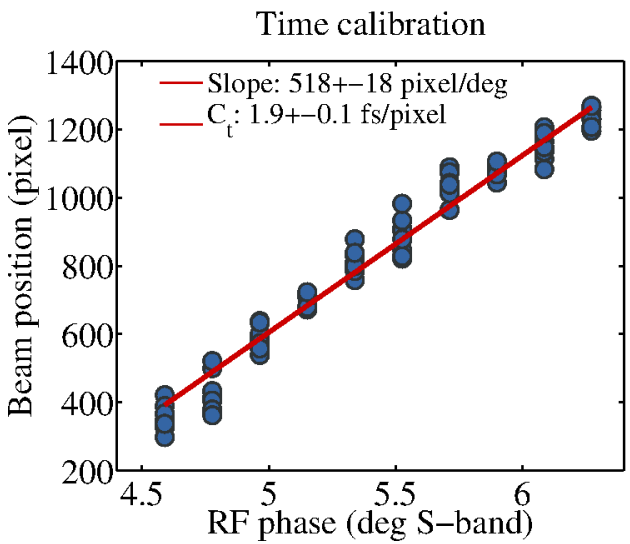

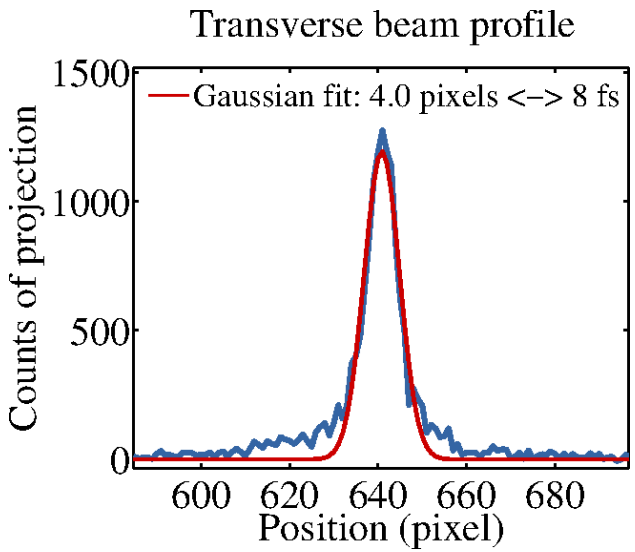

- Time calibration: Centroid offset versus RF phase ($\phi = \omega t \sim t$)
- Time resolution: Beam size without shearing by the TDS

Calibration, Resolution, and Impact of Jitter: Time

Time calibration: Scanning of RF phase

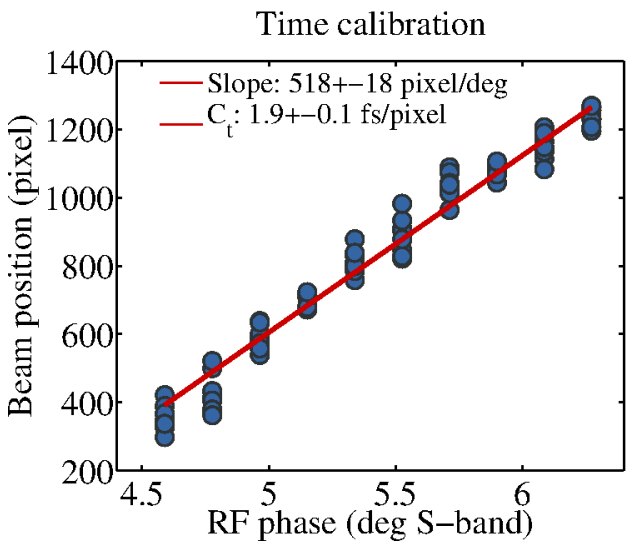

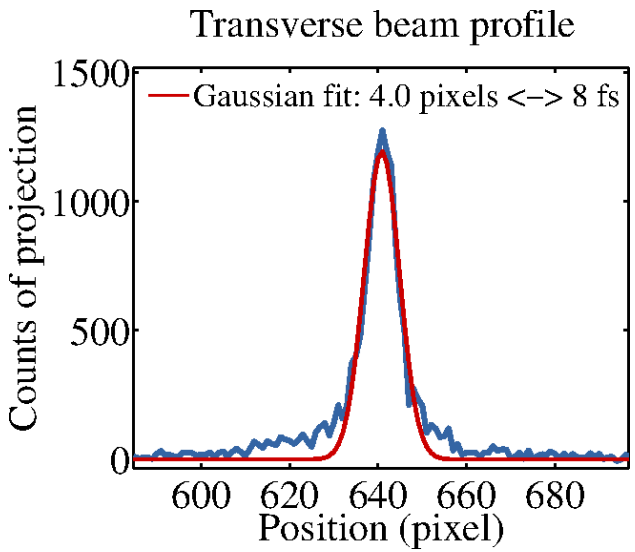

- Time calibration: Centroid offset versus RF phase ($\phi = \omega t \sim t$)
- Time resolution: Beam size without shearing by the TDS

Impact of jitter sources on tranverse jitter

- Might be a problem for calibration which is a multi-shot procedure
- The only relevant jitter is arrival time σ_t and RF phase jitter σ_ϕ
  $\rightarrow \sigma_x = S \cdot \sigma_t$ and $\sigma_x = S \cdot \omega^{-1} \cdot \sigma_\phi$

★ Basically this is under control for stable machines and can even be improved

Calibration, Resolution, and Impact of Jitter: Energy

Energy calibration: Scanning of magnet current (energy)

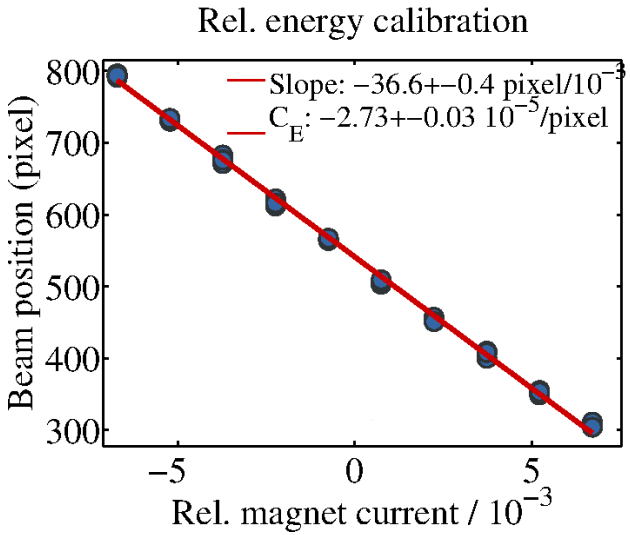

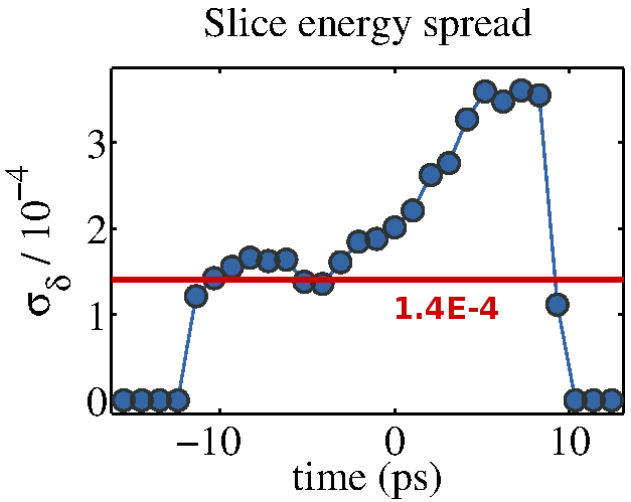

- Energy calibration: Centroid offset versus energy or simply magnet current ($\Delta I/I_0$)
- Energy resolution: Minimum slice energy spread of uncompressed bunches (reso. limited)

Calibration, Resolution, and Impact of Jitter: Energy

Energy calibration: Scanning of magnet current (energy)

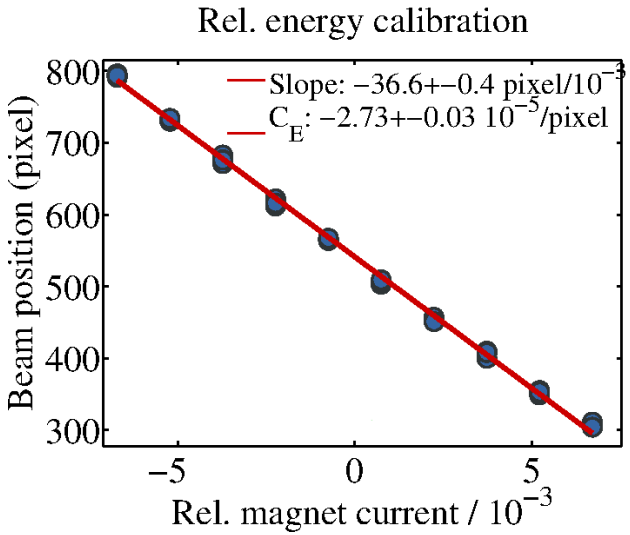

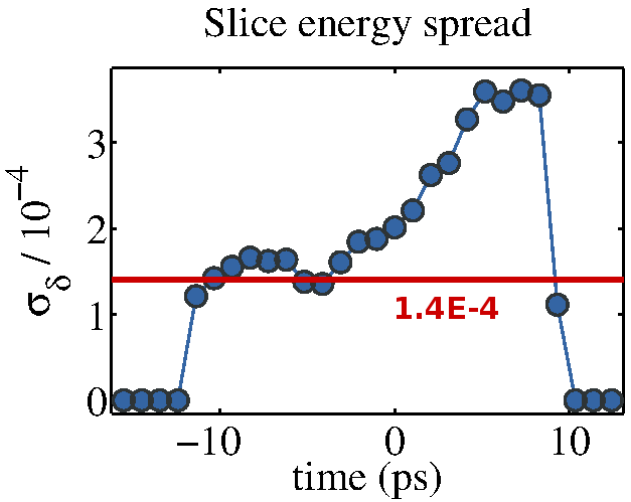

- Energy calibration: Centroid offset versus energy or simply magnet current ($\Delta I/I_0$)
- Energy resolution: Minimum slice energy spread of uncompressed bunches (reso. limited)

Impact of jitter sources on tranverse jitter

- Might be a problem for calibration which is a multishot procedure
- The only relevant jitter is energy jitter σ_δ
  $\rightarrow \sigma_y = D \cdot \sigma_\delta$

★ Basically this is under control, but pay attention to hysteresis effects

Intrinsic Effects: Induced Energy Spread, CSR and Wakefields

TDS-induced energy spread and chirp: Theory and Experiment

- Transverse deflecting structures induce energy spread (Panofsky-Wenzel theorem)
  Thin-lens matrix $\rightarrow \sigma_\delta = K\sigma_x = \frac{eVk}{pc}\sigma_x$
- Thick-lens matrix $\Rightarrow$ induced energy chirp

$$\begin{pmatrix} x_f \\ x'_f \\ t_f \\ \delta_f \end{pmatrix} = \begin{pmatrix} 1 & L & KL/2 & 0 \\ 0 & 1 & K & 0 \\ 0 & 0 & 1 & 0 \\ K & KL/2 & K^2L/6 & 1 \end{pmatrix} \cdot \begin{pmatrix} x_i \\ x'_i \\ t_i \\ \delta_i \end{pmatrix}$$

Intrinsic Effects: Induced Energy Spread, CSR and Wakefields

TDS-induced energy spread and chirp: Theory and Experiment

- Transverse deflecting structures induce energy spread (Panofsky-Wenzel theorem)
  Thin-lens matrix $\rightarrow \sigma_\delta = K\sigma_x = \frac{eVk}{pc}\sigma_x$
- Thick-lens matrix $\Rightarrow$ induced energy chirp

$$\begin{pmatrix} x_f \\ x'_f \\ t_f \\ \delta_f \end{pmatrix} = \begin{pmatrix} 1 & L & KL/2 & 0 \\ 0 & 1 & K & 0 \\ 0 & 0 & 1 & 0 \\ K & KL/2 & K^2L/6 & 1 \end{pmatrix} \cdot \begin{pmatrix} x_i \\ x'_i \\ t_i \\ \delta_i \end{pmatrix}$$

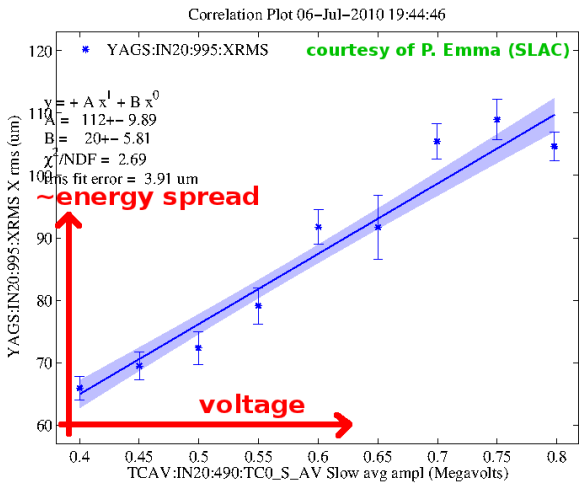

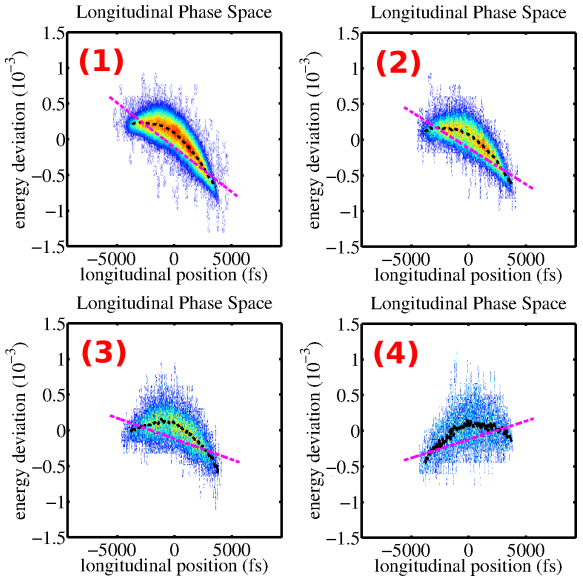

Intrinsic Effects: Induced Energy Spread, CSR and Wakefields

TDS-induced energy spread and chirp: Theory and Experiment

- Transverse deflecting structures induce energy spread (Panofsky-Wenzel theorem)
  Thin-lens matrix $\rightarrow \sigma_\delta = K\sigma_x = \frac{eVk}{pc}\sigma_x$
- Thick-lens matrix $\Rightarrow$ induced energy chirp

$$\begin{pmatrix} x_f \\ x'_f \\ t_f \\ \delta_f \end{pmatrix} = \begin{pmatrix} 1 & L & KL/2 & 0 \\ 0 & 1 & K & 0 \\ 0 & 0 & 1 & 0 \\ K & KL/2 & K^2L/6 & 1 \end{pmatrix} \cdot \begin{pmatrix} x_i \\ x'_i \\ t_i \\ \delta_i \end{pmatrix}$$

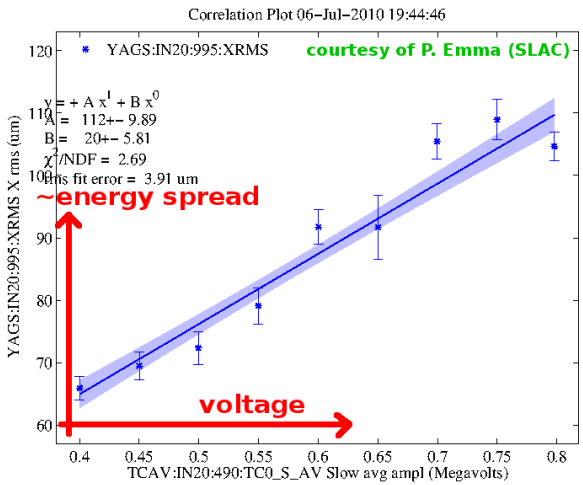

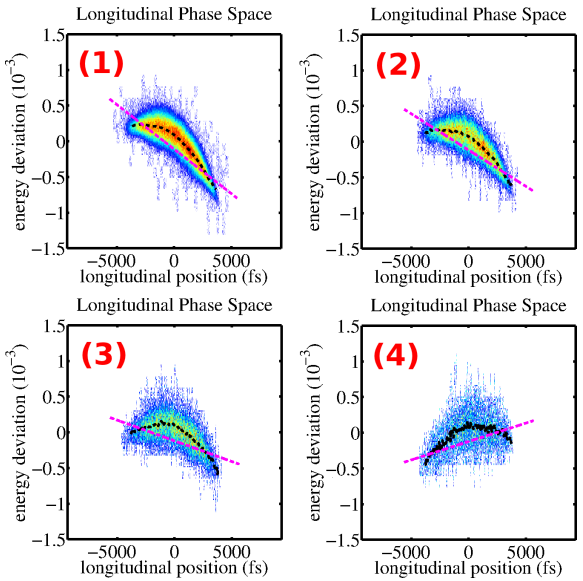

Coherent synchrotron radiation effects in the energy spectrometer

★ Basically negligible due to the fact that
- time is transformed (e.g. in x) in front of the spectrometer
- dispersion starts energy transformation (e.g. in y) before CSR is built up

Intrinsic Effects: Induced Energy Spread, CSR and Wakefields

TDS-induced energy spread and chirp: Theory and Experiment

- Transverse deflecting structures induce energy spread (Panofsky-Wenzel theorem)
  Thin-lens matrix $\rightarrow \sigma_\delta = K\sigma_x = \frac{eVk}{pc}\sigma_x$
- Thick-lens matrix $\Rightarrow$ induced energy chirp

$$\begin{pmatrix} x_f \\ x'_f \\ t_f \\ \delta_f \end{pmatrix} = \begin{pmatrix} 1 & L & KL/2 & 0 \\ 0 & 1 & K & 0 \\ 0 & 0 & 1 & 0 \\ K & KL/2 & K^2L/6 & 1 \end{pmatrix} \cdot \begin{pmatrix} x_i \\ x'_i \\ t_i \\ \delta_i \end{pmatrix}$$

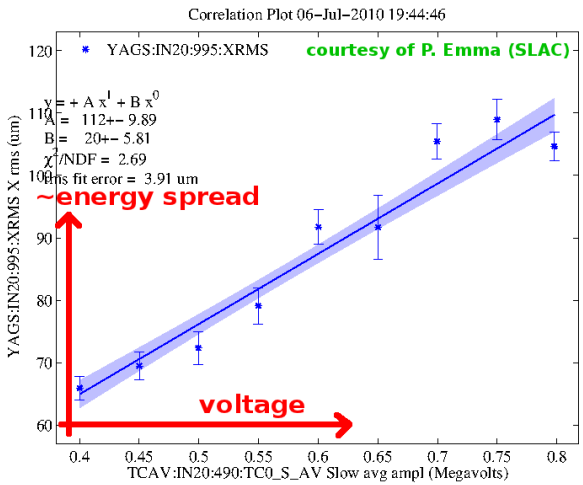

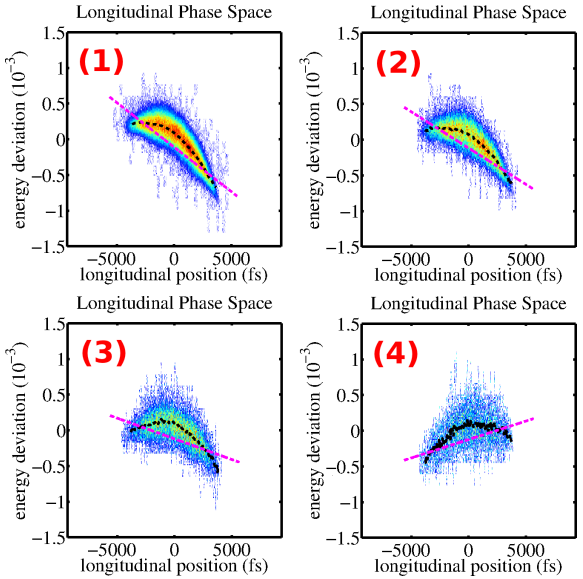

Wakefield effects

★ Basically negligible when having no large position offsets

Systematic Errors due to Initial Correlations in the Phase Space

Initial correlations in (x', t) may give different results when changing zero-crossing

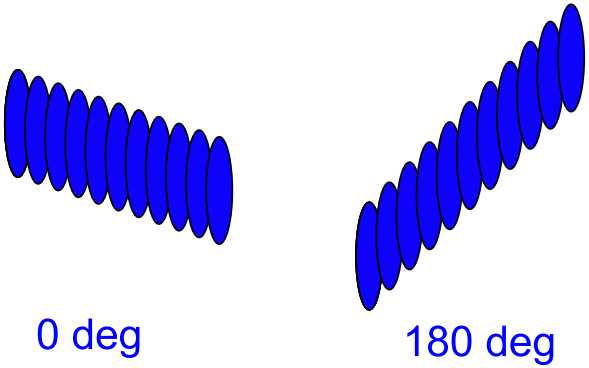

- $\sigma_x = \sqrt{\sigma_{x_0}^2 + (C \pm S)^2 \cdot \sigma_t^2}$

Systematic Errors due to Initial Correlations in the Phase Space

Initial correlations in (x', t) may give different results when changing zero-crossing

courtesy of H. Loos (SLAC)

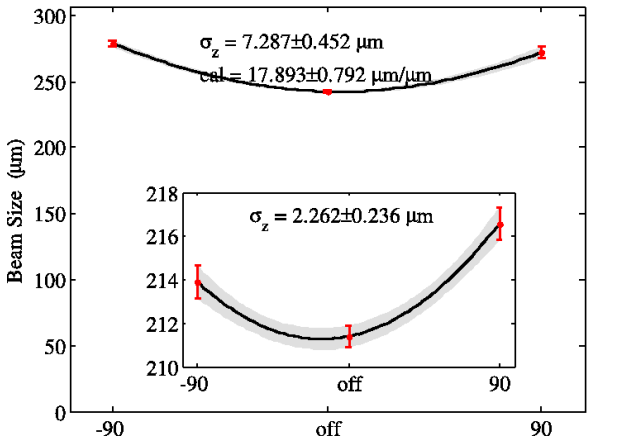

- $\sigma_x = \sqrt{\sigma_{x_0}^2 + (C \pm S)^2 \cdot \sigma_t^2}$

★ If C is a constant: simple calculation using values at $\pm S$ (0 and 180 deg)

Systematic Errors due to Initial Correlations in the Phase Space

Initial correlations in (x', t) may give different results when changing zero-crossing

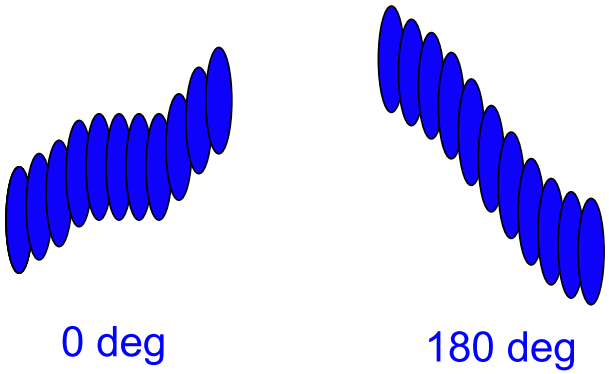

- $\sigma_x = \sqrt{\sigma_{x_0}^2 + (C \pm S)^2 \cdot \sigma_t^2}$
- ★ If C is a constant: simple calculation using values at $\pm S$ (0 and 180 deg)
- ★ If C varies along the bunch (i.e. $C(t)$): reconstruction from both projections is possible (idea and Ref. by H. Loos (SLAC))

Systematic Errors due to Initial Correlations in the Phase Space

Initial correlations in (x', t) may give different results when changing zero-crossing

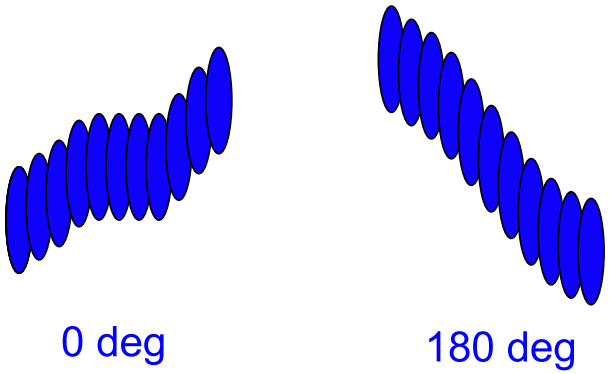

- $\sigma_x = \sqrt{\sigma_{x_0}^2 + (C \pm S)^2 \cdot \sigma_t^2}$
- ★ If C is a constant: simple calculation using values at $\pm S$ (0 and 180 deg)
- ★ If C varies along the bunch (i.e. $C(t)$): reconstruction from both projections is possible (idea and Ref. by H. Loos (SLAC))

Simulated measurements with both zero-crossings (0 and 180 deg)

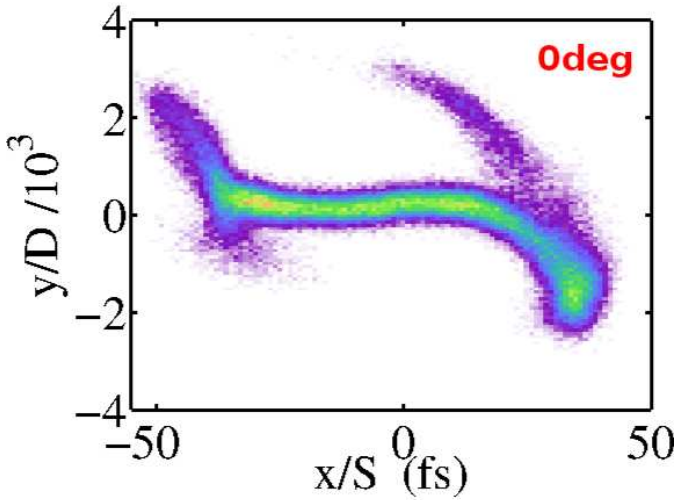

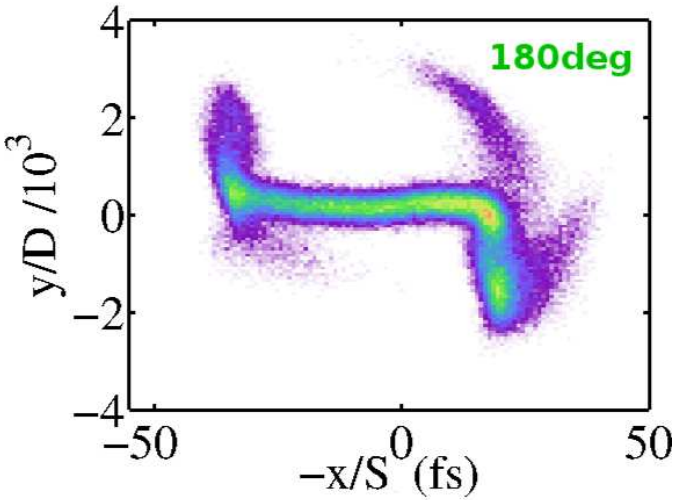

Systematic Errors due to Initial Correlations in the Phase Space

Initial correlations in (x', t) may give different results when changing zero-crossing

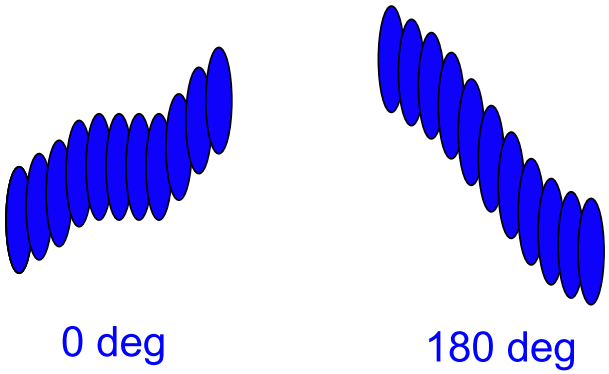

- $\sigma_x = \sqrt{\sigma_{x_0}^2 + (C \pm S)^2 \cdot \sigma_t^2}$

★ If C is a constant: simple calculation using values at $\pm S$ (0 and 180 deg)

★ If C varies along the bunch (i.e. $C(t)$): reconstruction from both projections is possible
(idea and Ref. by H. Loos (SLAC))

Simulated measurements with both zero-crossings (0 and 180 deg)

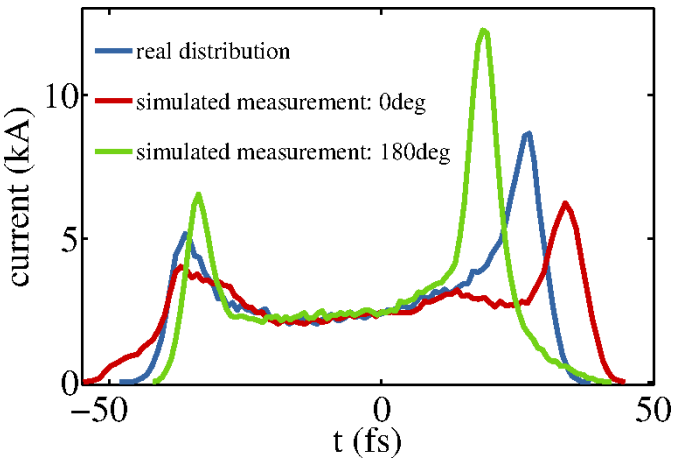

- Strong effects in head and tail

Systematic Errors due to Initial Correlations in the Phase Space

Initial correlations in (x', t) may give different results when changing zero-crossing

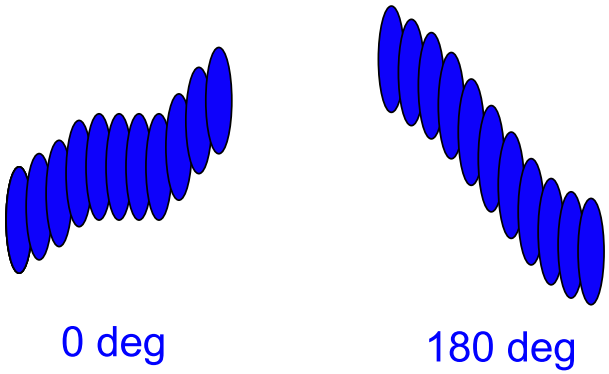

- $\sigma_x = \sqrt{\sigma_{x_0}^2 + (C \pm S)^2 \cdot \sigma_t^2}$
- ★ If C is a constant: simple calculation using values at $\pm S$ (0 and 180 deg)
- ★ If C varies along the bunch (i.e. $C(t)$): reconstruction from both projections is possible (idea and Ref. by H. Loos (SLAC))

Simulated measurements with both zero-crossings (0 and 180 deg)

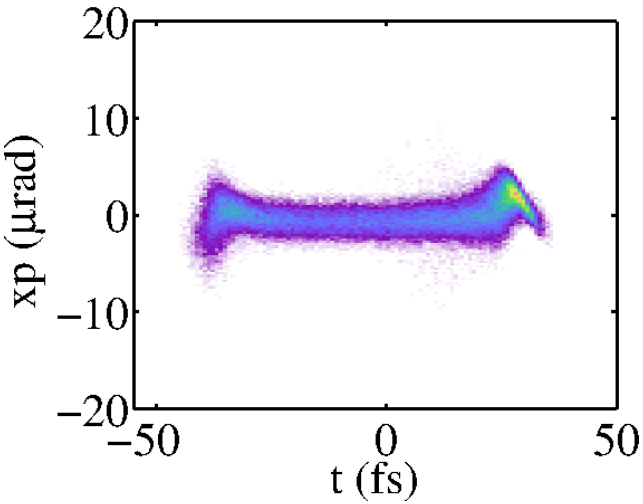

- Strong effects in head and tail
- ★ Linear scaling will not help

Systematic Errors due to Initial Correlations in the Phase Space

Initial correlations in (x', t) may give different results when changing zero-crossing

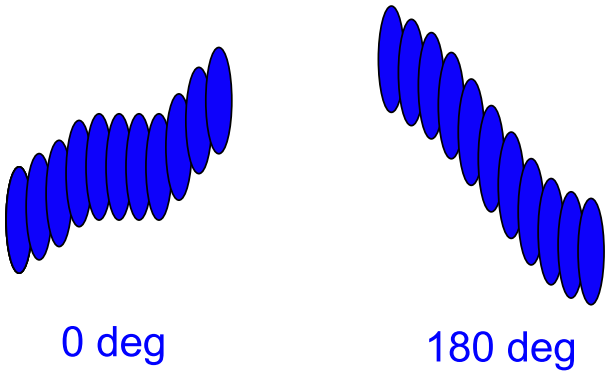

- $\sigma_x = \sqrt{\sigma_{x_0}^2 + (C \pm S)^2 \cdot \sigma_t^2}$
- ★ If C is a constant: simple calculation using values at $\pm S$ (0 and 180 deg)
- ★ If C varies along the bunch (i.e. $C(t)$): reconstruction from both projections is possible (idea and Ref. by H. Loos (SLAC))

Simulated measurements with both zero-crossings (0 and 180 deg)

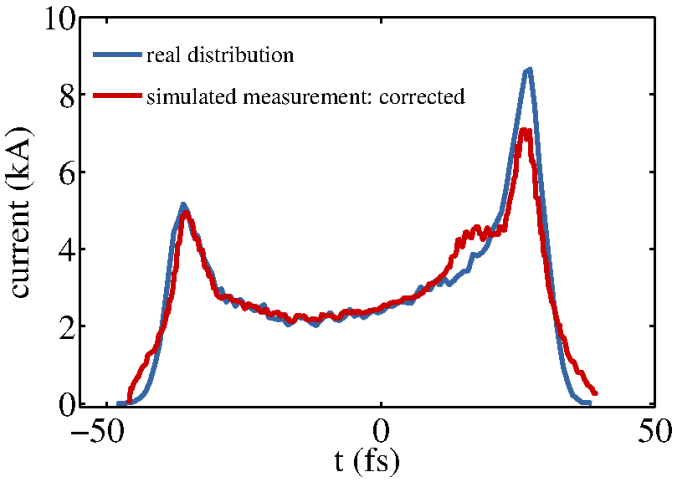

- Strong effects in head and tail
- ★ Linear scaling will not help
- ★ Reconstruction from two projections

Mitigation of Coherent Optical Transition Radiation: Simulations

Time coordinate along the energy spectrometer

- Longitudinal position after the spectrometer: $t_f = R_{53} \cdot y_i + R_{54} \cdot y_i' + t_i + R_{56} \cdot \delta_i$

Mitigation of Coherent Optical Transition Radiation: Simulations

Time coordinate along the energy spectrometer

- Longitudinal position after the spectrometer: $t_f = R_{53} \cdot y_i + R_{54} \cdot y_i' + t_i + R_{56} \cdot \delta_i$
- $\sigma_{t_f} \approx R_{53} \cdot \sigma_{y_i}$ and $R_{53} \approx \alpha$ i.e. the bending angle of the dipole
- $R_{53} \cdot \sigma_{y_i}$ smears out density modulations

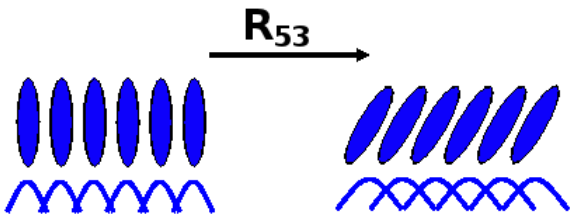

- Microbunches overlap and smear out

Mitigation of Coherent Optical Transition Radiation: Simulations

Time coordinate along the energy spectrometer

- Longitudinal position after the spectrometer: $t_f = R_{53} \cdot y_i + R_{54} \cdot y_i' + t_i + R_{56} \cdot \delta_i$
- $\sigma_{t_f} \approx R_{53} \cdot \sigma_{y_i}$ and $R_{53} \approx \alpha$ i.e. the bending angle of the dipole
- $R_{53} \cdot \sigma_{y_i}$ smears out density modulations

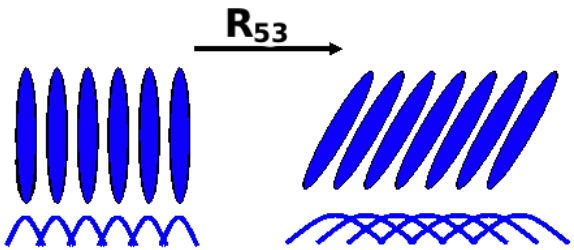

- Microbunches overlap and smear out
- Larger beam size $\rightarrow$ larger overlap

Mitigation of Coherent Optical Transition Radiation: Simulations

Time coordinate along the energy spectrometer

- Longitudinal position after the spectrometer: $t_f = R_{53} \cdot y_i + R_{54} \cdot y_i' + t_i + R_{56} \cdot \delta_i$
- $\sigma_{t_f} \approx R_{53} \cdot \sigma_{y_i}$ and $R_{53} \approx \alpha$ i.e. the bending angle of the dipole
- $R_{53} \cdot \sigma_{y_i}$ smears out density modulations

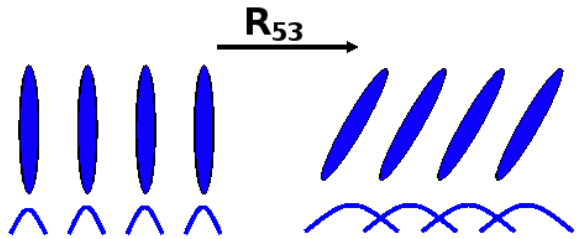

- Microbunches overlap and smear out
- Larger beam size $\rightarrow$ larger overlap
- Larger period $\rightarrow$ less overlap

Mitigation of Coherent Optical Transition Radiation: Simulations

Time coordinate along the energy spectrometer

- Longitudinal position after the spectrometer: $t_f = R_{53} \cdot y_i + R_{54} \cdot y_i' + t_i + R_{56} \cdot \delta_i$
- $\sigma_{t_f} \approx R_{53} \cdot \sigma_{y_i}$ and $R_{53} \approx \alpha$ i.e. the bending angle of the dipole
- $R_{53} \cdot \sigma_{y_i}$ smears out density modulations

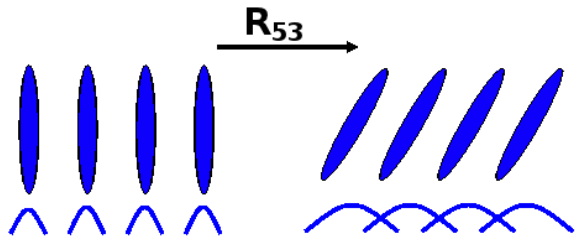

- Microbunches overlap and smear out
- Larger beam size $\rightarrow$ larger overlap
- Larger period $\rightarrow$ less overlap

Particle tracking simulation with initial density modulation

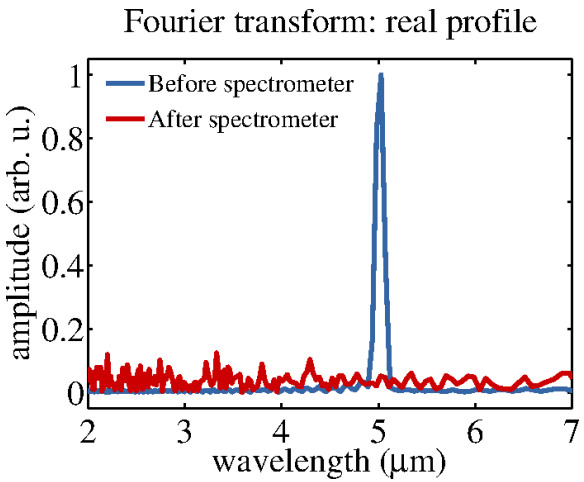

- $5\,\mu$m modulation in $(t, \delta)^{\mathrm{T}}$ before the spectrometer
- No modulation in $(t, \delta)^{\mathrm{T}}$ after the spectrometer

Mitigation of Coherent Optical Transition Radiation: Simulations

Time coordinate along the energy spectrometer

- Longitudinal position after the spectrometer: $t_f = R_{53} \cdot y_i + R_{54} \cdot y_i' + t_i + R_{56} \cdot \delta_i$
- $\sigma_{t_f} \approx R_{53} \cdot \sigma_{y_i}$ and $R_{53} \approx \alpha$ i.e. the bending angle of the dipole
- $R_{53} \cdot \sigma_{y_i}$ smears out density modulations

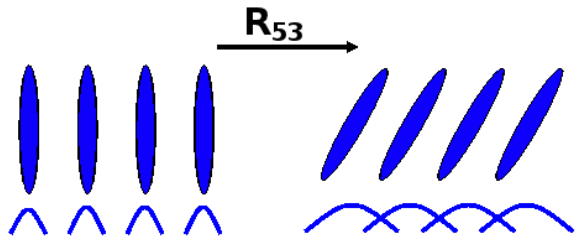

- Microbunches overlap and smear out
- Larger beam size $\rightarrow$ larger overlap
- Larger period $\rightarrow$ less overlap

Particle tracking simulation with initial density modulation

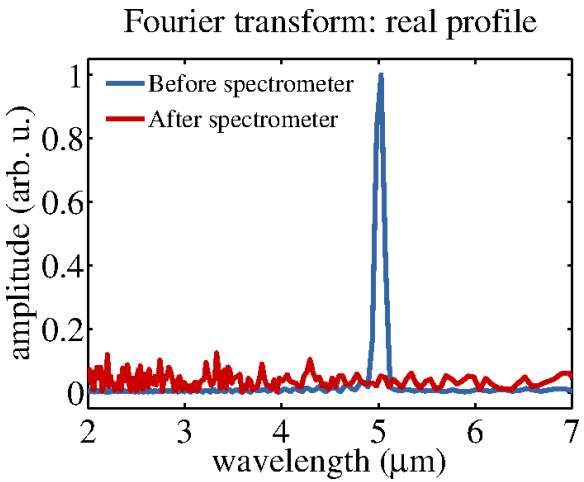

- $5\ \mu\mathrm{m}$ modulation in $(t, \delta)^{\mathrm{T}}$ before the spectrometer
- No modulation in $(t, \delta)^{\mathrm{T}}$ after the spectrometer
- ★ Wavelengths $\lambda_c \ll 2\pi R_{51}\sigma_x$ will be suppressed
- ★ Proposal: Strong COTR mitigation in an energy spectrometer $\Rightarrow$ emittance measurements

Longitudinal Phase Space Diagnostics at FERMI@Elettra

Courtesy of P. Craievich. For details: WEPA03.

Free Electron Laser for Multidisciplinary Investigations (FERMI)

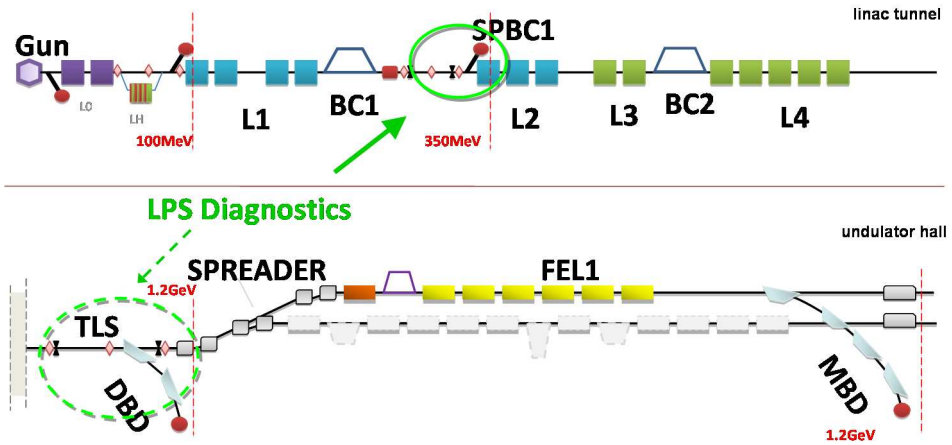

Longitudinal Phase Space Diagnostics at FERMI@Elettra

Courtesy of P. Craievich. For details: WEPA03.

Free Electron Laser for Multidisciplinary Investigations (FERMI)

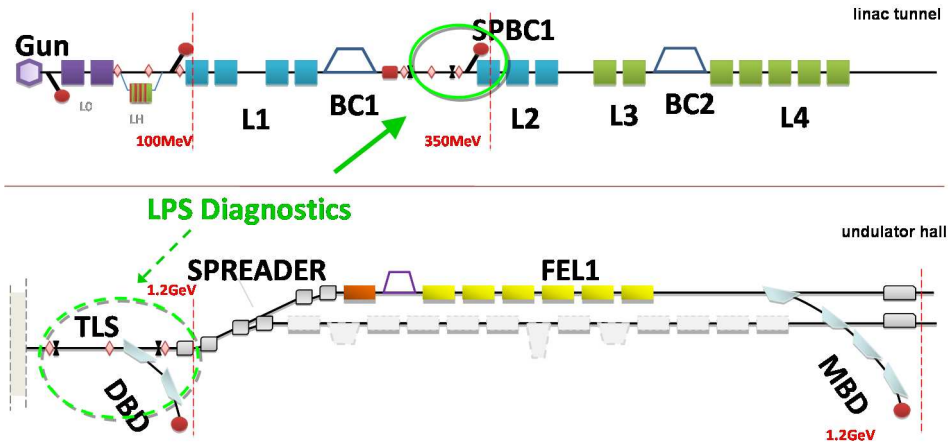

Longitudinal phase space diagnostics at FERMI@Elettra

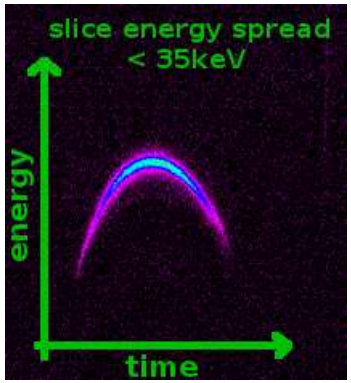

- LPS data in SPBC1 at low energy

Longitudinal Phase Space Diagnostics at FERMI@Elettra

Courtesy of P. Craievich. For details: WEPA03.

Free Electron Laser for Multidisciplinary Investigations (FERMI)

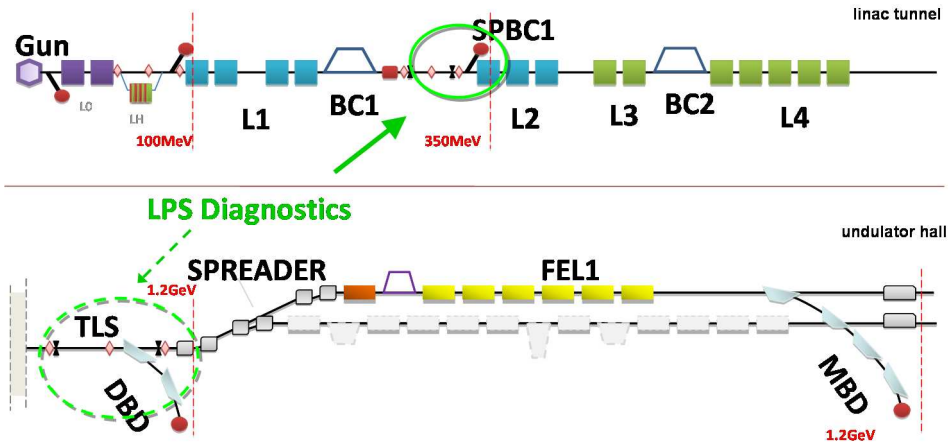

Longitudinal phase space diagnostics at FERMI@Elettra

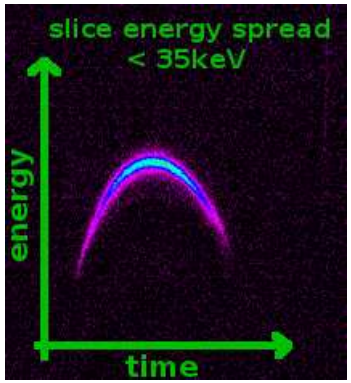

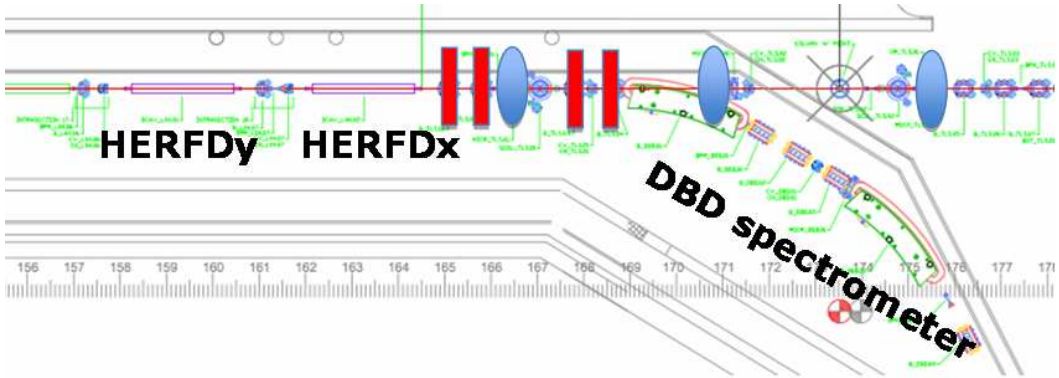

- LPS data in SPBC1 at low energy
- High energy TDS (both planes) will be installed soon

Longitudinal Phase Space Diagnostics at SACLA/SPring-8

Courtesy of Y. Otake.

SPring-8 Angstrom Compact Free-Electron Laser (SACLA)

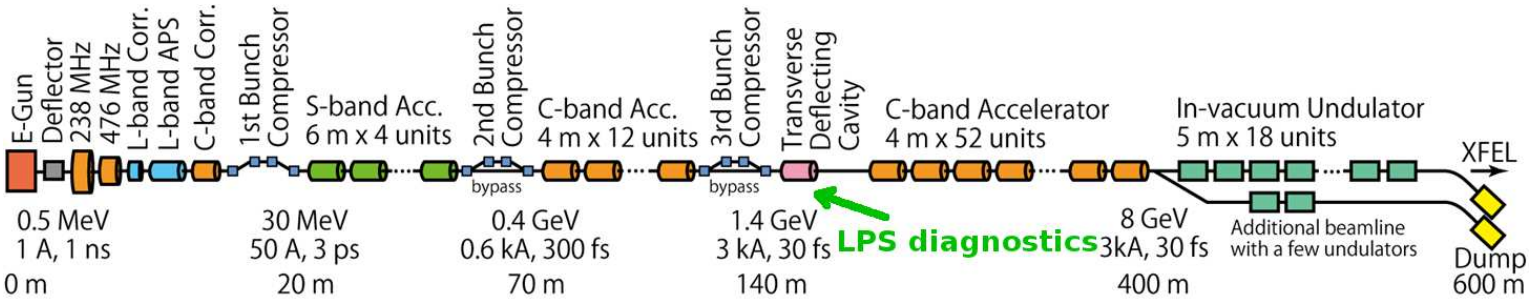

Longitudinal Phase Space Diagnostics at SACLA/SPring-8

Courtesy of Y. Otake.

SPring-8 Angstrom Compact Free-Electron Laser (SACLA)

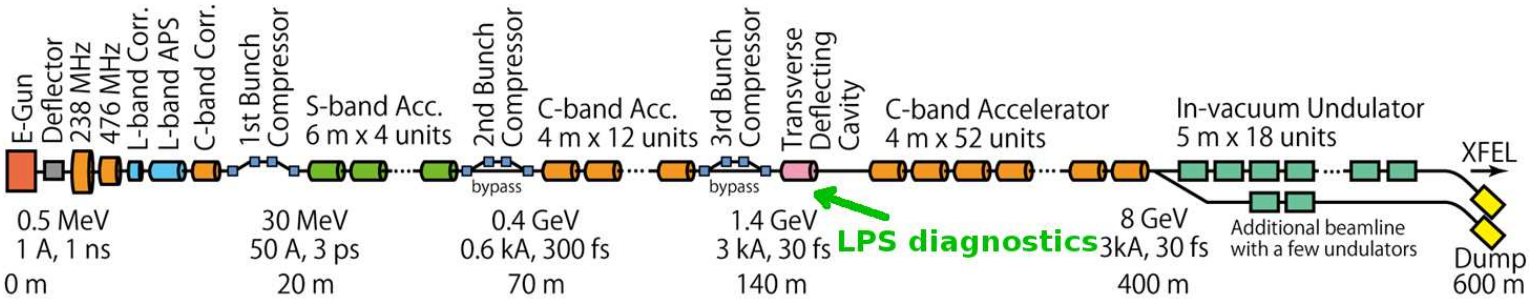

Longitudinal phase space diagnostics at SACLA

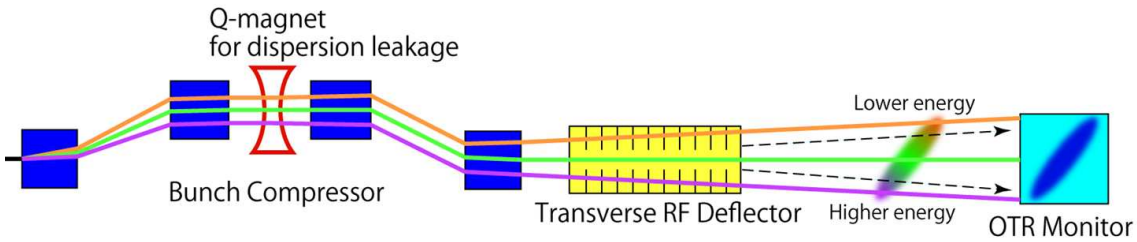

- Quadrupole kicks in a dispersive section
- Residual dispersion after the bunch compressor

Longitudinal Phase Space Diagnostics at SACLA/SPring-8

Courtesy of Y. Otake.

SPring-8 Angstrom Compact Free-Electron Laser (SACLA)

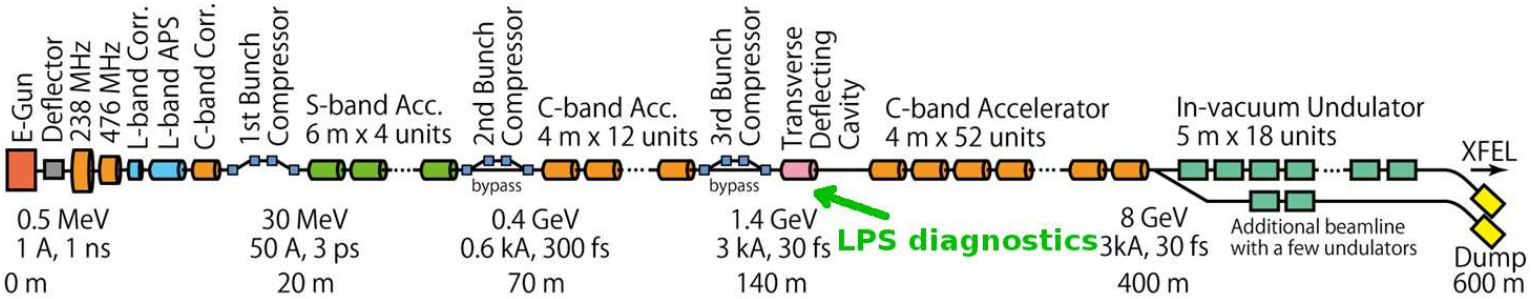

Longitudinal phase space diagnostics at SACLA

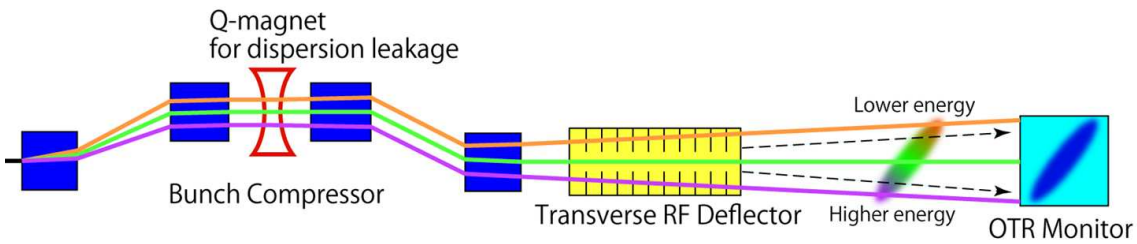

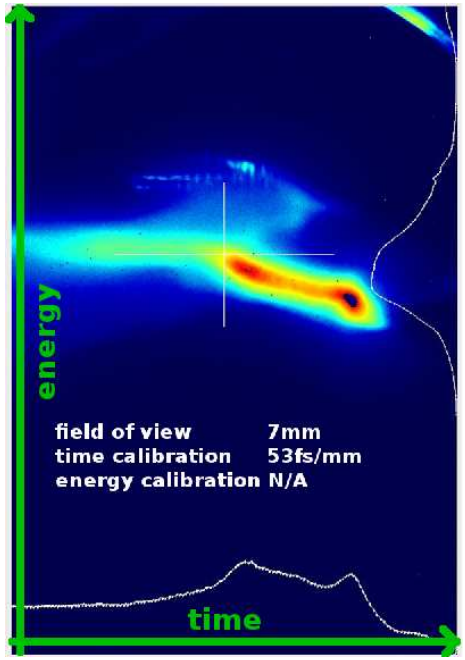

- Quadrupole kicks in a dispersive section
- Residual dispersion after the bunch compressor
- Still in commissioning phase
- Preliminary longitudinal phase space measurement ▶

Longitudinal Phase Space Diagnostics at LCLS/SLAC

Courtesy of Y. Ding, P. Emma, and H. Loos.

The Linac Coherent Light Source (LCLS)

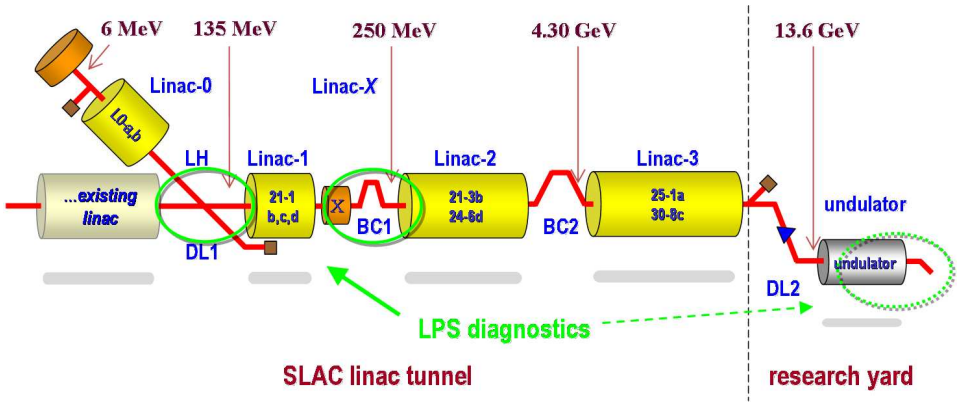

Longitudinal Phase Space Diagnostics at LCLS/SLAC

Courtesy of Y. Ding, P. Emma, and H. Loos.

The Linac Coherent Light Source (LCLS)

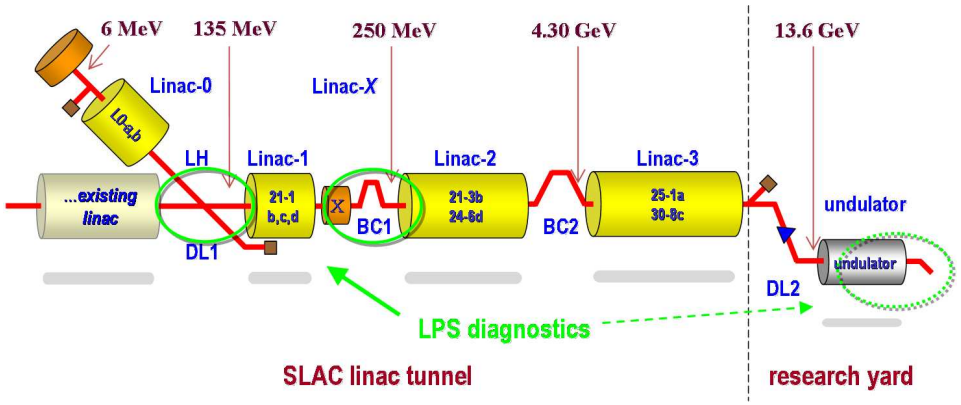

Longitudinal phase space diagnostics at LCLS

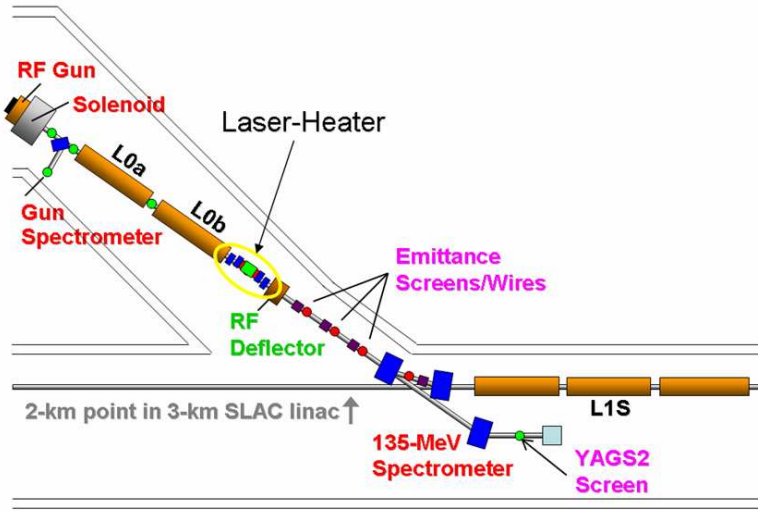

- Longitudinal phase space diagnostics
- Longitudinal phase space manipulation
  - Laser heater

Longitudinal Phase Space Diagnostics at LCLS/SLAC

Courtesy of Y. Ding, P. Emma, and H. Loos.

The Linac Coherent Light Source (LCLS)

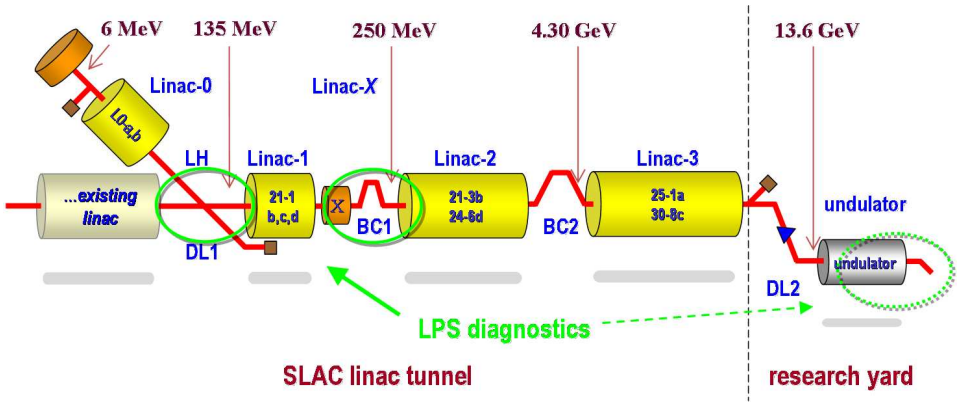

Longitudinal phase space diagnostics at LCLS

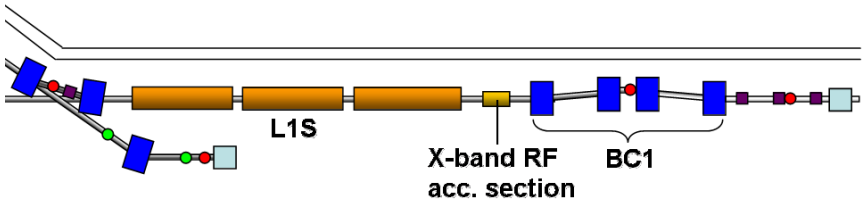

- Longitudinal phase space diagnostics
- Longitudinal phase space manipulation
  - Laser heater
- Longitudinal phase space linearization
  - X-band RF linearizer

Longitudinal Phase Space Diagnostics at LCLS/SLAC

Courtesy of Y. Ding, P. Emma, and H. Loos.

The Linac Coherent Light Source (LCLS)

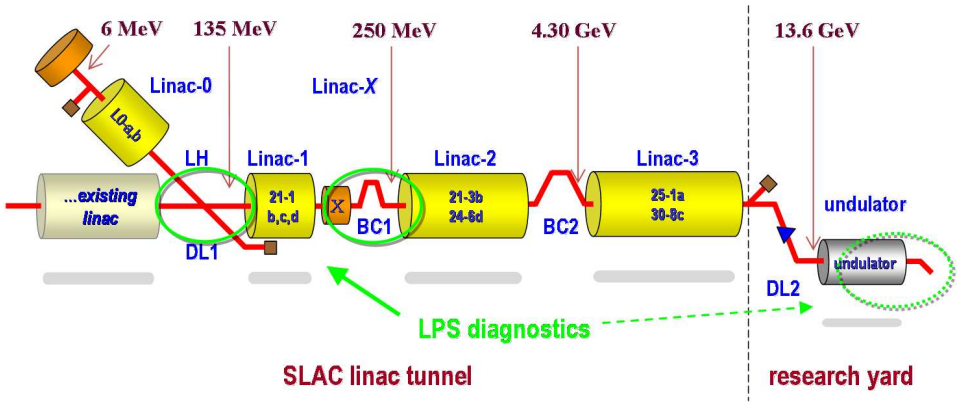

Longitudinal phase space diagnostics at LCLS

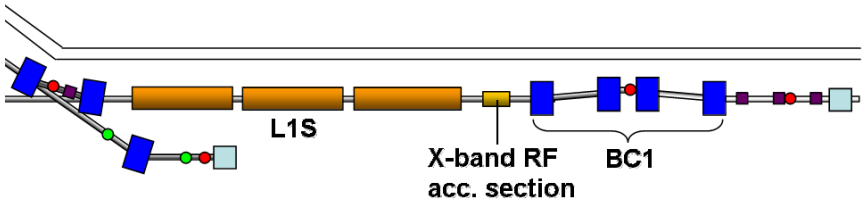

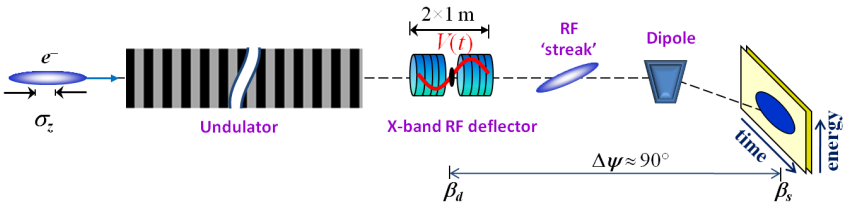

- Longitudinal phase space diagnostics
- Longitudinal phase space manipulation
  - Laser heater
- Longitudinal phase space linearization
  - X-band RF linearizer
- In preparation
  - X-band TDS after the undulators (project started this July)

Longitudinal Phase Space Diagnostics at FLASH/DESY

The Free-Electron Laser in Hamburg (FLASH)

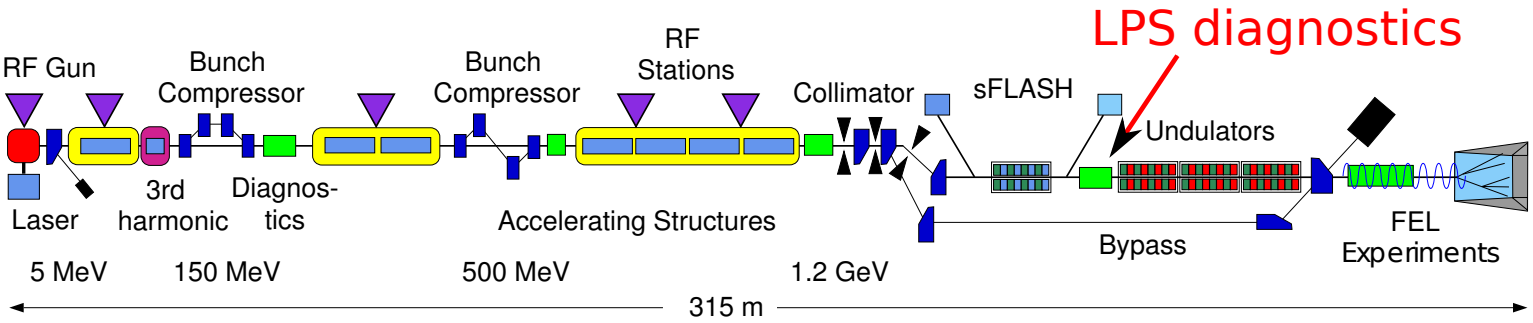

Longitudinal Phase Space Diagnostics at FLASH/DESY

The Free-Electron Laser in Hamburg (FLASH)

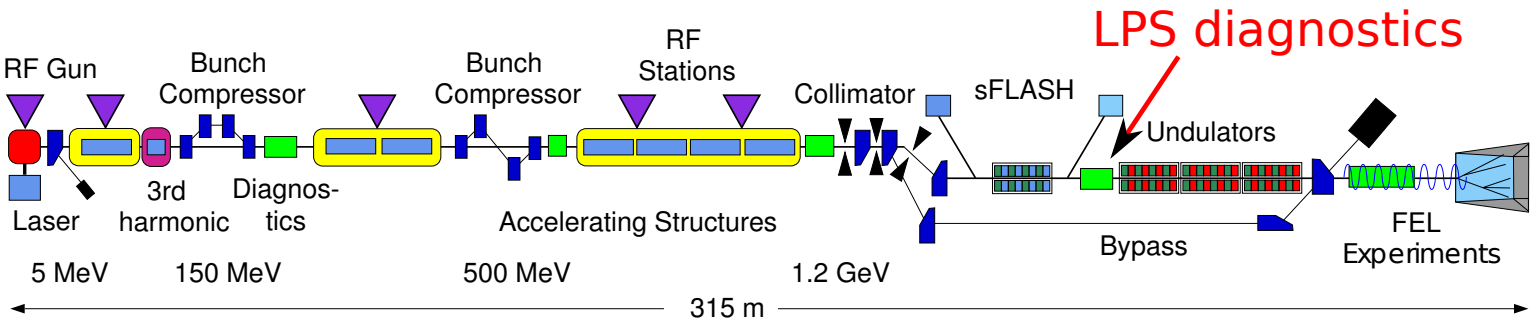

Longitudinal phase space diagnostics at FLASH

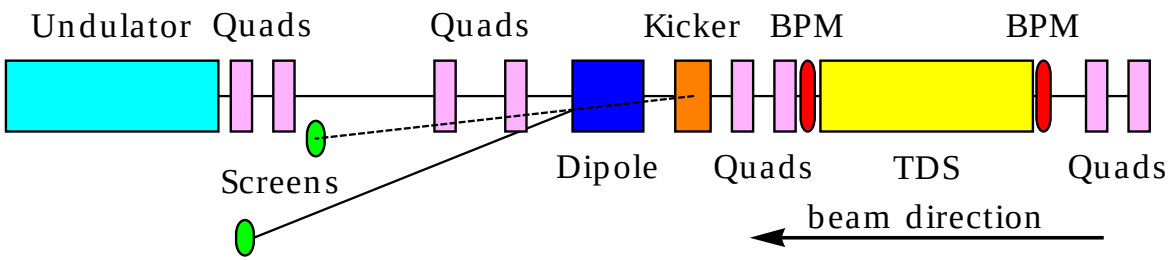

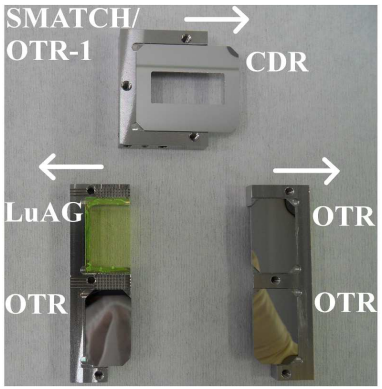

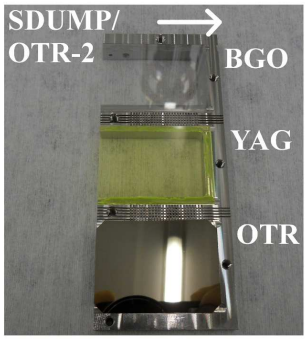

- Longitudinal phase space diagnostics in front of the undulators

Longitudinal Phase Space Diagnostics at FLASH/DESY

The Free-Electron Laser in Hamburg (FLASH)

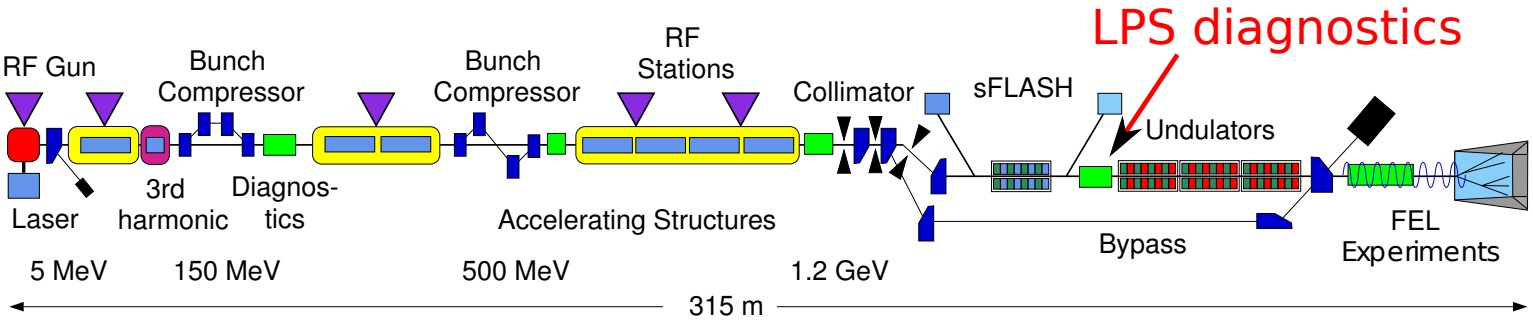

Longitudinal phase space diagnostics at FLASH

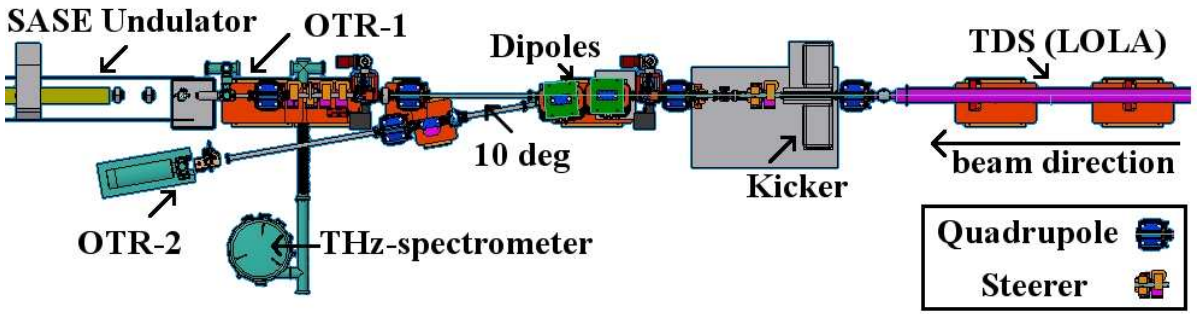

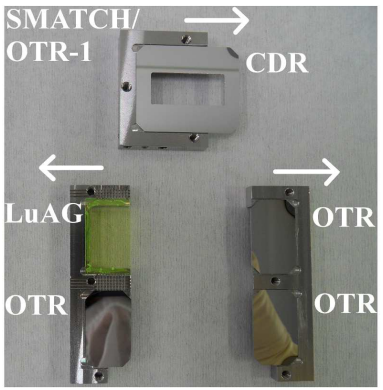

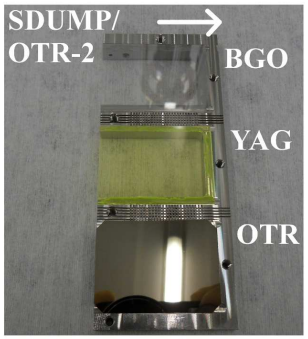

- Longitudinal phase space diagnostics in front of the undulators

Longitudinal Phase Space Diagnostics at FLASH/DESY

The Free-Electron Laser in Hamburg (FLASH)

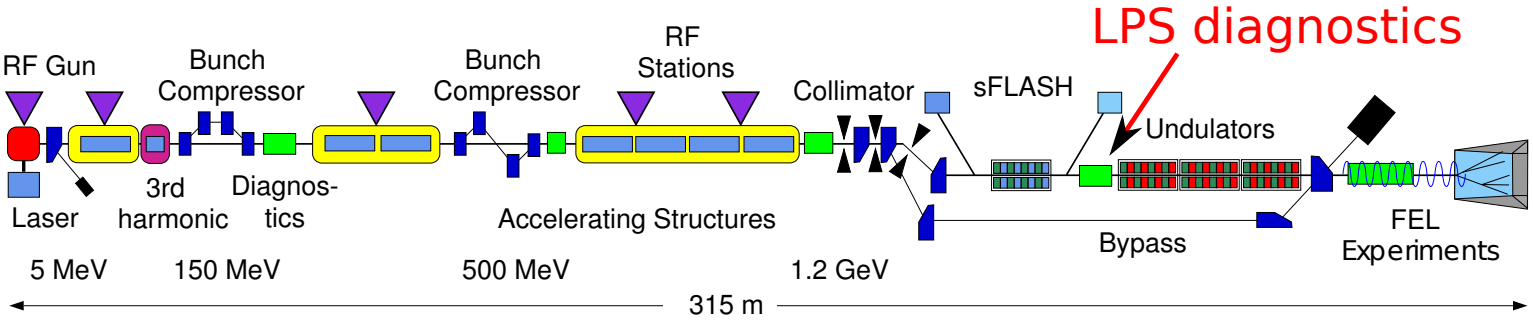

Longitudinal phase space diagnostics at FLASH

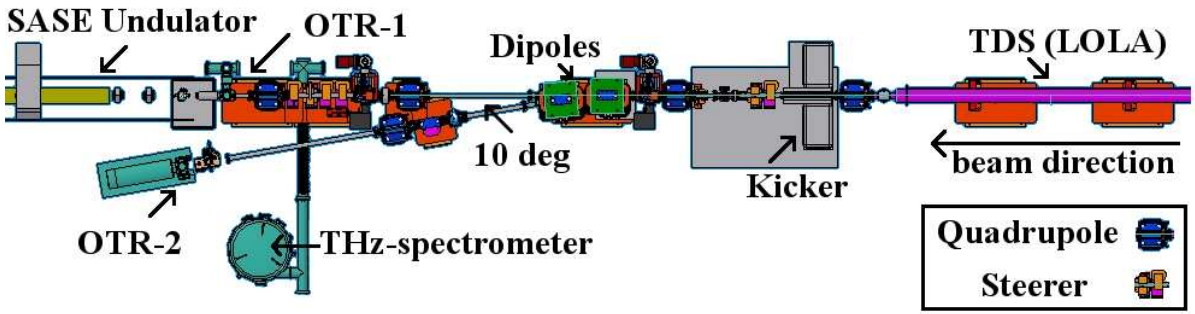

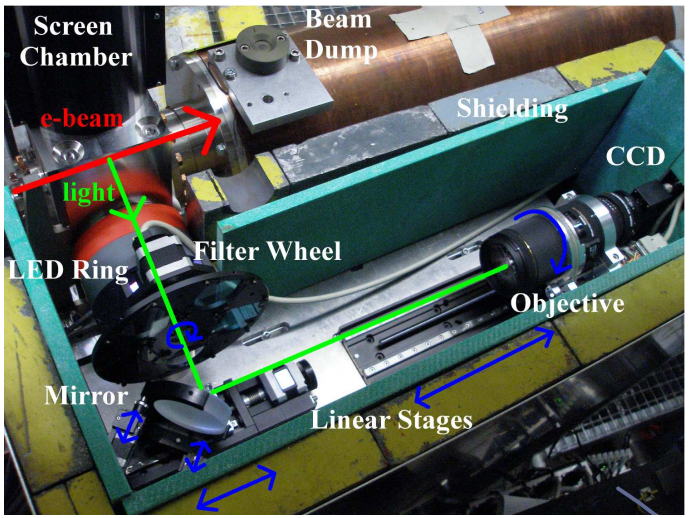

- Longitudinal phase space diagnostics in front of the undulators
- Indispensable for beam dynamics studies in general

Longitudinal Phase Space Diagnostics at FLASH/DESY

The Free-Electron Laser in Hamburg (FLASH)

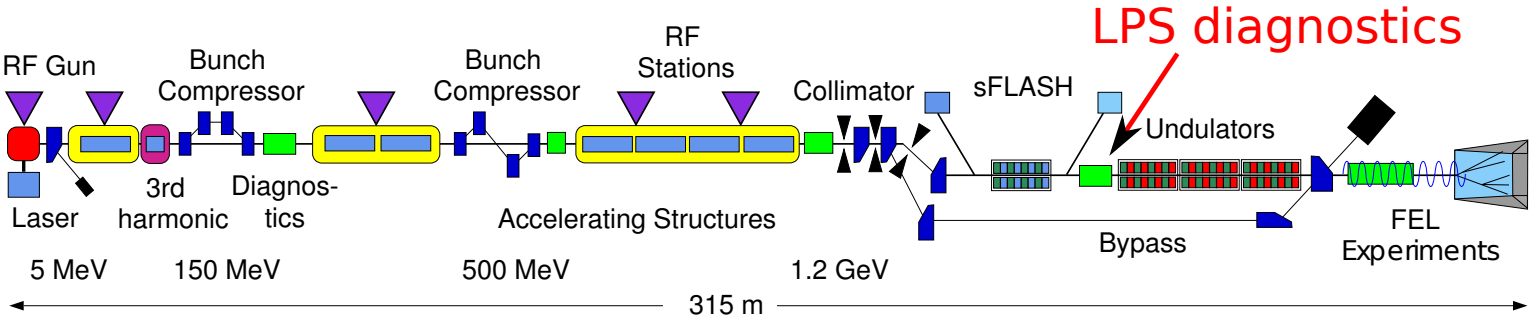

Longitudinal phase space diagnostics at FLASH

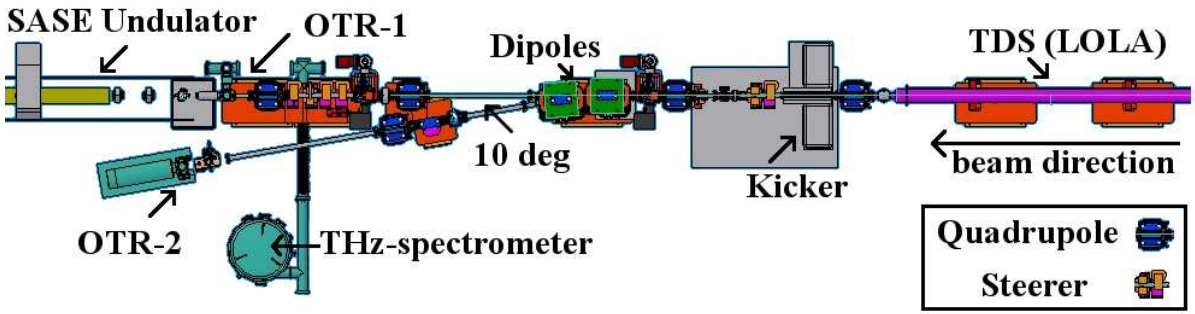

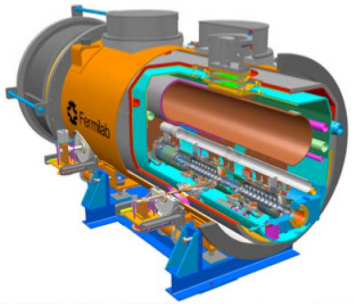

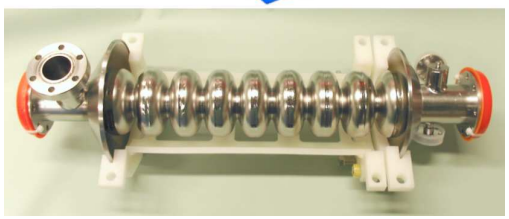

- Longitudinal phase space diagnostics in front of the undulators
- Indispensable for beam dynamics studies in general
- Longitudinal phase space linearizations with third-harmonic RF linearizer (3.9 GHz)

Longitudinal Phase Space Diagnostics at E-XFEL/DESY

European X-Ray Free Electron Laser (E-XFEL)

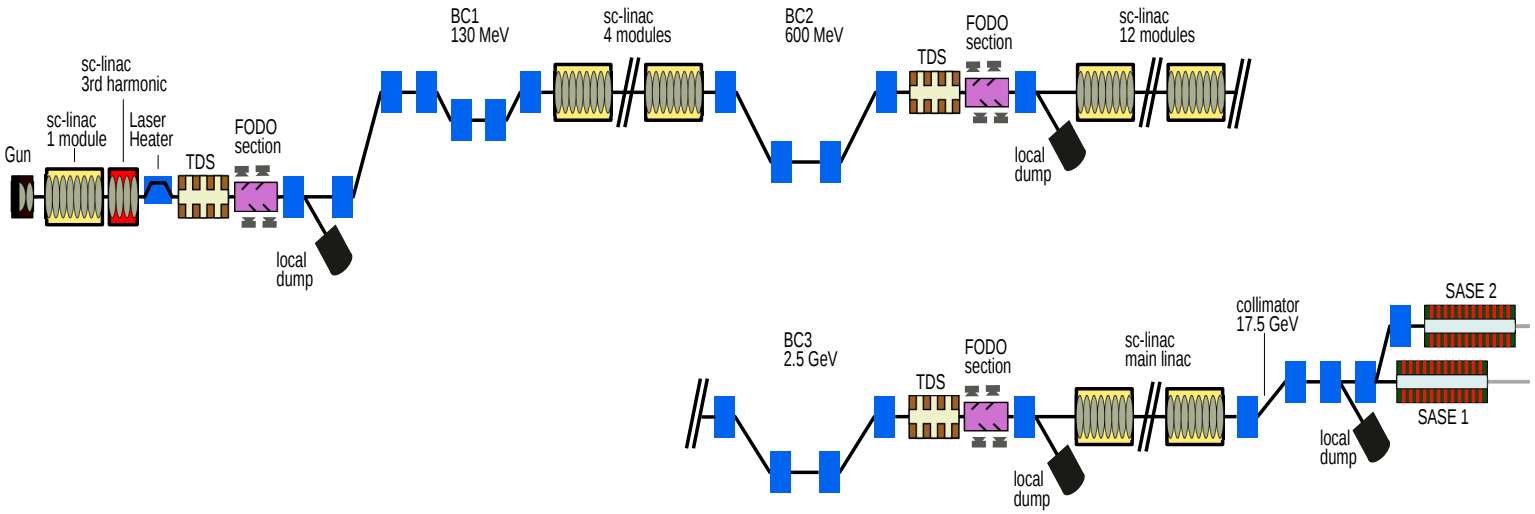

Longitudinal Phase Space Diagnostics at E-XFEL/DESY

European X-Ray Free Electron Laser (E-XFEL)

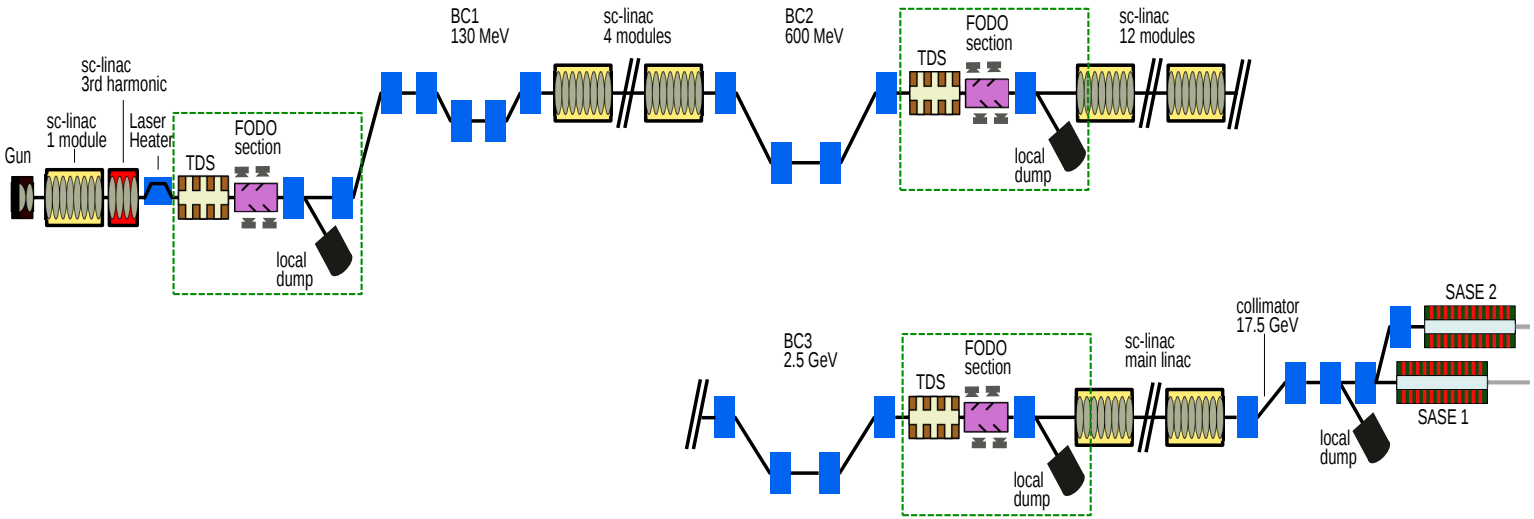

Longitudinal phase space diagnostics at E-XFEL

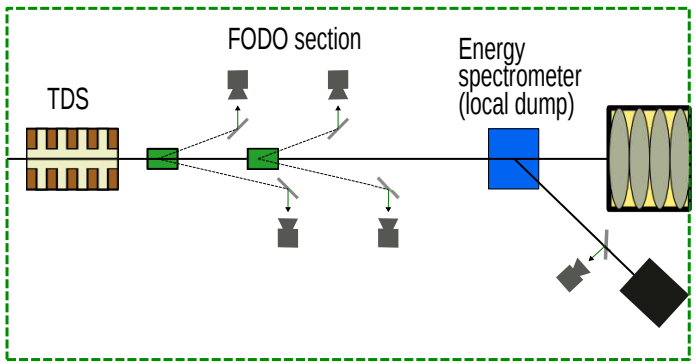

- Three setups for longitudinal phase space measurements (including slice emittance)
- Higher-harmonic RF linearizer and a laser heater
- Proposal: Apply longitudinal phase space diagnostics on individuals bunches of the train (septum magnet)

Longitudinal Phase Space Linearization at LCLS/SLAC

For details: TUOCAB02 by P. Emma *et al.* in the Proceedings of PAC'07

Linearization of the longitudinal phase space using an X-band RF linearizer

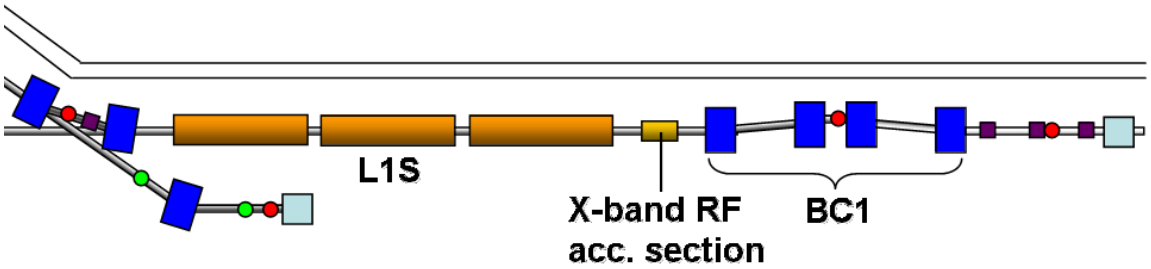

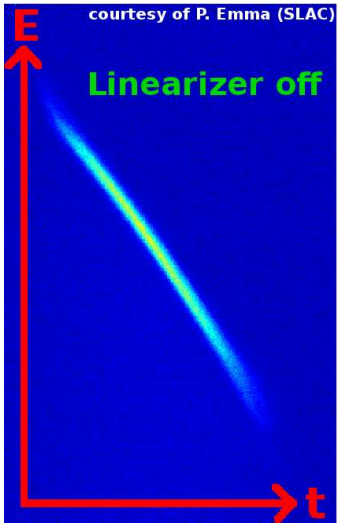

Measurements

- Longitudinal phase space (off-crest): X-band linearizer switched off

Longitudinal Phase Space Linearization at LCLS/SLAC

For details: TUOCAB02 by P. Emma *et al.* in the Proceedings of PAC'07

Linearization of the longitudinal phase space using an X-band RF linearizer

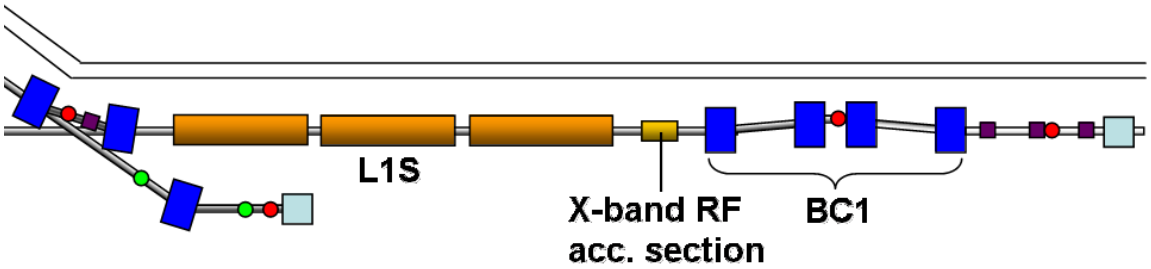

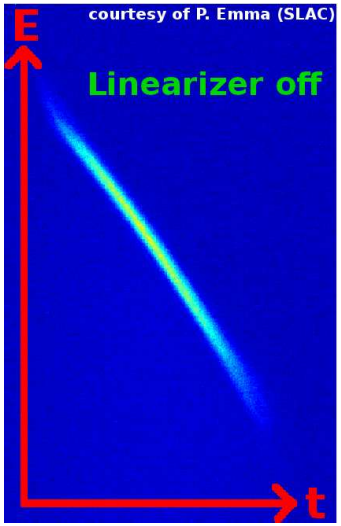

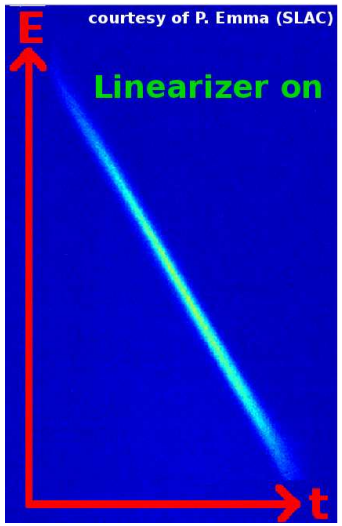

Measurements

- Longitudinal phase space (off-crest): X-band linearizer switched off
- Longitudinal phase space (off-crest): X-band linearizer switched on

Longitudinal Phase Space Linearization at LCLS/SLAC

For details: TUOCAB02 by P. Emma *et al.* in the Proceedings of PAC'07

Linearization of the longitudinal phase space using an X-band RF linearizer

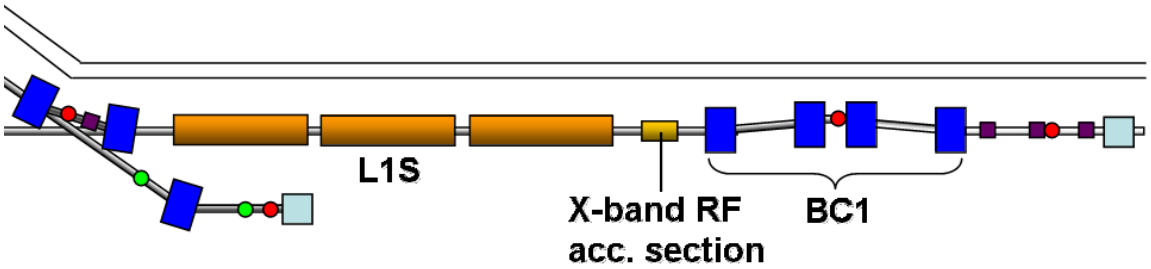

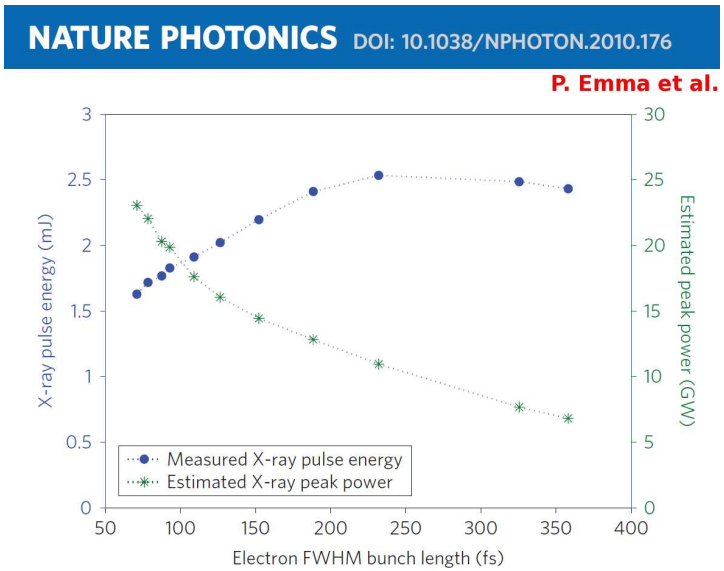

Measurements

- Longitudinal phase space (off-crest): X-band linearizer switched off
- Longitudinal phase space (off-crest): X-band linearizer switched on
- Control of the bunch lengths allows control of the FEL photon pulse durations (still a hot topic)

Longitudinal Phase Space Linearization at FLASH/DESY

Measurement of the longitudinal phase space: third-harmonic RF linearizer off

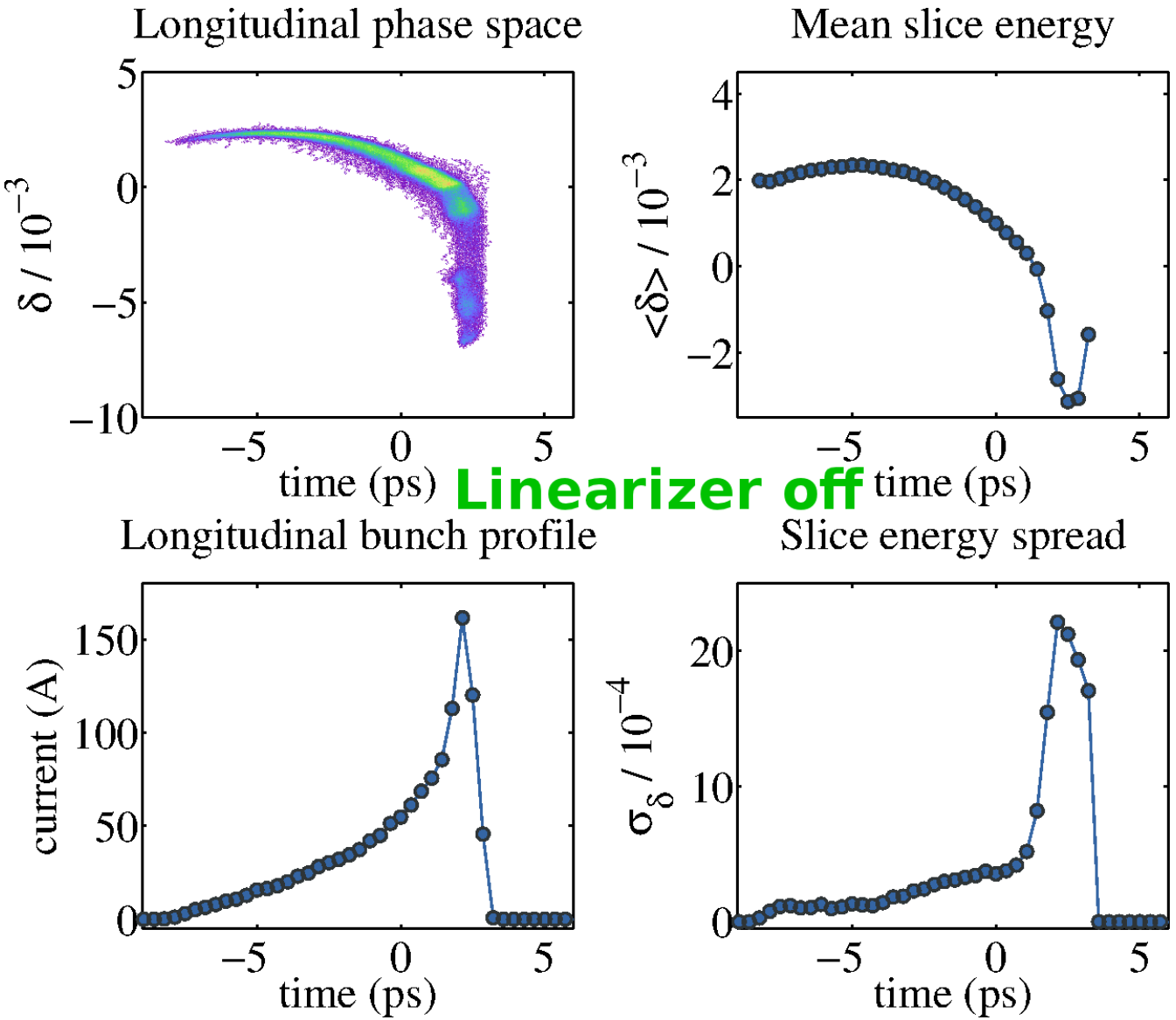

Longitudinal Phase Space Linearization at FLASH/DESY

Measurement of the longitudinal phase space: third-harmonic RF linearizer on

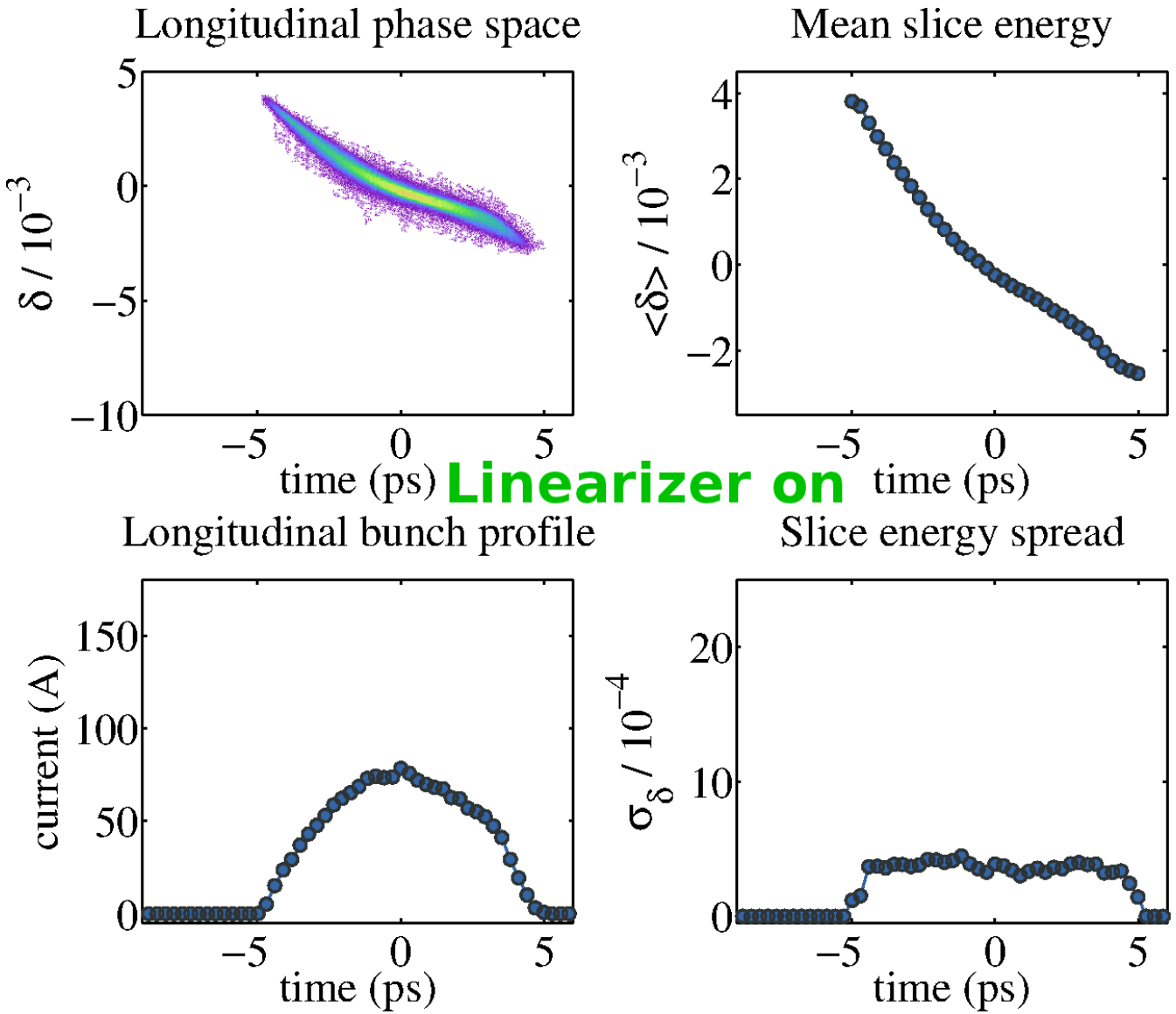

Longitudinal Phase Space Linearization at FLASH/DESY

Comparison: third-harmonic RF linearizer on/off

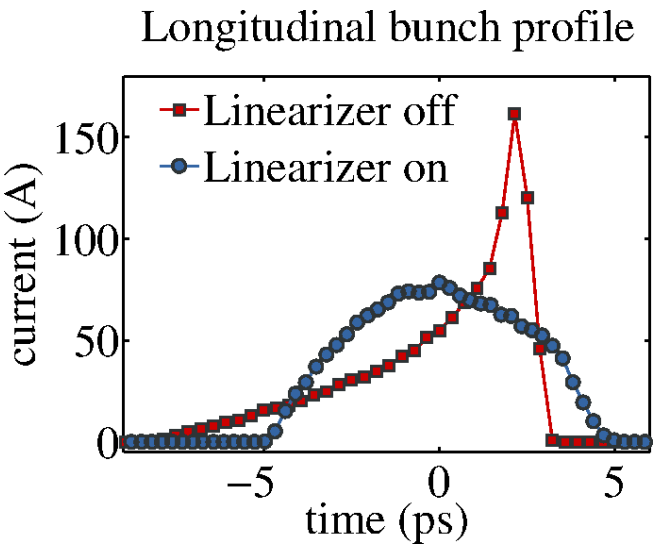

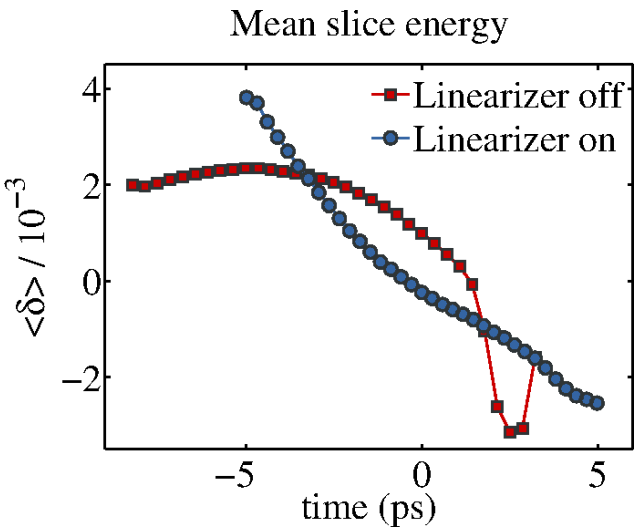

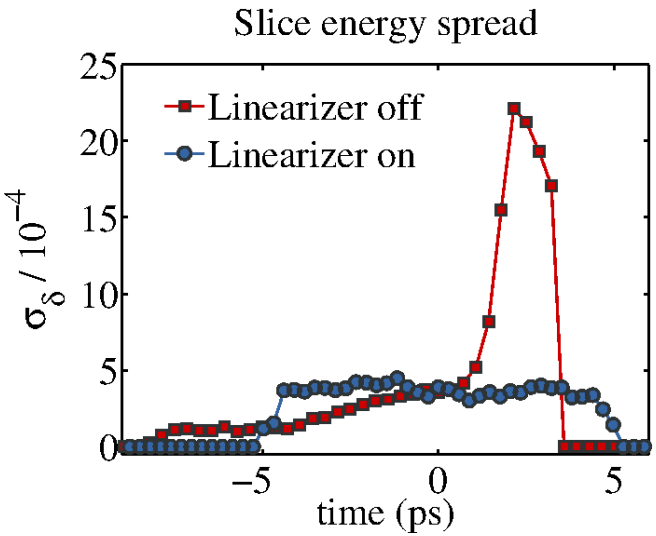

- Compression in a magnetic bunch compressor:
  $C^{-1} = (1 + h_1 R_{56}) + (h_2 R_{56} + 2h_1^2 T_{566}) t_i$
  - h_1,h_2: first and second order energy chirp
  - R_{56}, T_{566}: first and second oder longitudinal dispersion
- Eliminate time-dependency of C^{-1} by using a proper $h_2 \Rightarrow$ higher-harmonic RF system (dual-frequency)

Linear Compression using Dual-Frequency Linacs at FLASH/DESY

Measurements on linear bunch compression using only one bunch compressor

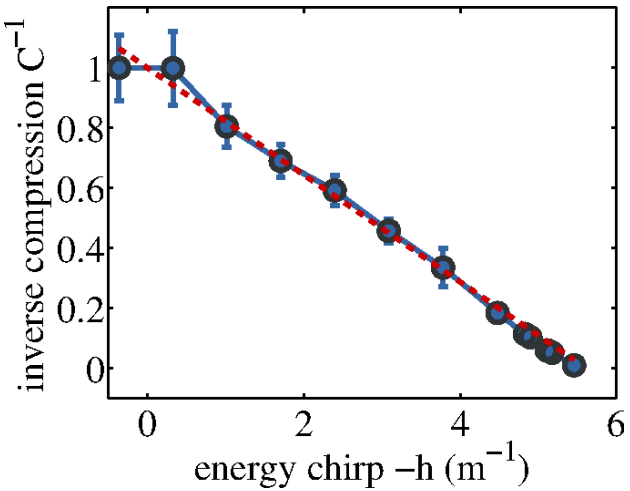

Linear Compression using Dual-Frequency Linacs at FLASH/DESY

Measurements on linear bunch compression using only one bunch compressor

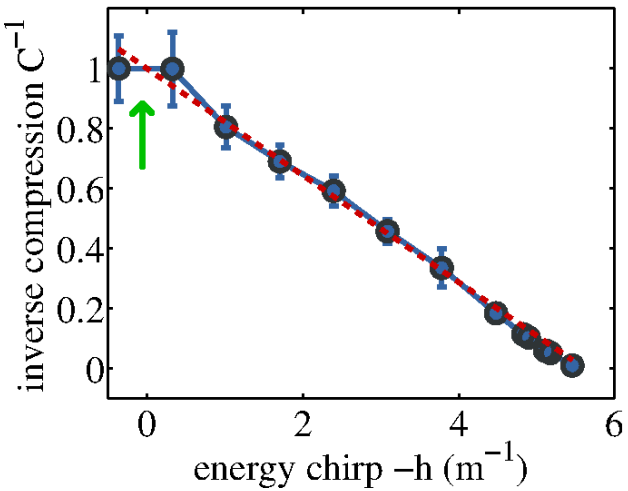

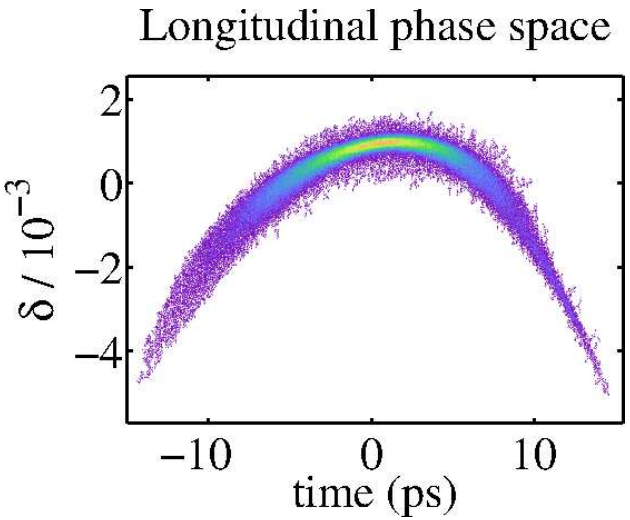

- Start with uncompressed bunches $(C^{-1} = 1)$

Linear Compression using Dual-Frequency Linacs at FLASH/DESY

Measurements on linear bunch compression using only one bunch compressor

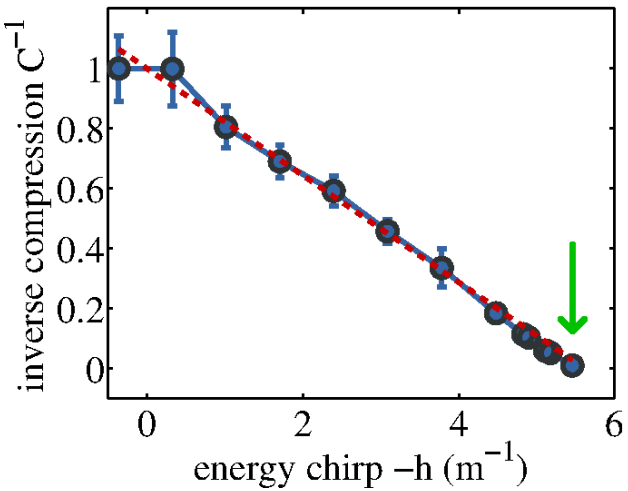

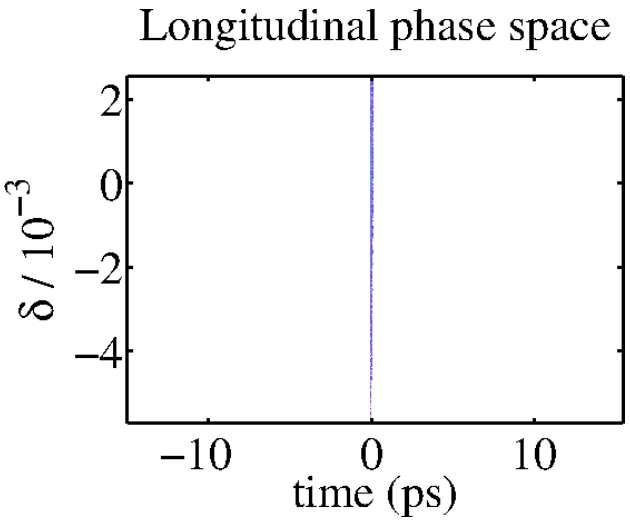

- Start with uncompressed bunches $(C^{-1} = 1)$
- End with compressed bunches $(C^{-1} \to 0)$

Linear Compression using Dual-Frequency Linacs at FLASH/DESY

Measurements on linear bunch compression using only one bunch compressor

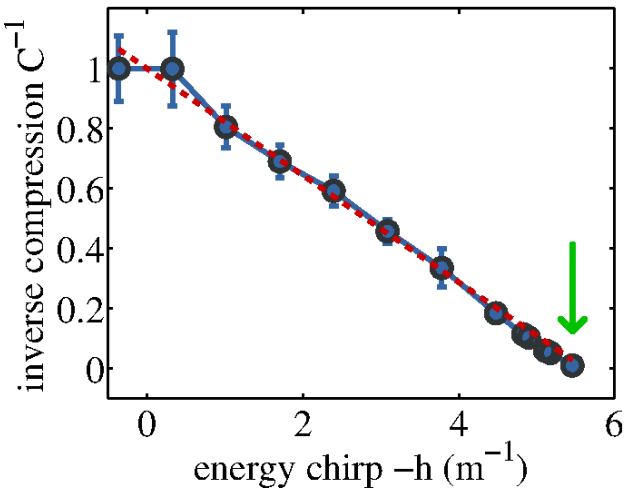

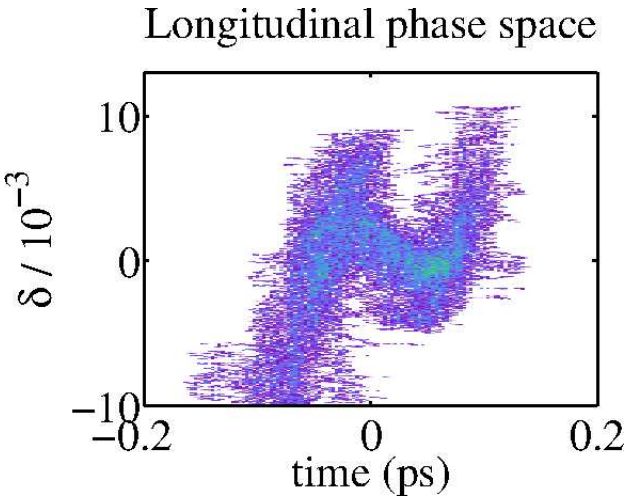

- Start with uncompressed bunches $(C^{-1} = 1)$
- End with compressed bunches $(C^{-1} \to 0)$

Linear Compression using Dual-Frequency Linacs at FLASH/DESY

Measurements on linear bunch compression using only one bunch compressor

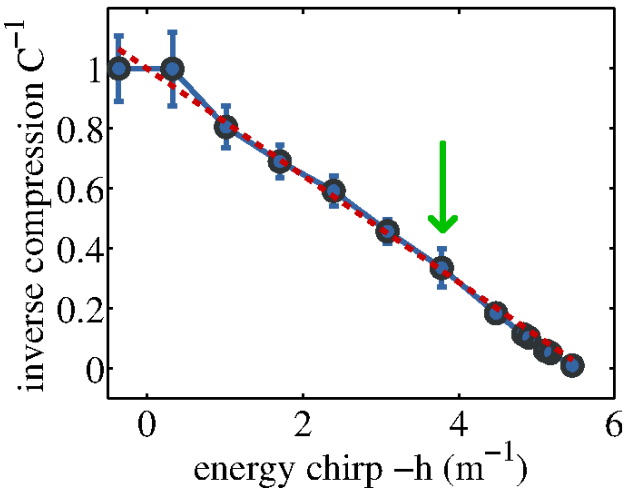

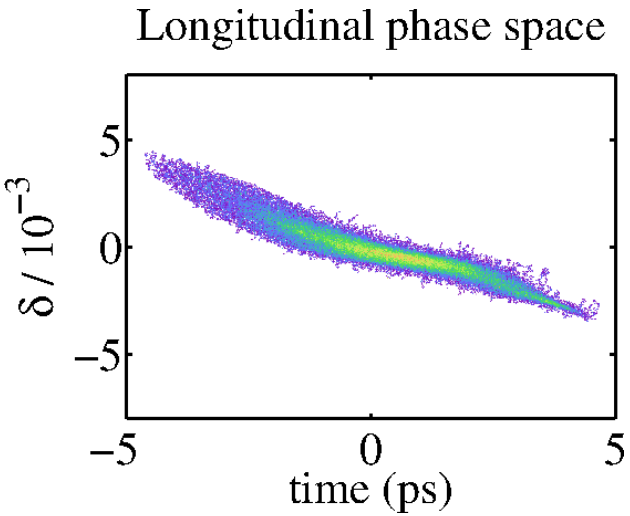

- Start with uncompressed bunches $(C^{-1} = 1)$
- End with compressed bunches $(C^{-1} \to 0)$

Linear Compression using Dual-Frequency Linacs at FLASH/DESY

Measurements on linear bunch compression using only one bunch compressor

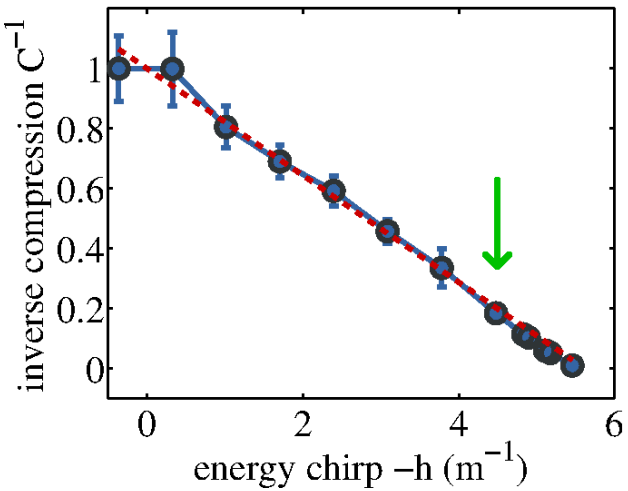

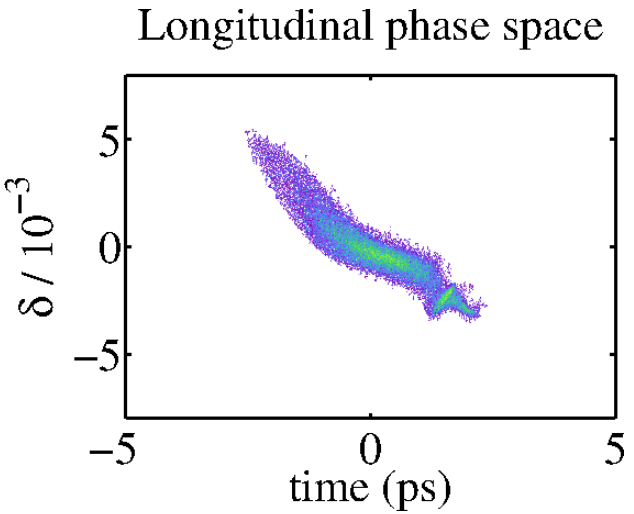

- Start with uncompressed bunches $(C^{-1} = 1)$
- End with compressed bunches $(C^{-1} \to 0)$

Linear Compression using Dual-Frequency Linacs at FLASH/DESY

Measurements on linear bunch compression using only one bunch compressor

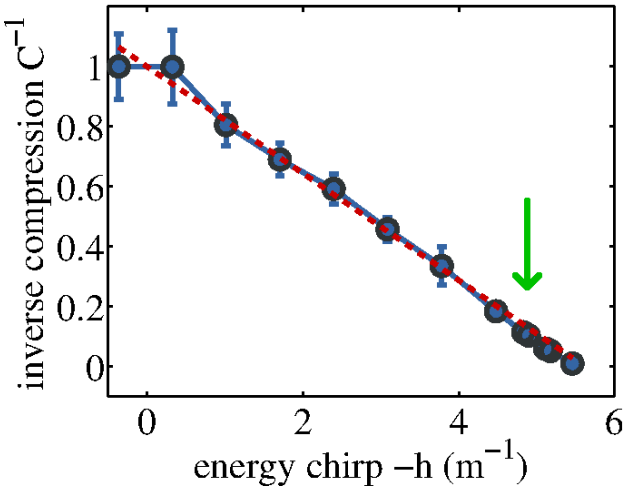

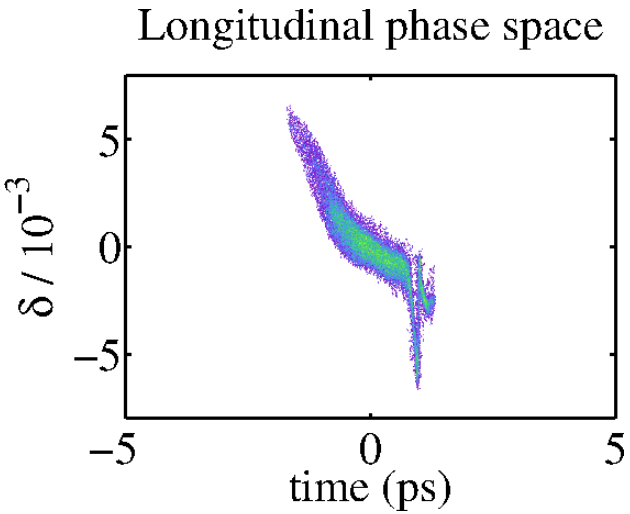

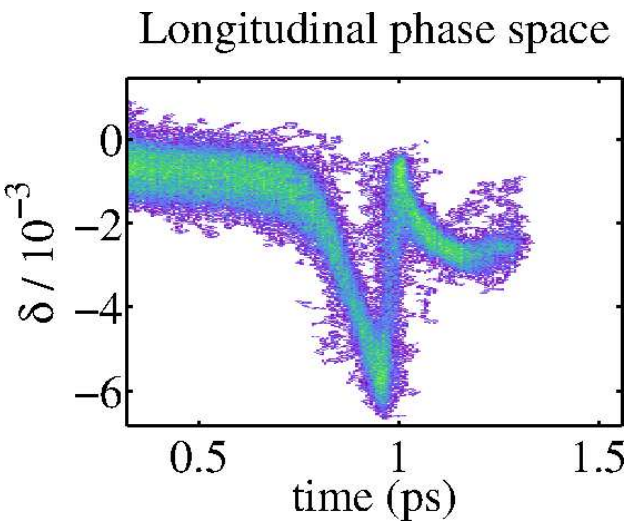

- Start with uncompressed bunches $(C^{-1} = 1)$
- End with compressed bunches $(C^{-1} \to 0)$
- ★ Strong local compression due to collective effects (not fully understood yet)

FEL Operation with Non-linear/Linear Compression at FLASH/DESY

The old non-linear compression mode

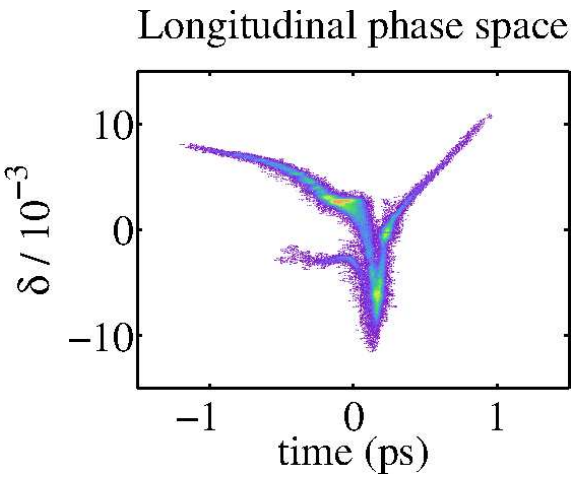

★ Non-linear compression: sharp leading spike (small charge fraction) with a long trailing tail

FEL Operation with Non-linear/Linear Compression at FLASH/DESY

FEL operation with new linear compression mode

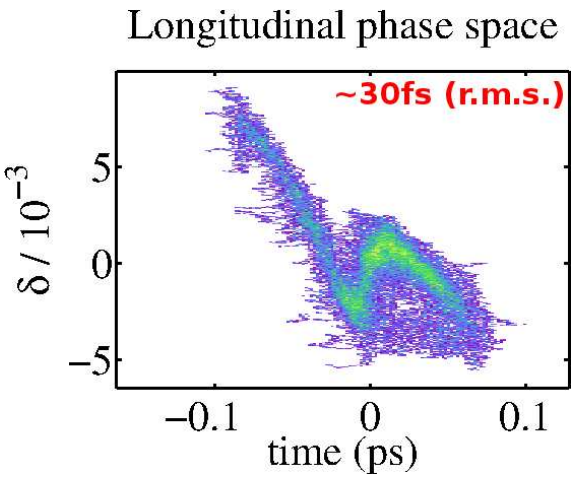

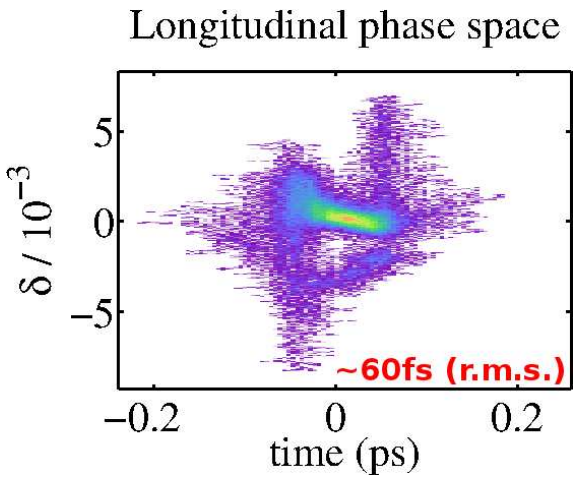

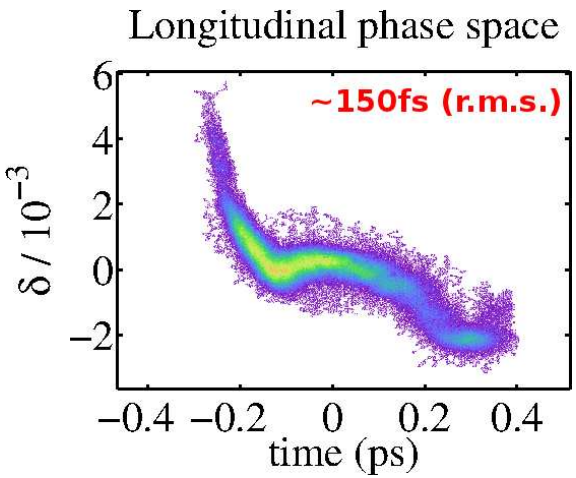

- ★ Non-linear compression: sharp leading spike (small charge fraction) with a long trailing tail
- ★ Linear compression: flexible bunch lengths and shapes (more regular but still complex)
- ★ Linear compression: more FEL pulse energies (at least $4\times$)

FEL Operation with Non-linear/Linear Compression at FLASH/DESY

FEL operation with new linear compression mode

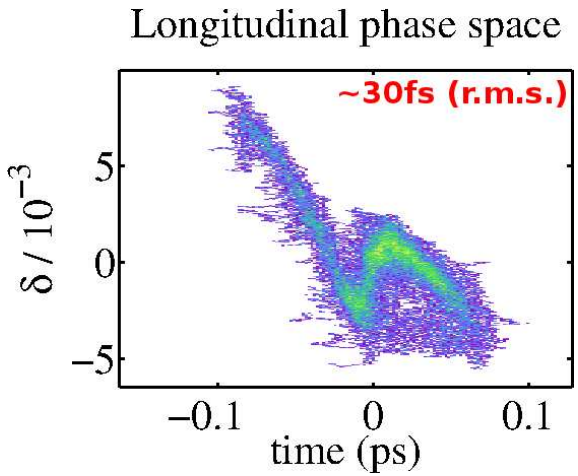

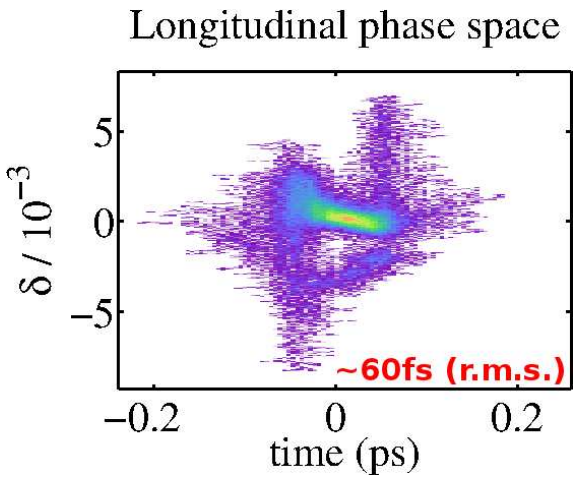

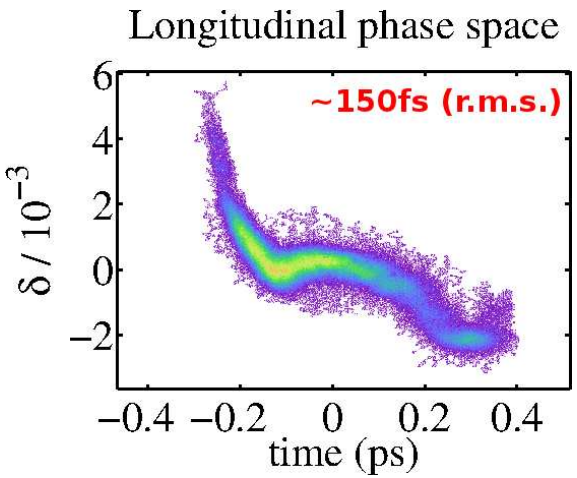

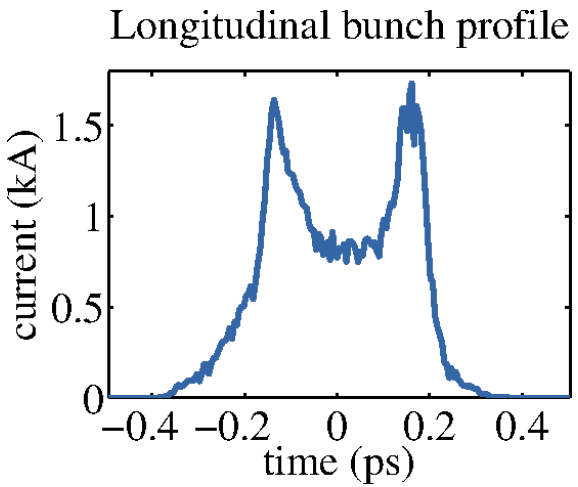

- ★ Non-linear compression: sharp leading spike (small charge fraction) with a long trailing tail
- ★ Linear compression: flexible bunch lengths and shapes (more regular but still complex)
- ★ Linear compression: more FEL pulse energies (at least $4\times$)
- Appearance of double-horns like at LCLS

FEL Operation with Non-linear/Linear Compression at FLASH/DESY

FEL operation with new linear compression mode

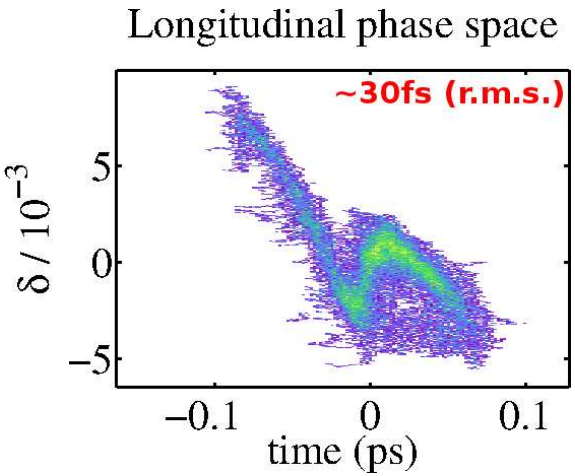

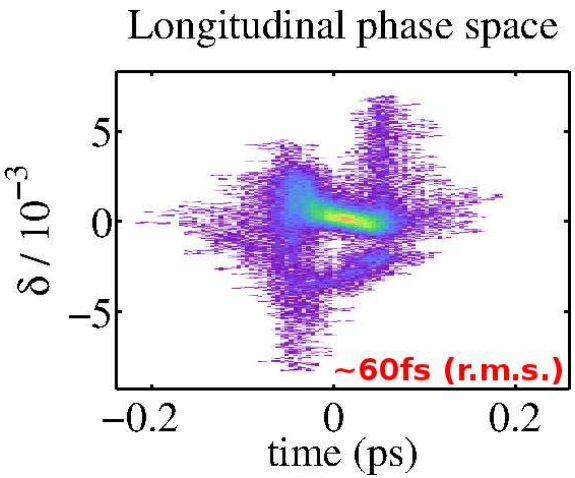

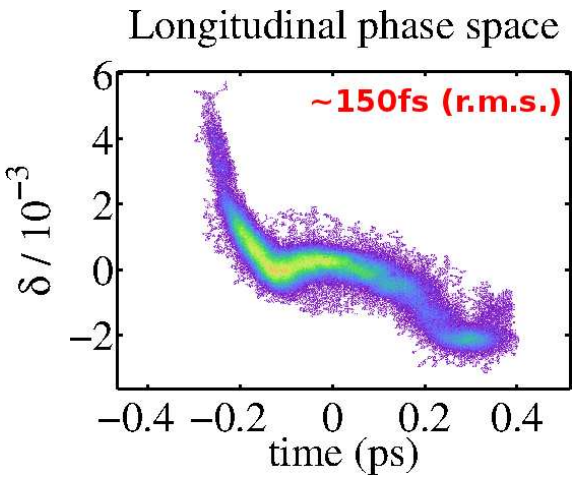

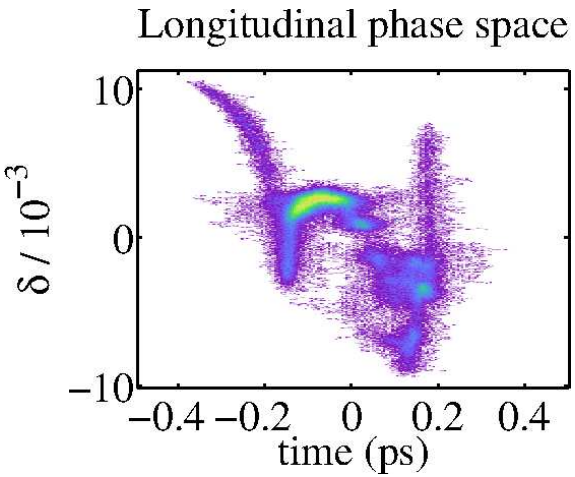

- ★ Non-linear compression: sharp leading spike (small charge fraction) with a long trailing tail
- ★ Linear compression: flexible bunch lengths and shapes (more regular but still complex)
- ★ Linear compression: more FEL pulse energies (at least $4\times$)
- ● Appearance of double-horns like at LCLS
- ★ Double-horns show some fragmentation

Tailoring the Longitudinal Phase Space for Wakefield Experiments

For details: P. Piot *et al.*, Fermilab preprint PUB-11-339-APC (2011)

Beam-driven acceleration with drive and witness bunch

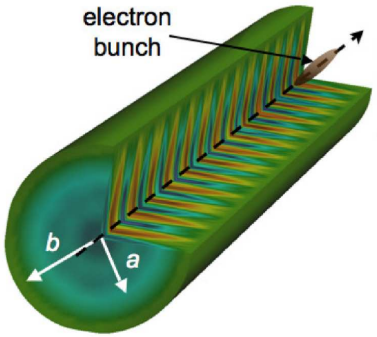

- Wakefield acceleration in dielectric structures using drive and witness bunches
- Transformer ratio $R = \frac{E_+}{E_-}$ is limited to ≤ 2 for symmetric current profiles

Tailoring the Longitudinal Phase Space for Wakefield Experiments

For details: P. Piot *et al.*, Fermilab preprint PUB-11-339-APC (2011)

Beam-driven acceleration with drive and witness bunch

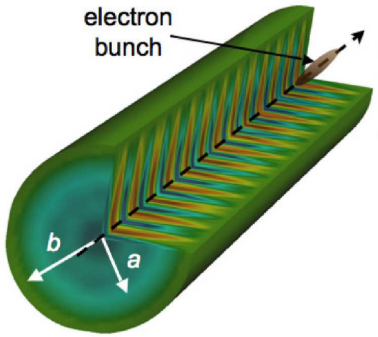

- Wakefield acceleration in dielectric structures using drive and witness bunches
- Transformer ratio $R = \frac{E_+}{E_-}$ is limited to ≤ 2 for symmetric current profiles
- Enhancement of the R by linearly ramped current profiles

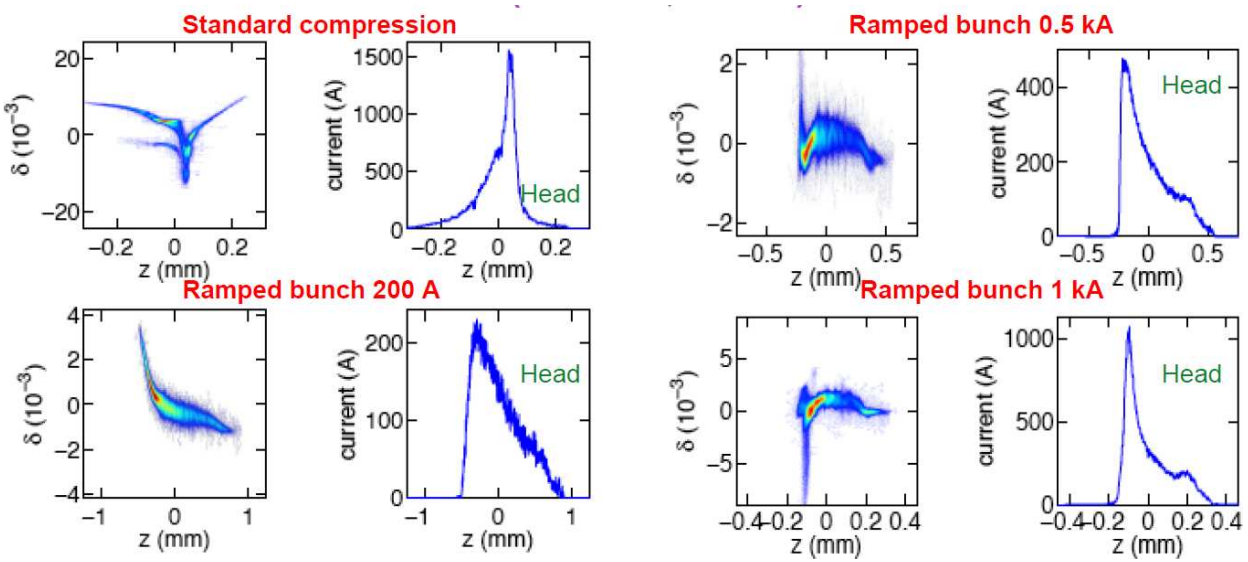

★ Linearly ramped current profiles (from experiment) enables (from simulations) $R > 6$

Observations of Microbunching Instabilities in Time-domain

Linearly chirped bunches with intensity modulations at FLASH/DESY and LCLS/SLAC

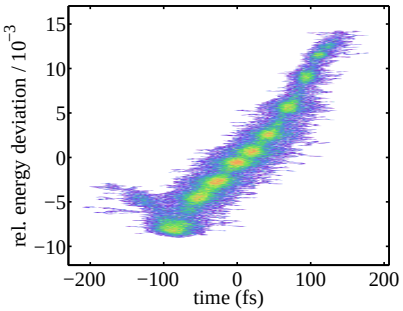

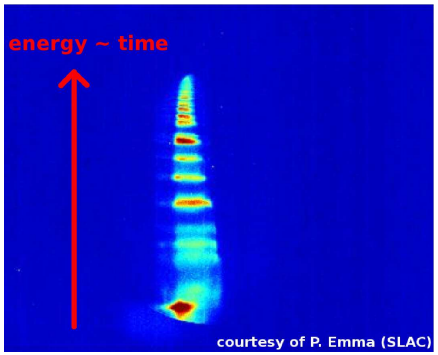

- Indication of microbunches
- Density modulations (FLASH)
- Energy modulations (LCLS)
  - chirped bunches $\rightarrow E \propto t$

Observations of Microbunching Instabilities in Time-domain

Linearly chirped bunches with intensity modulations at FLASH/DESY and LCLS/SLAC

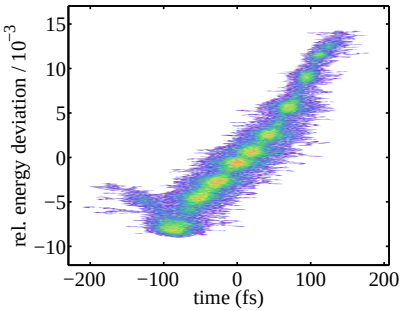

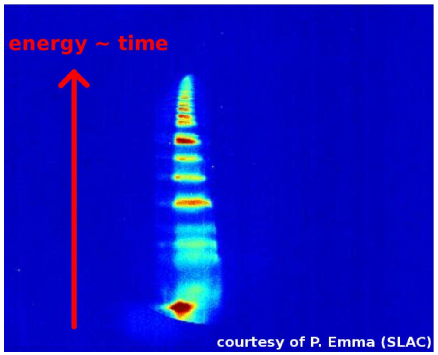

- Indication of microbunches
- Density modulations (FLASH)
- Energy modulations (LCLS)
  - chirped bunches $\rightarrow E \propto t$

Tilted microbunches and energy spread increase at FLASH/DESY

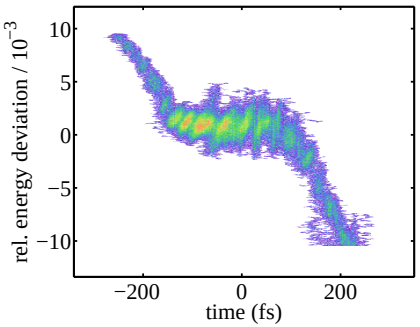

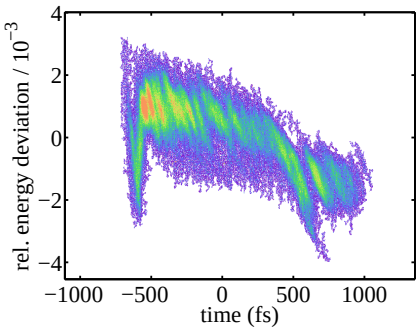

- Indication and observation of:
  - tilted microbunches
  - increased slice energy spread
- Common observation since operation with linear compression

★**Better control of slice energy spread is needed, especially for seeded FELs**

Mitigation of Coherent Optical Transition Radiation: Experiment

Compression instability: Charge 0.4 nC

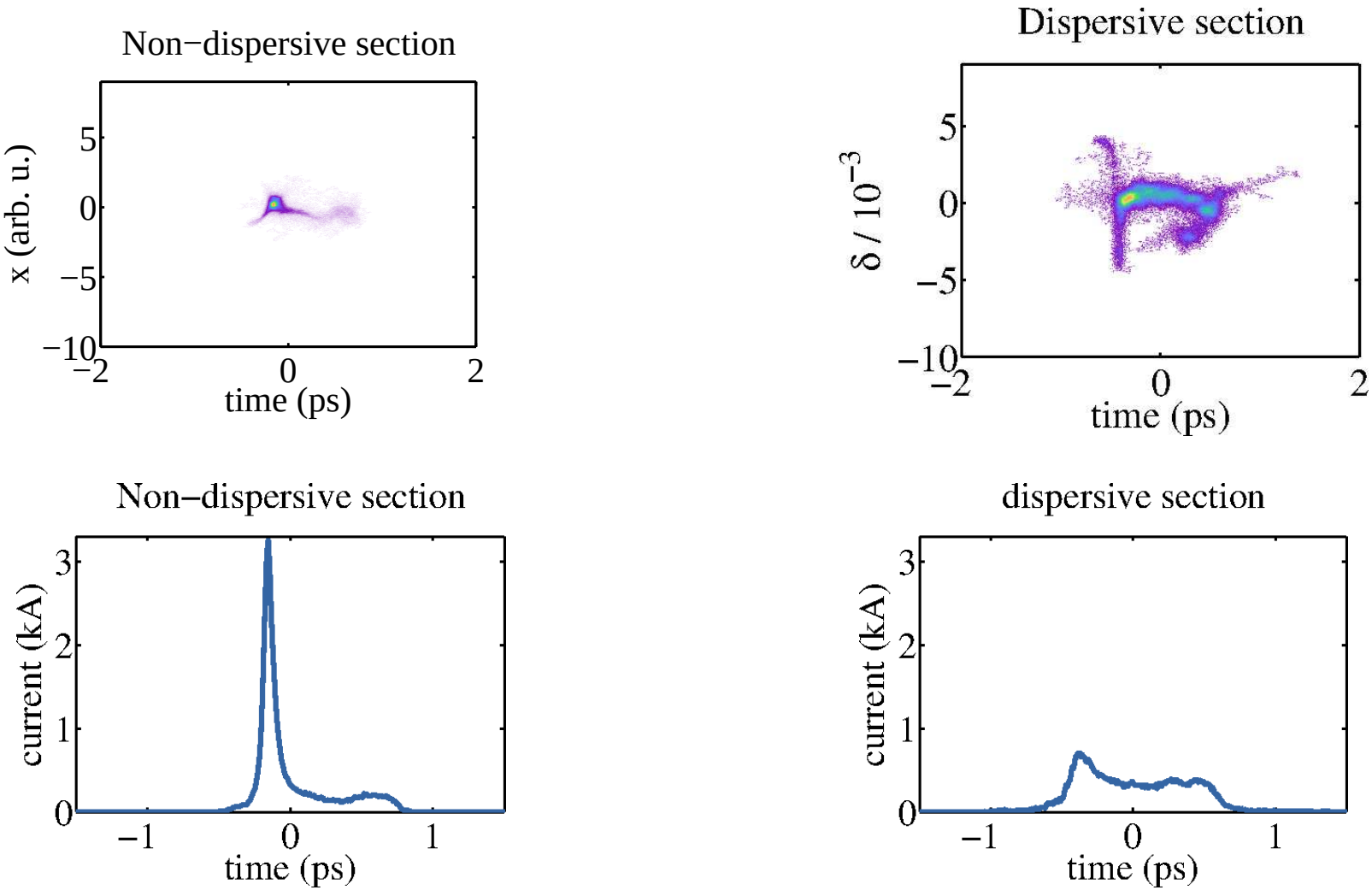

★ Strong discrepancy of current profiles between non-dispersive and dispersive section

Mitigation of Coherent Optical Transition Radiation: Experiment

Compression instability: Charge 0.5 nC

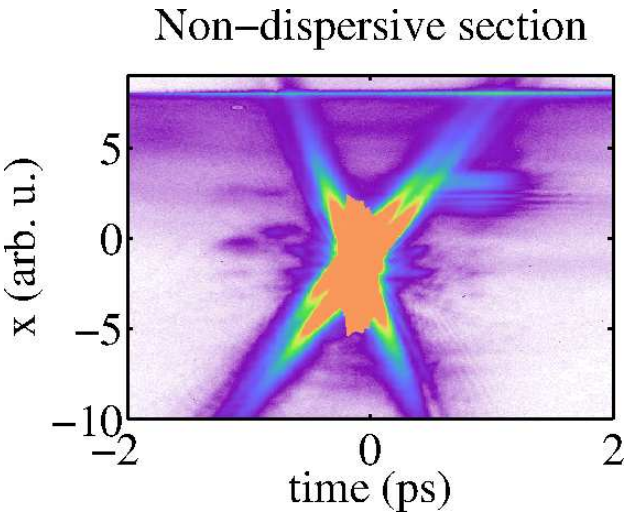

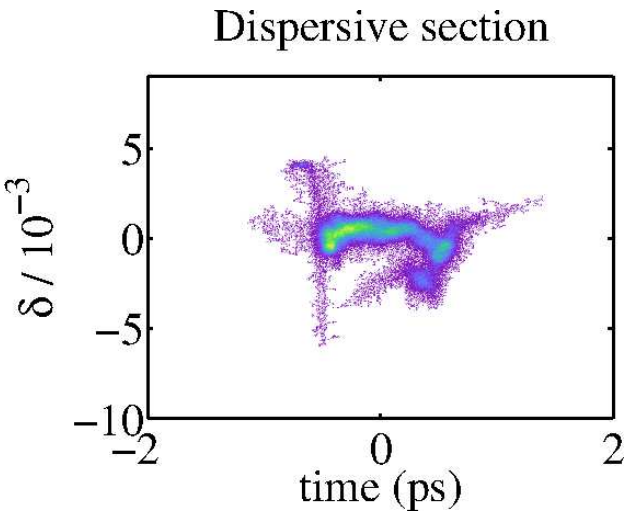

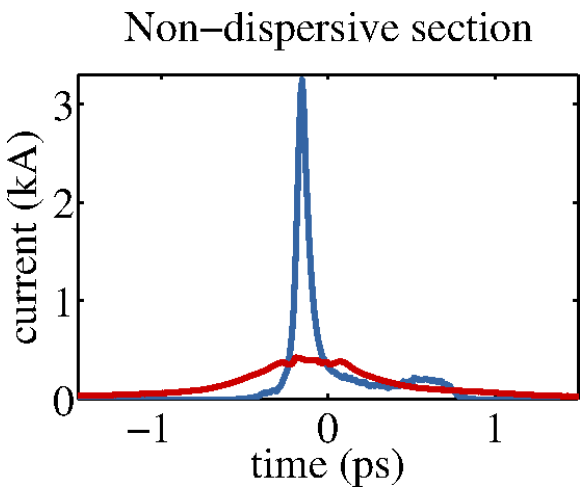

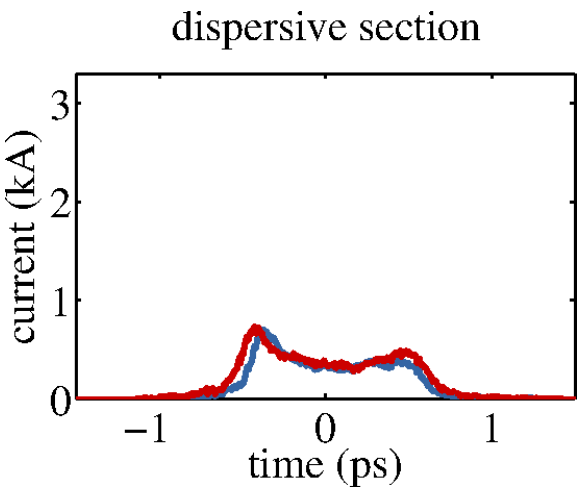

★ Local COTR emission spoils current profile measurement in non-dispersive section

Mitigation of Coherent Optical Transition Radiation: Experiment

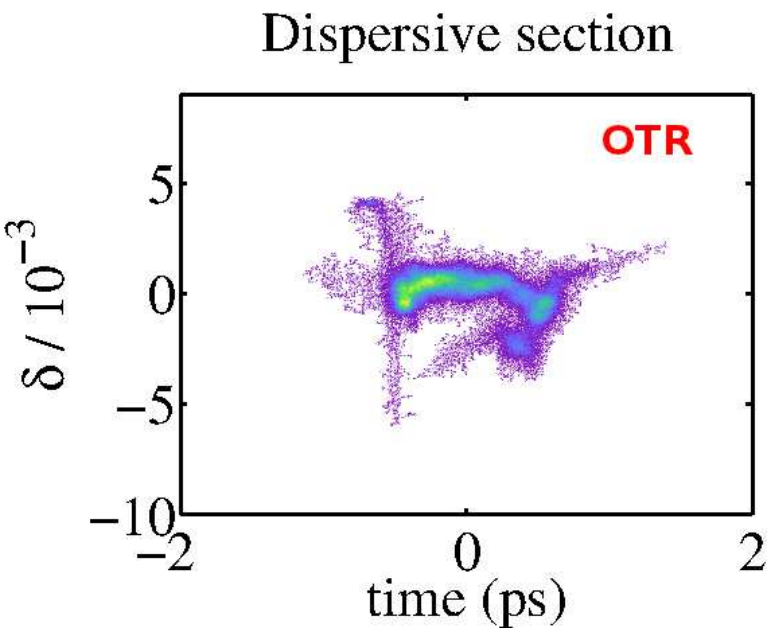

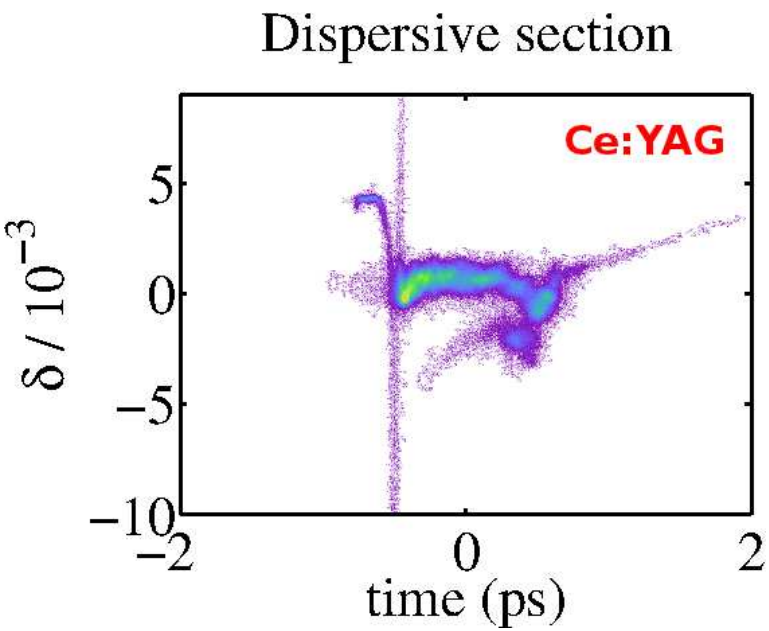

- ★ COTR is most probably generated by an ultra-short local spike
- ★ No indication for COTR in the dispersive section
- ● Poster on mitigation of COTR in the non-dispersive section at FLASH (M. Yan *et al.* THPB16)

Reversible Electron Beam Heater for Suppression of Microbunching Instabilities

For details: WEPB15 by Z. Huang *et al.* and WEOB4 by D. Xiang *et al.*

- Transverse deflecting structures induce energy spread (Panofsky-Wenzel theorem)
  ★ beam heating (cf. laser-heater)
- Energy spread is correlated, i.e. reversible
  ★ heat only where it's necessary

$$\begin{pmatrix} y_f \\ y'_f \\ t_f \\ \delta_f \end{pmatrix} = \begin{pmatrix} 1 & L & KL/2 & 0 \\ 0 & 1 & K & 0 \\ 0 & 0 & 1 & 0 \\ K & KL/2 & K^2L/6 & 1 \end{pmatrix} \cdot \begin{pmatrix} y_i \\ y'_i \\ t_i \\ \delta_i \end{pmatrix}$$

Reversible Electron Beam Heater for Suppression of Microbunching Instabilities

For details: WEPB15 by Z. Huang *et al.* and WEOB4 by D. Xiang *et al.*

- Transverse deflecting structures induce energy spread (Panofsky-Wenzel theorem)
  ★ beam heating (cf. laser-heater)
- Energy spread is correlated, i.e. reversible
  ★ heat only where it's necessary

$$\begin{pmatrix} y_f \\ y'_f \\ t_f \\ \delta_f \end{pmatrix} = \begin{pmatrix} 1 & L & KL/2 & 0 \\ 0 & 1 & K & 0 \\ 0 & 0 & 1 & 0 \\ K & KL/2 & K^2L/6 & 1 \end{pmatrix} \cdot \begin{pmatrix} y_i \\ y'_i \\ t_i \\ \delta_i \end{pmatrix}$$

Reversible beam heating combining two transverse deflecting structures (cavities)

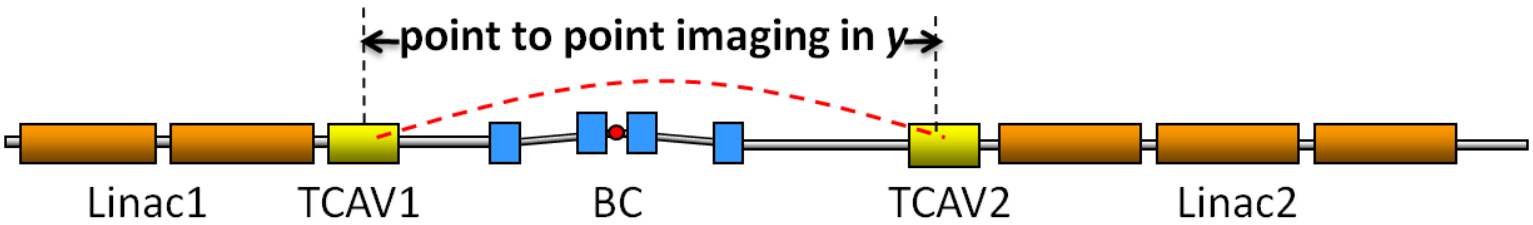

Reversible Electron Beam Heater for Suppression of Microbunching Instabilities

For details: WEPB15 by Z. Huang *et al.* and WEOB4 by D. Xiang *et al.*

- Transverse deflecting structures induce energy spread (Panofsky-Wenzel theorem)
  ★ beam heating (cf. laser-heater)
- Energy spread is correlated, i.e. reversible
  ★ heat only where it's necessary

$$\begin{pmatrix} y_f \\ y'_f \\ t_f \\ \delta_f \end{pmatrix} = \begin{pmatrix} 1 & L & KL/2 & 0 \\ 0 & 1 & K & 0 \\ 0 & 0 & 1 & 0 \\ K & KL/2 & K^2L/6 & 1 \end{pmatrix} \cdot \begin{pmatrix} y_i \\ y'_i \\ t_i \\ \delta_i \end{pmatrix}$$

Reversible beam heating combining two transverse deflecting structures (cavities)

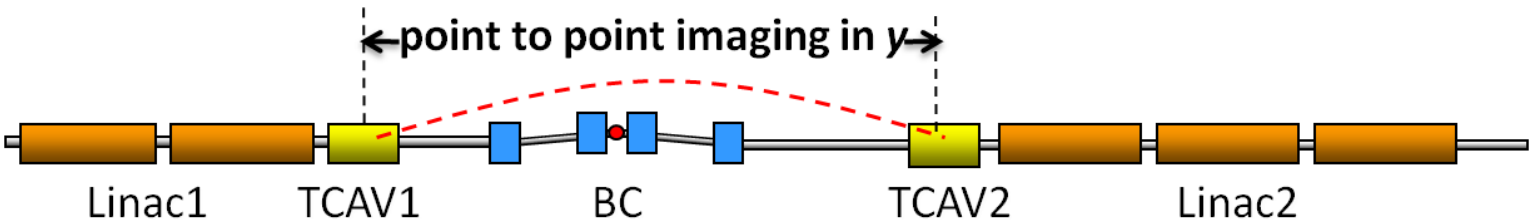

- Transport matrix: TCAV1 $\rightarrow$ TCAV2 (streaking $\perp$ bending plane)
- ★ $K_1 R_{56}$: effective energy spread for microbunching suppression
- ★ energy spread and spatial chirp cancelation

$$\begin{pmatrix} a + \frac{bL_2}{2} + \frac{K_1 K_2 R_{56} L_2}{2} & \frac{L_2}{2a} & 0 & \frac{K_2 L_2 R_{56}}{2} \\ b + K_1 K_2 R_{56} & a^{-1} & 0 & K_2 R_{56} \\ K_1 R_{56} & 0 & 1 + hR_{56} & R_{56} \\ 0 & 0 & 0 & \frac{1}{1+hR_{56}} \end{pmatrix}$$

Reversible Electron Beam Heater for Suppression of Microbunching Instabilities

For details: WEPB15 by Z. Huang *et al.* and WEOB4 by D. Xiang *et al.*

Demonstration setup with parameters comparable to a proposal at LBNL (NGLS)

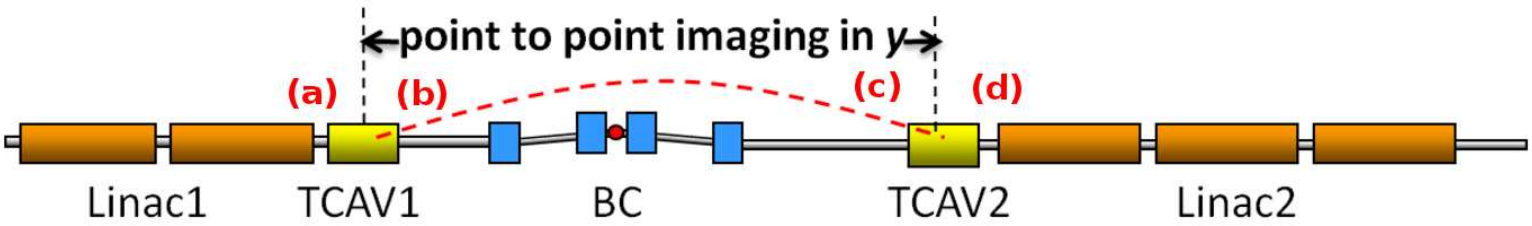

- Longitudinal phase space:
  - start with $1\,\mathrm{keV}$ slice energy spread
  - compression $C \approx 13$

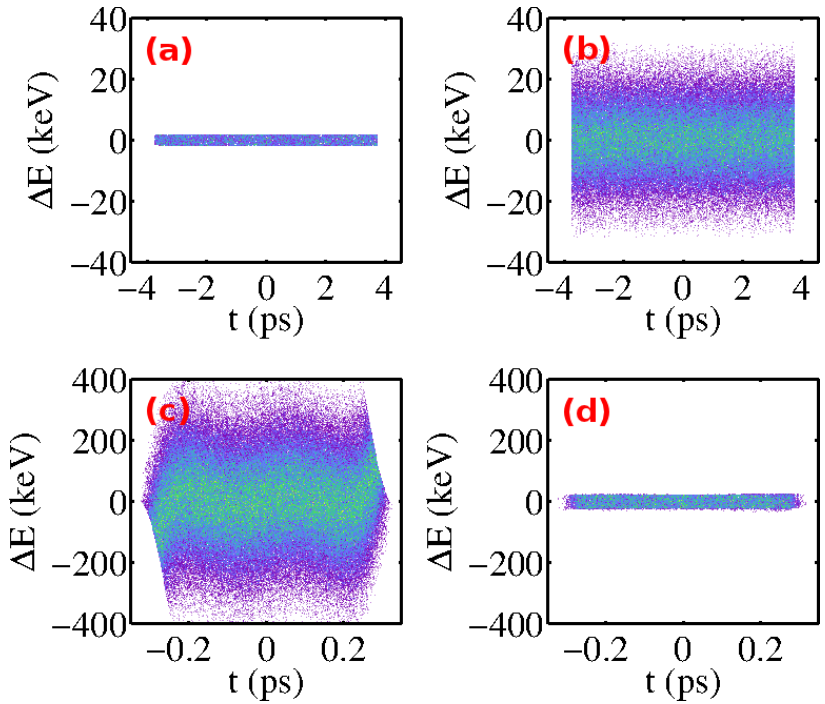

Reversible Electron Beam Heater for Suppression of Microbunching Instabilities

For details: WEPB15 by Z. Huang *et al.* and WEOB4 by D. Xiang *et al.*

Demonstration setup with parameters comparable to a proposal at LBNL (NGLS)

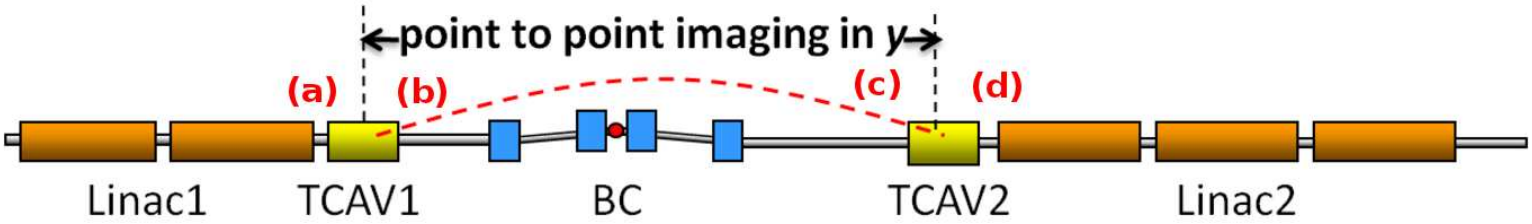

- Longitudinal phase space:
  - start with $1\,\mathrm{keV}$ slice energy spread
  - compression of about $C \approx 13$
- ★ Perfect cancelation of additional energy spread induced by TCAV1
  - CSR: small differences in the tails

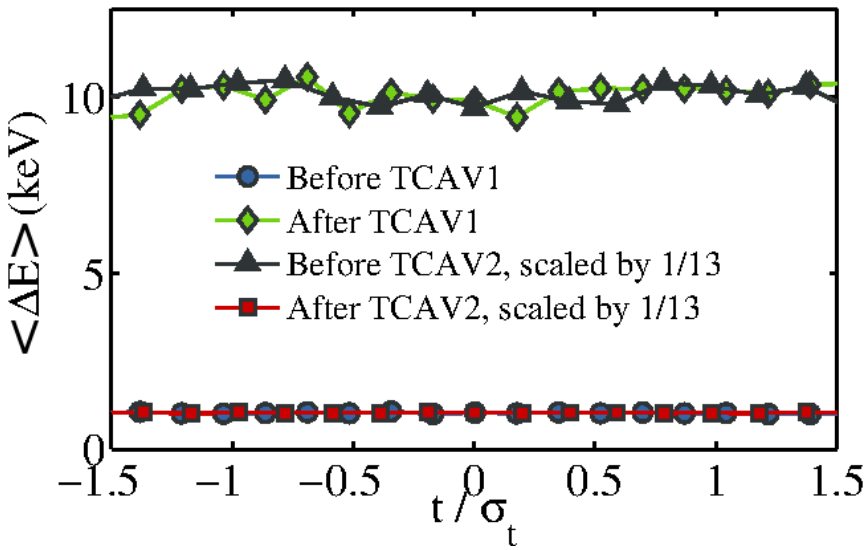

Reversible Electron Beam Heater for Suppression of Microbunching Instabilities

For details: WEPB15 by Z. Huang *et al.* and WEOB4 by D. Xiang *et al.*

Demonstration setup with parameters comparable to a proposal at LBNL (NGLS)

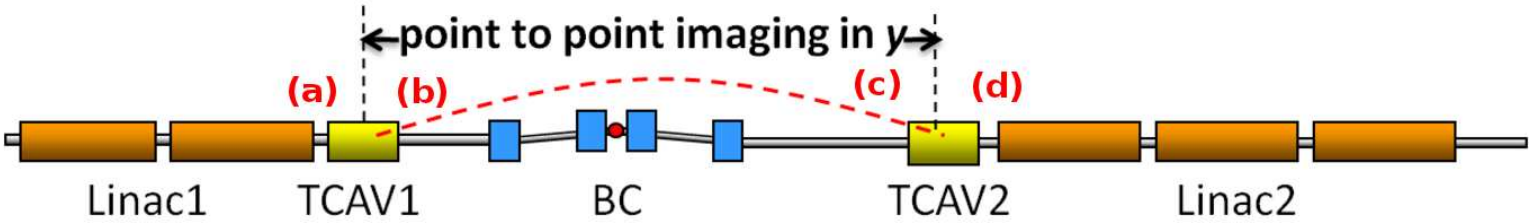

- ► Longitudinal phase space:
  - start with $1\,\mathrm{keV}$ slice energy spread
  - compression of about $C \approx 13$
- ★ Perfect cancelation of additional energy spread induced by TCAV1
  - CSR: small differences in the tails
- ★ CSR-driven microbunching:
  - start with 5% density modulation
- ★ TCAV-heater switched off

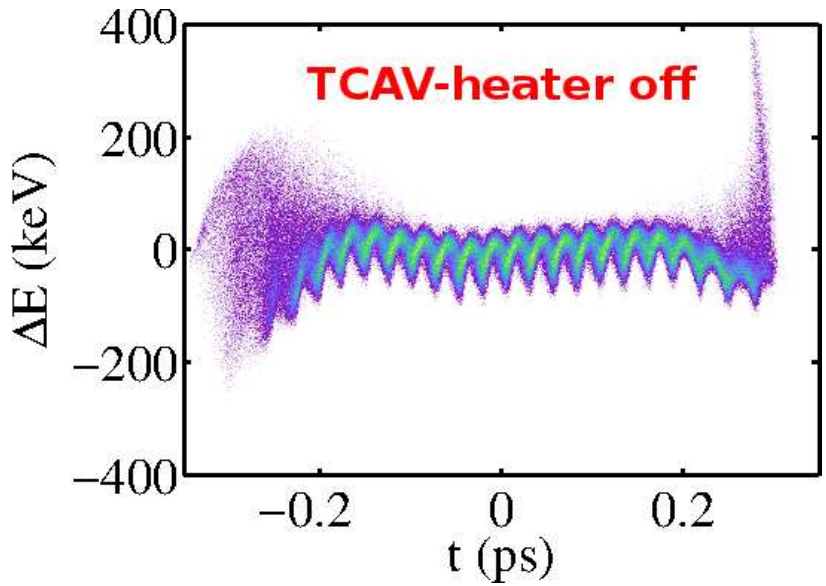

Reversible Electron Beam Heater for Suppression of Microbunching Instabilities

For details: WEPB15 by Z. Huang *et al.* and WEOB4 by D. Xiang *et al.*

Demonstration setup with parameters comparable to a proposal at LBNL (NGLS)

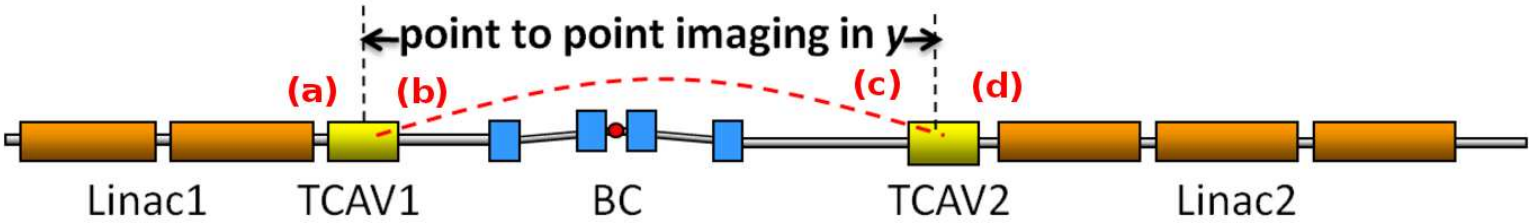

- ► Longitudinal phase space:
  - start with $1\,\mathrm{keV}$ slice energy spread
  - compression of about $C \approx 13$
- ★ Perfect cancelation of additional energy spread induced by TCAV1
  - CSR: small differences in the tails
- ★ CSR-driven microbunching:
  - start with 5% density modulation
- ★ TCAV-heater switched on

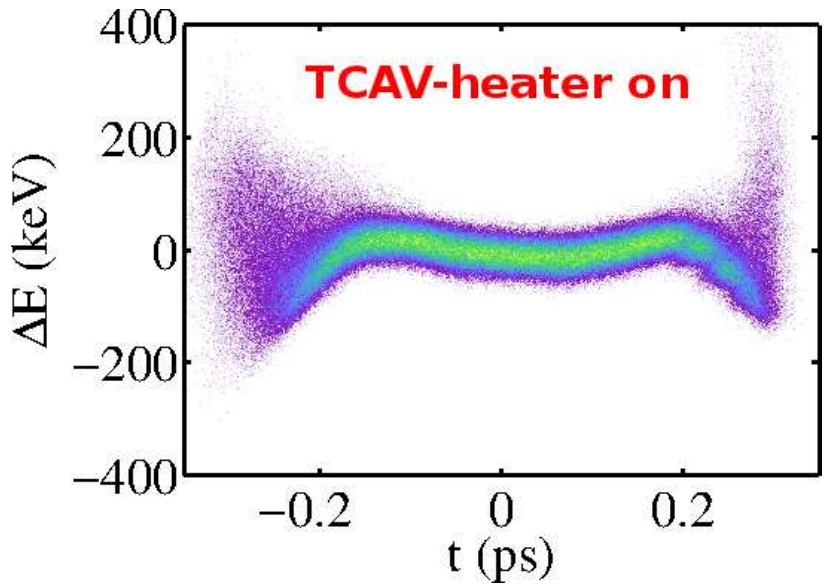

Longitudinal phase space diagnostics comes for free

Time-resolved X-ray Diagnostics with Femtosecond Resolution in Free-Electron Lasers For details: WEPA01 and THOCI2 by Y. Ding *et al.*

Longitudinal phase space diagnostics right after the undulators

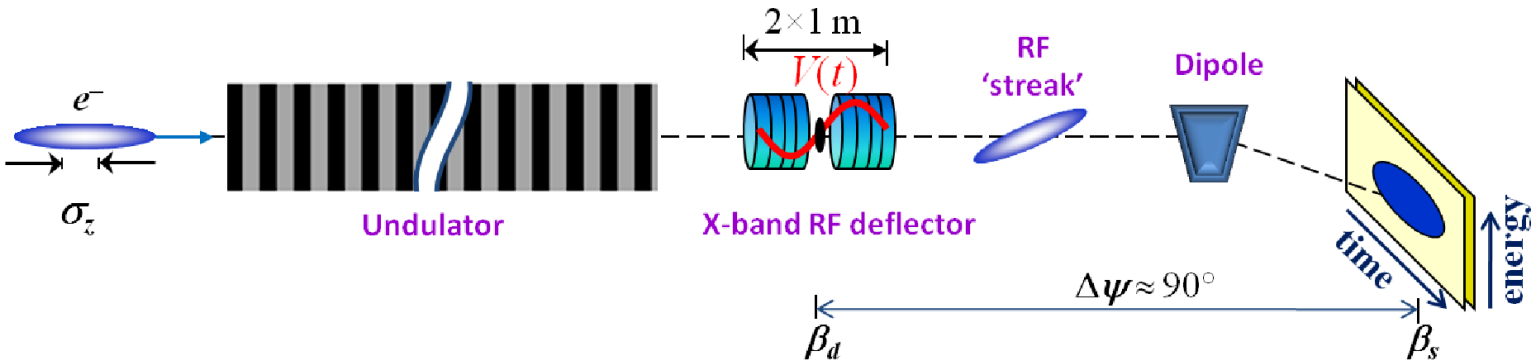

Time-resolved X-ray Diagnostics with Femtosecond Resolution in Free-Electron Lasers

For details: WEPA01 and THOCI2 by Y. Ding *et al.*

Longitudinal phase space diagnostics right after the undulators

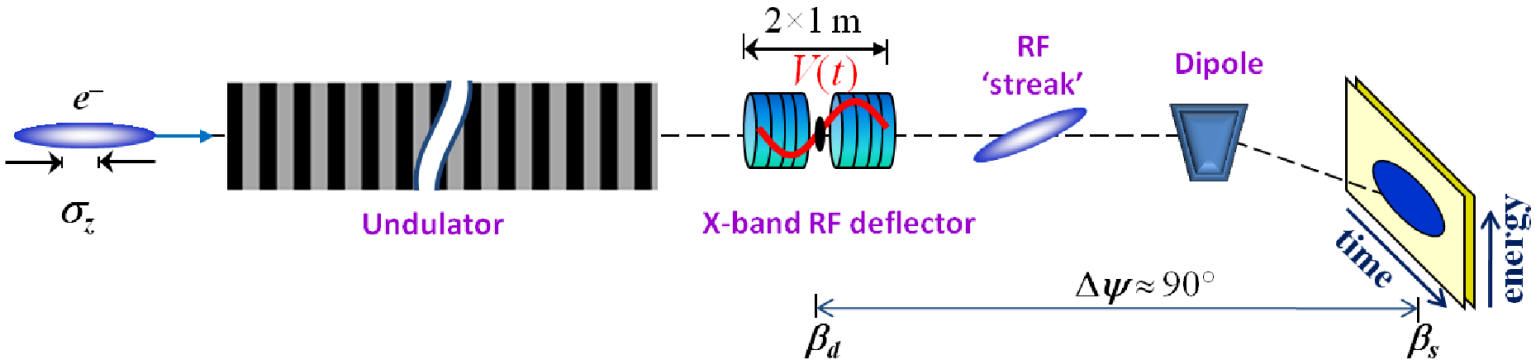

FEL: Genesis -> Tracking: elegant

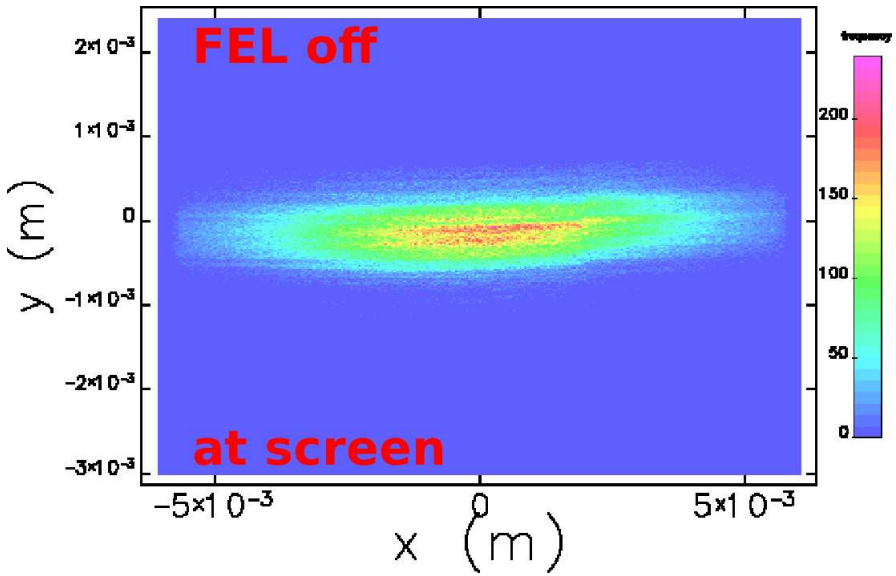

Time-resolved X-ray Diagnostics with Femtosecond Resolution in Free-Electron Lasers

For details: WEPA01 and THOCI2 by Y. Ding *et al.*

Longitudinal phase space diagnostics right after the undulators

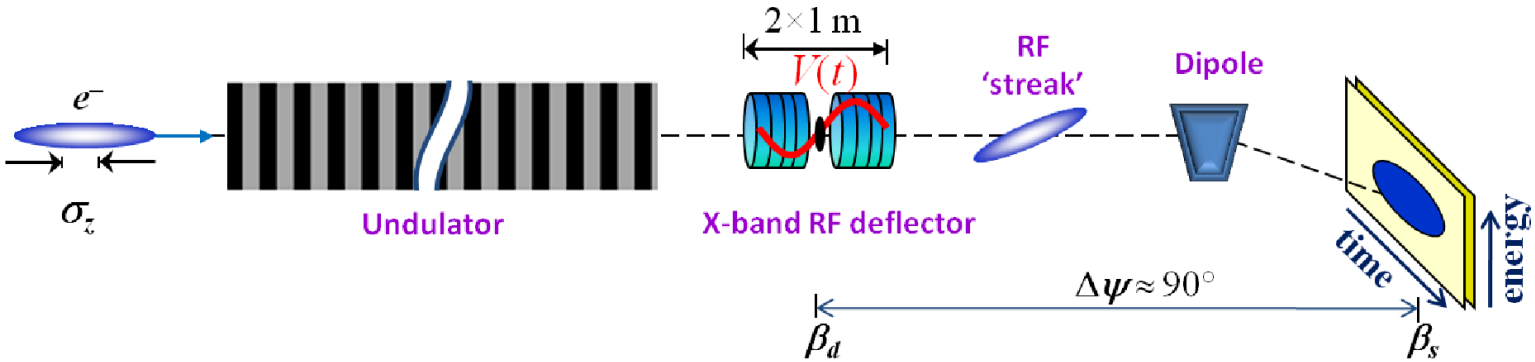

FEL: Genesis -> Tracking: elegant

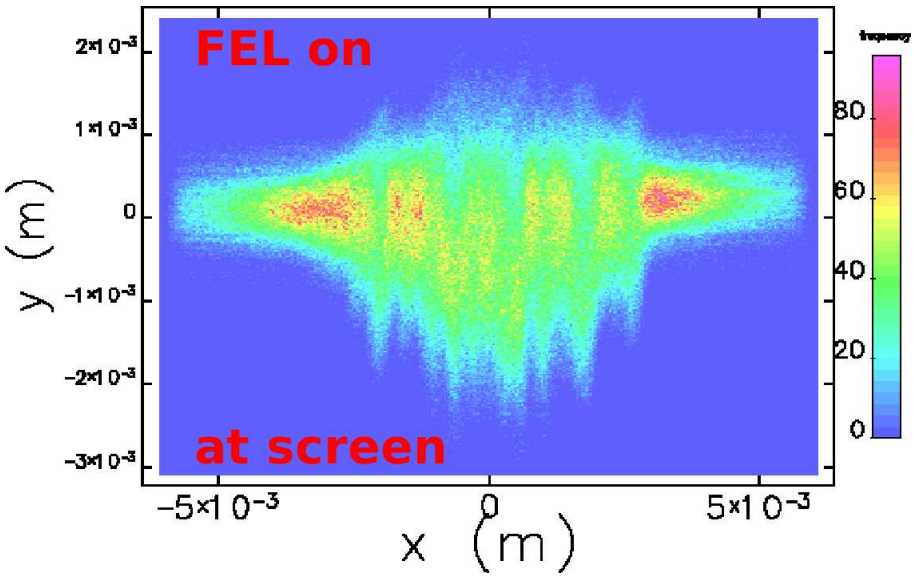

Time-resolved X-ray Diagnostics with Femtosecond Resolution in Free-Electron Lasers

For details: WEPA01 and THOCI2 by Y. Ding *et al.*

Longitudinal phase space diagnostics right after the undulators

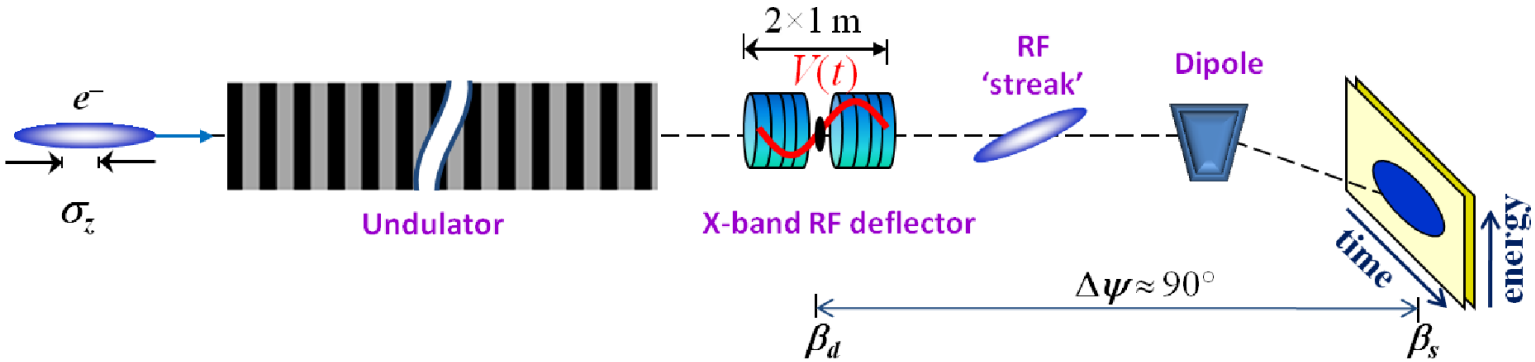

FEL: Genesis -> Tracking: elegant

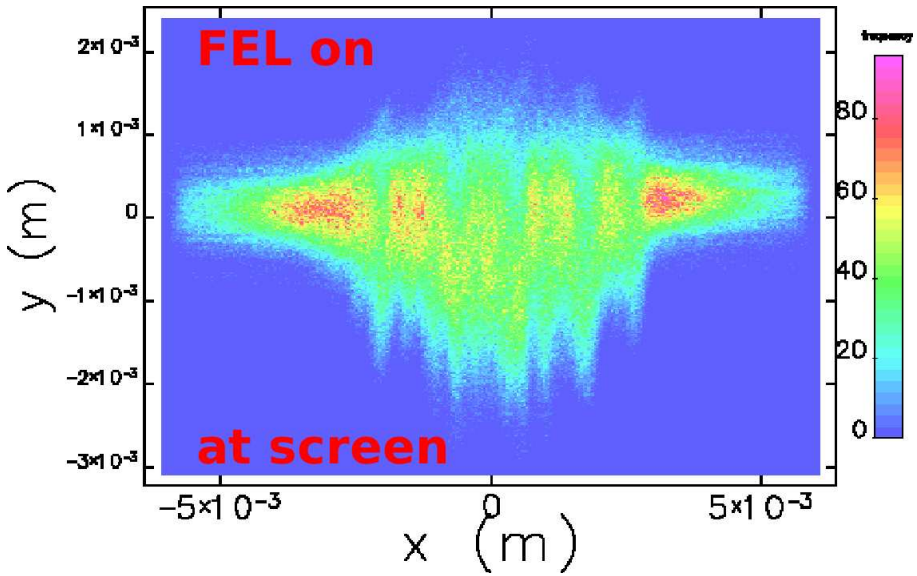

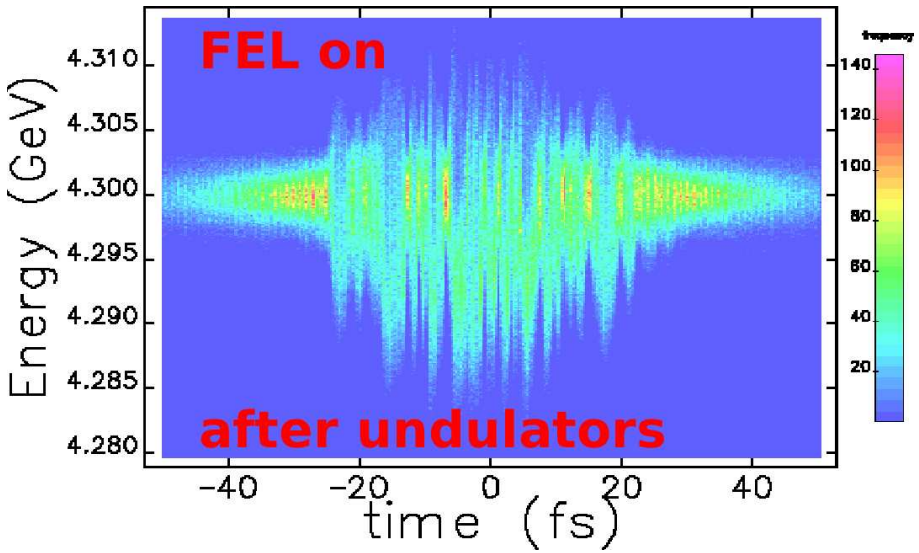

Time-resolved X-ray Diagnostics with Femtosecond Resolution in Free-Electron Lasers For details: WEPA01 and THOCI2 by Y. Ding *et al.*

Longitudinal phase space diagnostics right after the undulators

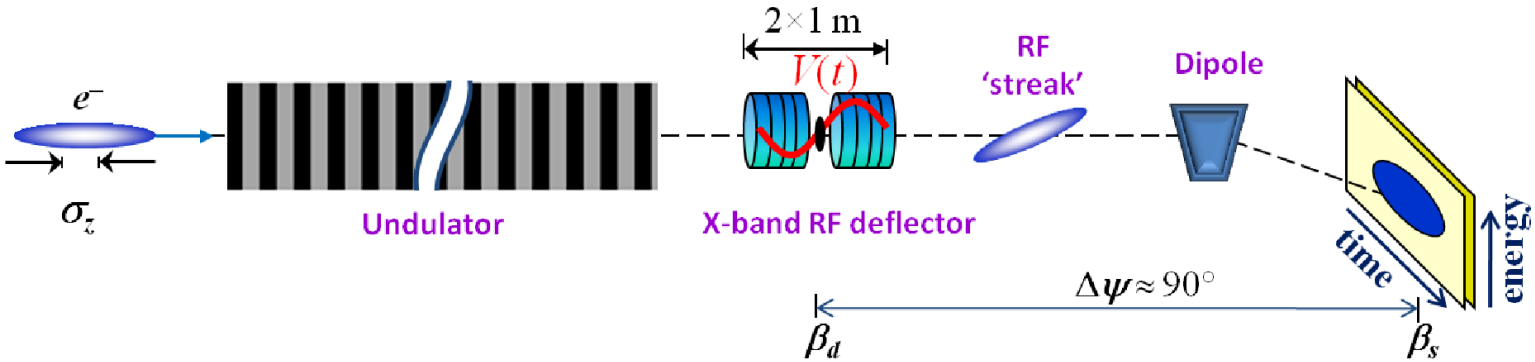

FEL: Genesis -> Tracking: elegant

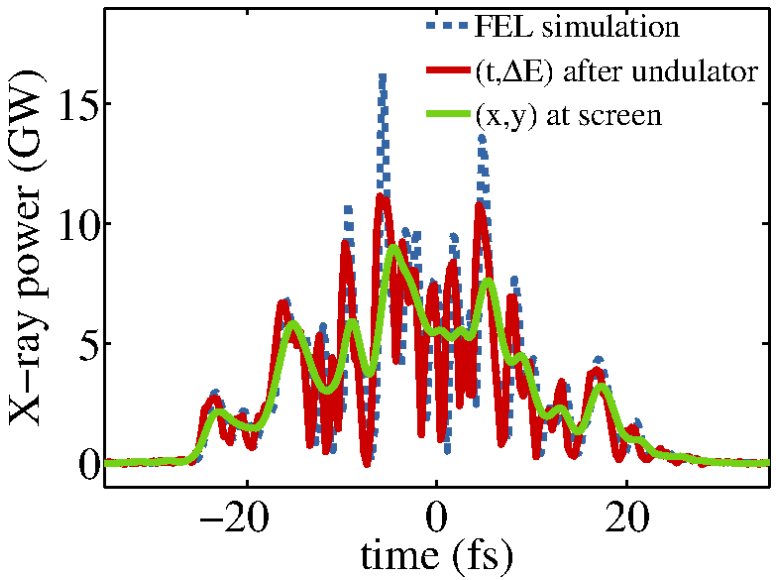

- Time-dependent energy loss and spread due to FEL process
- Correlation with temporal FEL photon pulse profile (replica of FEL photon pulse)

Time-resolved X-ray Diagnostics with Femtosecond Resolution in Free-Electron Lasers

For details: WEPA01 and THOCI2 by Y. Ding *et al.*

Longitudinal phase space diagnostics right after the undulators

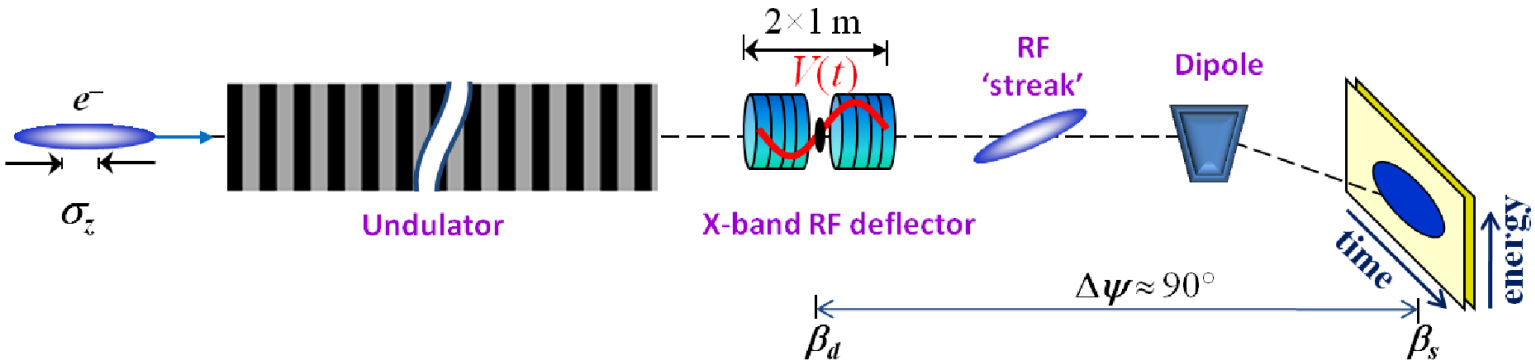

FEL: Genesis -> Tracking: elegant

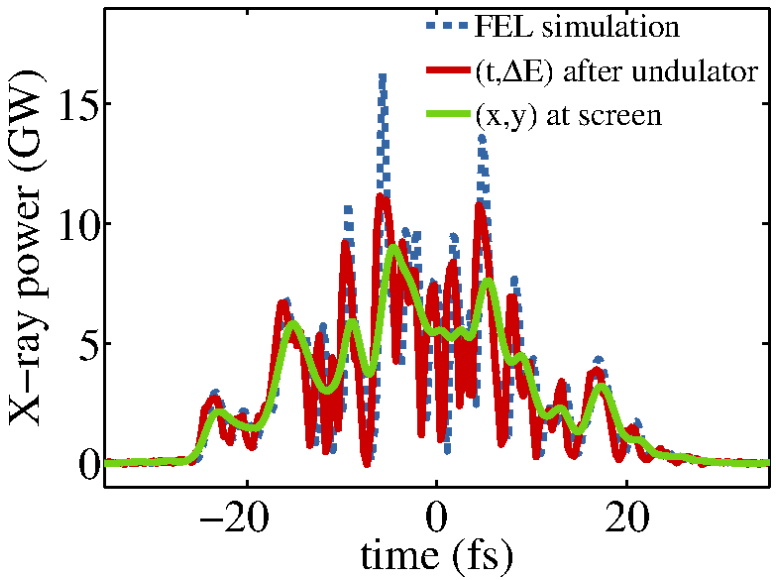

- Time-dependent energy loss and spread due to FEL process
- Correlation with temporal FEL photon pulse profile (replica of FEL photon pulse)
- ★ All features of high-resolution longitudinal phase space diagnostics (electrons beams):
  - independent of FEL wavelength
  - high-dynamic range
  - single-shot temporal profiles

Summary and Conclusions

Longitudinal phase space diagnostics based on TDS and energy spectrometer

- ★ Provide useful information on electron beams
- ★ Both with high resolution, high dynamic range, and single-shot capability

Summary and Conclusions

Longitudinal phase space diagnostics based on TDS and energy spectrometer

- ★ Provide useful information on electron beams
- ★ Both with high resolution, high dynamic range, and single-shot capability
- ★ Mitigation of coherent radiation effects of screen based diagnostics, e.g. COTR

Summary and Conclusions

Longitudinal phase space diagnostics based on TDS and energy spectrometer

- ★ Provide useful information on electron beams
- ★ Both with high resolution, high dynamic range, and single-shot capability
- ★ Mitigation of coherent radiation effects of screen based diagnostics, e.g. COTR
- ★ Be aware of systematic errors and the definition and meaning of resolution

Summary and Conclusions

Longitudinal phase space diagnostics based on TDS and energy spectrometer

- ★ Provide useful information on electron beams
- ★ Both with high resolution, high dynamic range, and single-shot capability
- ★ Mitigation of coherent radiation effects of screen based diagnostics, e.g. COTR
- ★ Be aware of systematic errors and the definition and meaning of resolution

Control of the longitudinal phase space by dual-frequency linear accelerators

- ★ Higher harmonic RF systems for longitudinal phase space linearizations
  - linear compression
- ★ Improvement of FEL performance in terms of pulse length tunabilty and intensity

Summary and Conclusions

Longitudinal phase space diagnostics based on TDS and energy spectrometer

- ★ Provide useful information on electron beams
- ★ Both with high resolution, high dynamic range, and single-shot capability
- ★ Mitigation of coherent radiation effects of screen based diagnostics, e.g. COTR
- ★ Be aware of systematic errors and the definition and meaning of resolution

Control of the longitudinal phase space by dual-frequency linear accelerators

- ★ Higher harmonic RF systems for longitudinal phase space linearizations
  - linear compression
- ★ Improvement of FEL performance in terms of pulse length tunabilty and intensity
- ★ Flexible longitudinal pulse shaping in general (e.g. for wakefield experiments)

Summary and Conclusions

Longitudinal phase space diagnostics based on TDS and energy spectrometer

- ★ Provide useful information on electron beams
- ★ Both with high resolution, high dynamic range, and single-shot capability
- ★ Mitigation of coherent radiation effects of screen based diagnostics, e.g. COTR
- ★ Be aware of systematic errors and the definition and meaning of resolution

Control of the longitudinal phase space by dual-frequency linear accelerators

- ★ Higher harmonic RF systems for longitudinal phase space linearizations
  - linear compression
- ★ Improvement of FEL performance in terms of pulse length tunabilty and intensity
- ★ Flexible longitudinal pulse shaping in general (e.g. for wakefield experiments)

Special applications of longitudinal phase space diagnostics

- ★ May provide useful information on X-ray pulses
- ★ Reversible Electron Beam Heater for Suppression of Microbunching Instabilities

Acknowledgments

Thanks for lots of helpful information and discussions to ...

- P. Evtushenko at Jlab
- P. Craievich at Elettra
- D. Filippetto at LBNL
- Y. Otake at SPring-8
- P. Piot and H. Edwards at Fermilab
- Y. Ding, P. Emma, J. Frisch, Z. Huang, and H. Loos at SLAC
- my colleagues at DESY and at the University of Hamburg

Acknowledgments

Thanks for lots of helpful information and discussions to ...

- P. Evtushenko at Jlab
- P. Craievich at Elettra
- D. Filippetto at LBNL
- Y. Otake at SPring-8
- P. Piot and H. Edwards at Fermilab
- Y. Ding, P. Emma, J. Frisch, Z. Huang, and H. Loos at SLAC
- my colleagues at DESY and at the University of Hamburg

Thank you for your attention!